

UCSF

UC San Francisco Electronic Theses and Dissertations

Title

Studies of the Carcinoma-Associated Fibroblast in Human Oral Squamous Cell Carcinoma

Permalink

<https://escholarship.org/uc/item/9g36f9r2>

Author

Connelly, Stephen Thaddeus

Publication Date

2011

Peer reviewed|Thesis/dissertation

Studies of the Carcinoma-Associated Fibroblast in Human Oral
Squamous Cell Carcinoma

by

S. Thaddeus Connelly

DISSERTATION

Submitted in partial satisfaction of the requirements for the degree of

DOCTOR OF PHILOSOPHY

in

Oral and Craniofacial Sciences

in the

GRADUATE DIVISION

of the

UNIVERSITY OF CALIFORNIA, SAN FRANCISCO

Copyright 2011

by

S. Thaddeus Connelly

Dedication and Acknowledgements

I dedicate this work to my wife Pathima, my son Sebastien, my Mother Nancy and Father Steve as well as my brothers and sister, Corey, Adam and Heather. Thank you for all of your support and encouragement.

Thank you to everyone who helped me along the way. My entire extended family on both of my Mother and Father's sides as well as my wife's family.

A special thanks to the scientific and clinical mentors that I have had in the past twenty years; Drs. Donna Albertson, Brian Schmidt, Richard Jordan, Dan Ramos, M.A. Pogrel, Shelley Miyasaki, Jon Horvitz, Paul Shepard and Rebeka Silva.

Thank you to the Albertson Lab; especially Bing Huey and Aditi Bhattacharya, I could not have done this without the help of either of you.

Thank you to the members of my committee; Drs. Donna Albertson (Chair), Jon Levine, Randal Kramer and Dan Ramos.

Portions of Chapter 3 have been taken from a previously published work, as indicated in the chapter, from our laboratory with a minor contribution from the author.

Snijders, A. M. *et al.* Stromal control of oncogenic traits expressed in response to the overexpression of GLI2, a pleiotropic oncogene. *Oncogene* **28**, 625-637, doi:10.1038/onc.2008.421 (2009).

**Studies of the Carcinoma-Associated Fibroblast in Human Oral Squamous
Cell Carcinoma
S. Thaddeus Connelly**

Abstract

Our understanding of the development and progression of oral squamous cell carcinoma (Oral SCC) remains limited. This is reflected by the fact that oral cancer is associated with one of the poorest 5-year survival rates of any malignancy in the body. It is becoming increasingly evident that the underlying stroma has an important role to play in tumorigenesis. Our studies focus on the central controller of the stroma, the fibroblast and its tumor-associated counterpart, the carcinoma-associated fibroblast (CAF). The molecular and functional characteristics of CAFs associated with Oral SCC remain incomplete. Thus, we studied the influence of the stroma on the tumor microenvironment through a histologic evaluation of cancerous and pre-cancerous lesions. Additionally, we assessed the molecular response that CAFs and fibroblasts display to TGF β or TGF β -mediated stimulation by direct measurement of expression levels of downstream genes and in an organotypic co-culture system, respectively. Lastly, we used expression profiling, immunofluorescence and functional assays of CAFs and normal fibroblasts (NFs) in an attempt to classify a CAF specific expression signature, CAF subsets or cellular origin and to identify CAF genes or gene pathways that might contribute to proliferation, migration and invasion. The results demonstrate that the stromal lymphocytic infiltrate increases with lesion severity of pre-cancers with the most in Oral SCC, indicating a causal relationship. Fibroblast response to TGF β or TGF β -mediated stimulation was varied based on anatomic site and this heterogeneity was further appreciated in the results of the immunofluorescence and expression profiling, however these studies confirmed that α SMA is a robust CAF marker. Despite the heterogeneity in the CAF/NF expression profiles, a set of genes was found and validated to be differentially expressed between gingiva CAFs and NFs and tongue and gingival fibroblasts in general. Finally, analysis of fibroblast groups defined through functional assays reveal differential gene expression between fibroblasts that are most or least inhibitory to keratinocyte/tumor cell line proliferation and those that increase or decrease invasion/migration. SFRP2 from the proliferation assay and DKK1 from the invasion/migration assay are both differentially expressed negative modulators of WNT signaling, indicating a potentially important pathway in the reciprocal tumor/stroma evolutionary relationship.

Table of Contents

Chapter 1

Characterization of the Stromal Lymphocytic Infiltrate in Pre-Neoplastic and Neoplastic Lesions

1.1 Introduction	2
1.2 Methods	4
1.3 Results	6
1.4 Discussion	13

Chapter 2

Derivation of Oral Fibroblast Strains from Human Surgical Specimens

2.1 Introduction	17
2.2 Methods	20
2.3 Results	24
2.4 Discussion	24

Chapter 3

Anatomic Variation in Oral Fibroblast Response to TGF β or TGF β - Mediated Stimulation.

3.1 Introduction	49
3.2 Methods	61
3.3 Results	66
3.4 Discussion	71

Chapter 4

Immunofluorescence Study Seeking to Identify Carcinoma-Associated Fibroblast Subsets and Cell-of-Origin.

4.1 Introduction	75
4.2 Methods	76
4.3 Results	78
4.4 Discussion	84

Chapter 5

mRNA Expression Profiling of Carcinoma-Associated and Normal Fibroblasts

5.1 Introduction	88
5.2 Methods	89

5.3 Results	97
5.4 Discussion	109

Chapter 6

Proliferation and Invasion/Migration Assays Reveal Subsets of Fibroblasts with Differential Gene Expression

6.1 Introduction	116
6.2 Methods	116
6.3 Results	121
6.4 Discussion	131

List of Tables

Chapter 1

Table 1.1 Patient characteristics for pathology review cohort

Chapter 2

Table 2.1 Listing of derived primary cell strains

Table 2.2 Study population characteristics

Table 2.3 Success of primary cell strain cultures

Table 2.4 Cell strain survival by cell type and anatomic subset

Chapter 3

Table 3.1 Antibodies used for immunofluorescence and immunohistochemistry

Chapter 4

Table 4.1 Antibodies used for immunofluorescence

Table 4.2 Fibroblast strains used for the immunofluorescence study

Table 4.3 Positive fluorescence for each marker per anatomic subgroup

Chapter 5

Table 5.1 CAF/NF strains used from the expression arrays

Table 5.2 Gene function and cancer relevance of differentially expressed genes

Table 5.3 Validation of 15 genes that were differentially expressed

Table 5.4 qPCR Validation results

Chapter 6

Table 6.1 Same individual CAF/NF pairs with differing inhibition of proliferation.

Table 6.2 Fibroblast strains divided into least and most inhibiting to proliferation.

List of Figures

Chapter 1

Figure 1.1 Criteria for PVL lesions

Figure 1.2 Inflammation level in PVL, OED and Oral SCC

Figure 1.3 Photomicrographs of infiltrate in increasingly severe OED lesions

Figure 1.4 Infiltrate increases as severity of dysplasia increases

Figure 1.5 Infiltrate increases as severity of PVL increases

Figure 1.6 Infiltrate increases as severity of dysplasia increases in PVL

Figure 1.7 No relationship between grade of Oral SCC and infiltrate

Chapter 2

Figure 2.1 Success of culturing according to sex of tissue donor

Figure 2.2 Overall success of cell strain establishment in the normal keratinocyte, normal fibroblast and carcinoma-associated fibroblast groups

Figure 2.3a NK culture results by anatomic site

Figure 2.3b NF culture results by anatomic site

Figure 2.3c CAF culture results by anatomic site

Figure 2.4a NK culture results by site based on sex

Figure 2.4b NF culture results by site based on sex

Figure 2.4c CAF culture results by site based on sex

Figure 2.4d Culture results by type based on sex

Figure 2.5a NK culture results per age group

Figure 2.5b NF culture results per age groups

Figure 2.5c CAF culture results per age groups

Figure 2.6a NK culture success over time

Figure 2.6b NF culture success over time

Figure 2.6c CAF culture success over time

Figure 2.7 Survival of maxillary versus mandibular cultures

Chapter 3

Figure 3.1 Organotypic co-culture

Figure 3.2 GLI2 induces transdifferentiation of fibroblasts

Figure 3.3 GLI2 induces TGF β mediated differentiation of fibroblasts

Figure 3.4 Anatomic variation in fibroblast response to TGF β

Chapter 4

Figure 4.1 Pancytokeratin and vimentin markers

Figure 4.2 α SMA and FSP-1 markers

Figure 4.3 PDGFR β and NG2 markers

Figure 4.4 α SMA signal in the CAF/NF gingiva and tongue pairs

Chapter 5

Figure 5.1 Configuration of the RNA QC PCR array

Figure 5.2 Unsupervised hierarchical clustering of top 10% most differentially expressed genes in the entire 24-sample data set

Figure 5.3 Unsupervised hierarchical clustering of top 10% most differentially expressed genes among the gingival data set

Figure 5.4 Unsupervised hierarchical clustering of top 10% most differentially expressed genes among the tongue fibroblast data set

Figure 5.5 Ten genes were identified as being differentially expressed based on the level of fold change in expression and the significance level for gingival CAFs compared to gingival NFs

Figure 5.6 Eight genes were identified as being differentially expressed based on the level of fold change in expression and the significance level for tongue fibroblasts compared to gingival fibroblasts

Chapter 6

Figure 6.1 Proliferation experiment results for HaCaT and OSC20

Figure 6.2 Proliferation rates based on CAF/NF, tongue and gingiva groups

Figure 6.3 Proliferation results comparing rates of HaCaT versus OSC20

Figure 6.4 51 differentially expressed genes in the different fibroblast groups

Figure 6.5 Ratios of invasion/migration for repeat experiments

Figure 6.6 Most reproducible fibroblast strains in the invasion/migration assay

Figure 6.7 Comparison of fibroblasts that increased/decreased invasion/migration and their effect on proliferation

Figure 6.8 Differential expression of 14 genes found in the invasion/migration assay

**Chapter 1: Characterization of the Stromal Lymphocytic Infiltrate in
Pre-Neoplastic and Neoplastic Lesions.**

Introduction.

The importance of the interactions between epidermal tumor cells and their surrounding microenvironment has been increasingly brought to light. The main components of the tumor microenvironment are the tumor cells themselves and the various tumor associated elements, which include the endothelial cells and supporting elements of the vasculature, neural processes and associated cells, protein constituents of the extracellular matrix, local and infiltrating cells of the immune system and fibroblasts¹. Their importance and role in the development and progression of cancers, including human oral squamous cell carcinoma (Oral SCC) are being elucidated. For example, the vascular mediators VEGF and VEGFR have been shown to be a reliable prognostic tool in Oral SCC, predicting poor disease-free survival, poor overall survival and metastatic disease². The neural system is not only present to relay to the brain information from distal sources but it is a highly interactive component of the microenvironment controlling such processes as neurogenic inflammation. As an illustration of this fact, patients that have Oral SCCs that are associated with high levels of pain have a lower disease free survival rate and lower overall survival rate^{3,4}. Hyaluronic acid, a major building block of the extracellular matrix, has been shown to interact with CD44 receptors in complexes, which include the often over expressed (in head and neck cancers) epidermal growth factor receptor, leading to downstream activation of components of the Ras and RhoA pathways leading to cell migration, growth and tumor survival⁵. The presence of carcinoma-associated fibroblasts, the main topic of this thesis are often present in the microenvironment of Oral SCC, and patients that have tumors with increased

numbers have a poorer disease-free rate and lower rates of overall survival. Then, finally, the inflammatory infiltrate, the subject of this current chapter, has been shown to play a role in solid tumors in general⁶ and Oral SCC⁷ in particular.

In order to explore the role of the inflammatory infiltrate we have studied a rare clinical entity of the oral cavity called proliferative verrucous leukoplakia (PVL). PVL is a persistent, recurrent, multi-focal pre-cancerous lesion that has a higher rate (50-70%) of malignant transformation than all other oral pre-malignant lesions. It predominately occurs in middle-age women and is not generally associated with any of the traditional oral cancer risk factors such as tobacco and alcohol use⁸. Thus, PVL contrasts with the more common and much better studied form of pre-cancer, oral epithelial dysplasia (OED), which has a transformation rate of less than 16% and is strongly associated with tobacco and alcohol use. Little is known about the underlying causes of PVL, whether the precipitating lesions are located in the epithelial or stromal cells and although an association with HPV infection has been supported by some studies, this has not been confirmed by others ref. It is clear, histologically that the normal pattern of epithelial differentiation has been disrupted and, interestingly the initial clinical appearance often resembles lichen planus, and in fact taken out of clinical context, PVL can be mistaken for lichen planus. Lichen planus, has a well-characterized immunologic pathogenesis and classically has a readily identifiable dense band of inflammatory infiltrate just underlying the epidermal lesion upon histologic examination⁹. Thus, we have a rare disease entity with a high propensity for transforming into a more malignant form, which shares

clinical characteristics with another more common oral mucosal disease that has a well characterized associated inflammatory infiltrate. Additionally, given that PVL presents as an increasingly severe spectrum of lesions (see below), it seems as though it would be informative to investigate the association between the levels of the inflammatory infiltrate within this spectrum of related lesions and then compare them to lesions with lower rates of transformation, the OEDs as well as Oral SCCs. In summary, it is the aim of this chapter to present our initial observations regarding the relationship of lesion severity and the level of the inflammatory infiltrate in PVLs, OEDs and Oral SCCs. Potentially, these data will lead to more meaningful functional and prognostic characterizations of the infiltrate associated with preneoplasias and neoplasias of the oral cavity.

Methods.

A pathology report review was carried out on cases selected from the University of California San Francisco's Oral Cancer Tissue Bank using the key words "Proliferative Verrucous Leukoplakia" and "PVL". Data were gathered from a total of 102 pathology reports, including demographic data, anatomic site of the biopsy, whether a previous biopsy had been performed and whether there was dysplasia detected within the biopsy specimen. From this initial review, a detailed histological review of haematoxylin and eosin (H&E) slides was undertaken using 65 randomly selected PVL cases from the pathology report review, and then for comparison, 60 oral squamous carcinoma and 61 oral epithelial dysplasias were randomly selected from the Tissue Bank. The PVL

cases were graded on a 5-point scaling system based on Hansen's original 10-point system (Figure 1.1)¹⁰. The 5-point scaling system grades lesions in an increasing order of severity from hyperkeratosis, verruciform hyperkeratosis, verrucous hyperplasia, verrucous carcinoma and ending with squamous cell carcinoma. The oral squamous cell carcinoma specimens were evaluated for being either poorly, moderately or well-differentiated. Additionally, the oral epithelial dysplasias were scored as being mild, moderate, severe or carcinoma-*in situ*. For each slide, a score was given quantifying the amount of inflammatory infiltrate that was present in the surrounding stroma, which was designated as none, mild, moderate or severe. All evaluations were carried out at both 10X and 20X on a Zeiss upright microscope and a board-certified Oral Pathologist did the scoring.

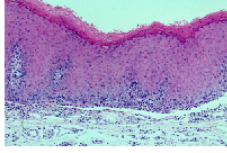
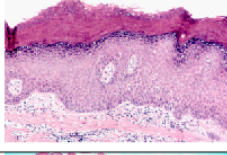
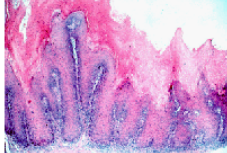
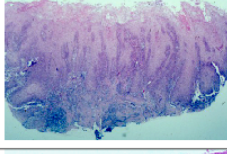
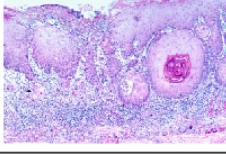
Histologic Lesion	Grade Number	Hansen's Grade	Histologic Features	Micrograph
Hyperkeratosis	1	2	hyperkeratosis only	
Verruciform Hyperkeratosis	2		verruciform profile no acanthosis ± mild OED	
Verrucous Hyperplasia	3	4	verruciform profile acanthosis no stromal invasion	
Verrucous Carcinoma	4	6	verruciform profile acanthosis stromal invasion	
Squamous Cell Carcinoma	5	8-10	cellular atypia pleomorphism stromal invasion	

Figure 1.1 Histological criteria for the progressive PVL lesions.
Results.

PVL pathology report review is consistent with previous published data showing that PVL is more a problem for women than men and that it tends to be a recurrent multifocal disease entity. The results of the PVL pathology report review are consistent with previously published results (Table 1.1) demonstrating that PVL tends to affect females more often than males. Additionally, the multifocal and recurrent nature of PVL is reflected in the relatively equal anatomic distribution of the biopsy sites and high percentage of pathology reports that were associated with a previous biopsy. Haematoxylin and eosin (H&E) stained slides from 65 PVL cases were randomly selected for review from the 102 cases in the report

review. Thirty-one percent of the cases in the report review stated that there was dysplasia in the primary lesion, whereas 43% of the H&E slides had dysplasia. The differing ratios of dysplasia between the two groups was mainly a result of the random nature in which the H&E cases were selected out of the report review group, there were only three cases which were deemed to have dysplasia in the H&E review, but not listed as such in the pathology report and this was not significant. It seems you might want to say that the difference is not significant.

Table 1. 1 Patient characteristics for pathology review cohort

	Number	%
Total patients	102	
Males	44	43
Females	58	57
Previous Biopsy	54	53
Anatomic site		
Anterior Maxillary Gingiva	17	17
Posterior Maxillary Gingiva	18	18
Hard Palate	10	10
Anterior Mandibular Gingiva	16	16
Posterior Mandibular Gingiva	17	17
Buccal Mucosa	10	10
Tongue	15	15
Dysplasia		
Positive in the path report	31/102	31
Positive per slide review	28/65	43
Path report and slide discrepancy	3	1

Oral SCC has a significantly higher level of inflammatory infiltrate than either PVL or OED.

For the between group analysis, scoring of the inflammatory infiltrate in the underlying stroma from the PVL cases (n=65) as compared to oral squamous cell carcinoma (Oral SCC, n=60) and oral epithelial dysplasia (OED, n=61) reveals that there is a significantly more intense inflammatory infiltrate associated with Oral SCC compared to PVL and OED (p=0.003, Kruskal Wallis rank sum test).

When comparing the inflammatory infiltrate scores by pairs, there is a statistically significant difference between the OEDs and the Oral SCCs (p=0.0096, Wilcoxon rank sum test) and the PVLs and the Oral SCCs (p=0.02, Wilcoxon rank sum test) but not between the PVL and OED groups (p=0.25, Wilcoxon rank sum test) (Figure 1.2).

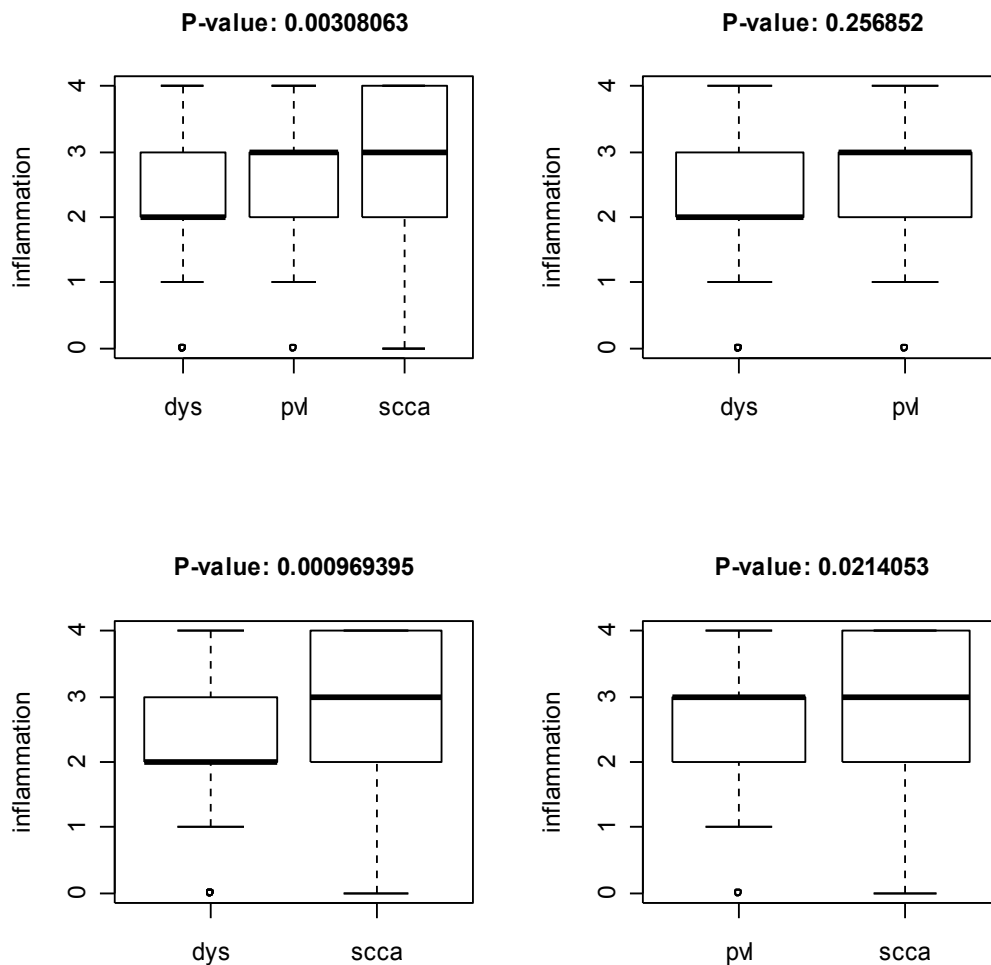
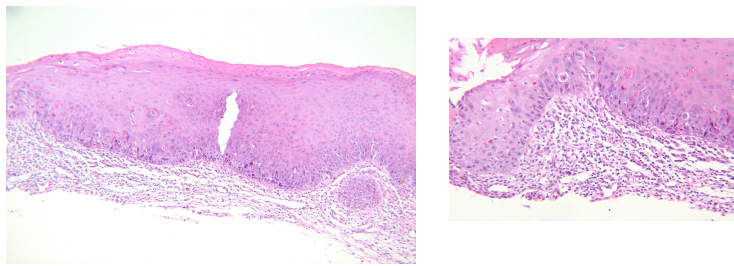


Figure 1.2 : Top left graph is a box-plot demonstrating the results Kruskal Wallis rank sum test comparing the levels of inflammation among the PVL, Oral SCC and OED groups. The other 3 figures so the results of the Wilcoxon rank sum test comparing types in pairs. Inflammation from dysplasia is significantly different from SCCA inflammation. PVL inflammation is also significantly different from that of SCCA at the 5% level of significance but is less so than when comparing dysplasia and SCCA.

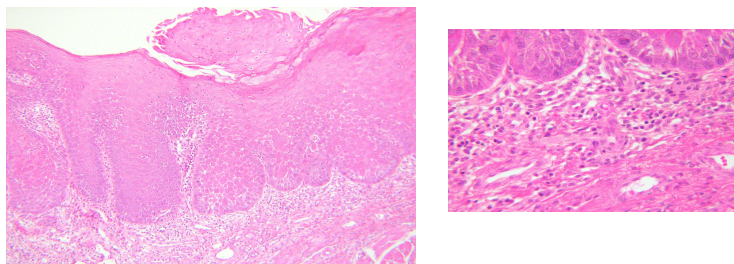
The level of inflammatory infiltrate increases as the severity of dysplasia increases in OED and PVL and as the grade on the modified Hansen scale for PVL increases.

Analysis of the inflammatory infiltrate within-group scores demonstrates that in the OED group, as the grade of dysplasia increases from mild, moderate, severe and carcinoma-in situ (CIS), the level of infiltrate increases (p=0.0014, Kruskal Wallis rank sum test). Figure 1.3 represents typical OED graded as mild,

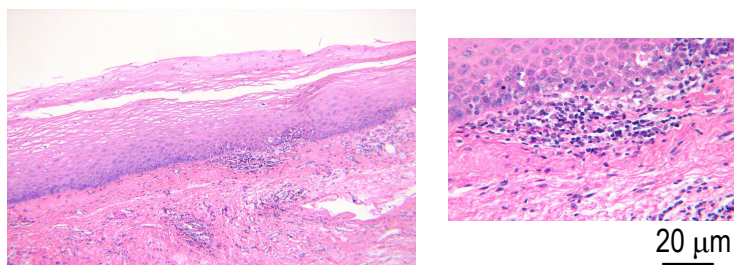
moderate and severe and the increasing inflammatory infiltrates associated with each increasingly severe lesion.



Severe Dysplasia – Severe Infiltrate



Moderate Dysplasia – Moderate Infiltrate



100 μ m
10x

Mild Dysplasia – Mild Infiltrate

20 μ m
20x

Figure 1.3. Increasingly severe levels of OED are associated with increasing levels of inflammatory infiltrate.

This relationship becomes even more statistically significant if the analysis is done excluding CIS ($p=0.0005$, Kruskal Wallis rank sum test) (Figure 1.4). In a similar manner, as the grade of PVL increases from hyperkeratosis, verruciform hyperkeratosis, verrucous hyperplasia, verrucous carcinoma and Oral SCC, so does the level of infiltrate increase ($p=3.98 \times 10^{-5}$, Kruskal Wallis rank sum test) (Figure 1.5). Further, for PVL lesions that have dysplasia within them, there is a statistically significant increase in the inflammatory infiltrate as the level of

dysplasia increases from none, mild, moderate and severe ($p=0.02$, Kruskal Wallis rank sum test) (Figure 1.6). This relationship is less significant than between PVL grades and infiltrate. Lastly, Figure 1.7 demonstrates that there is no statistical difference in the level of stromal infiltrate among Oral SCCs from lesions graded as poorly, moderately or well differentiated.

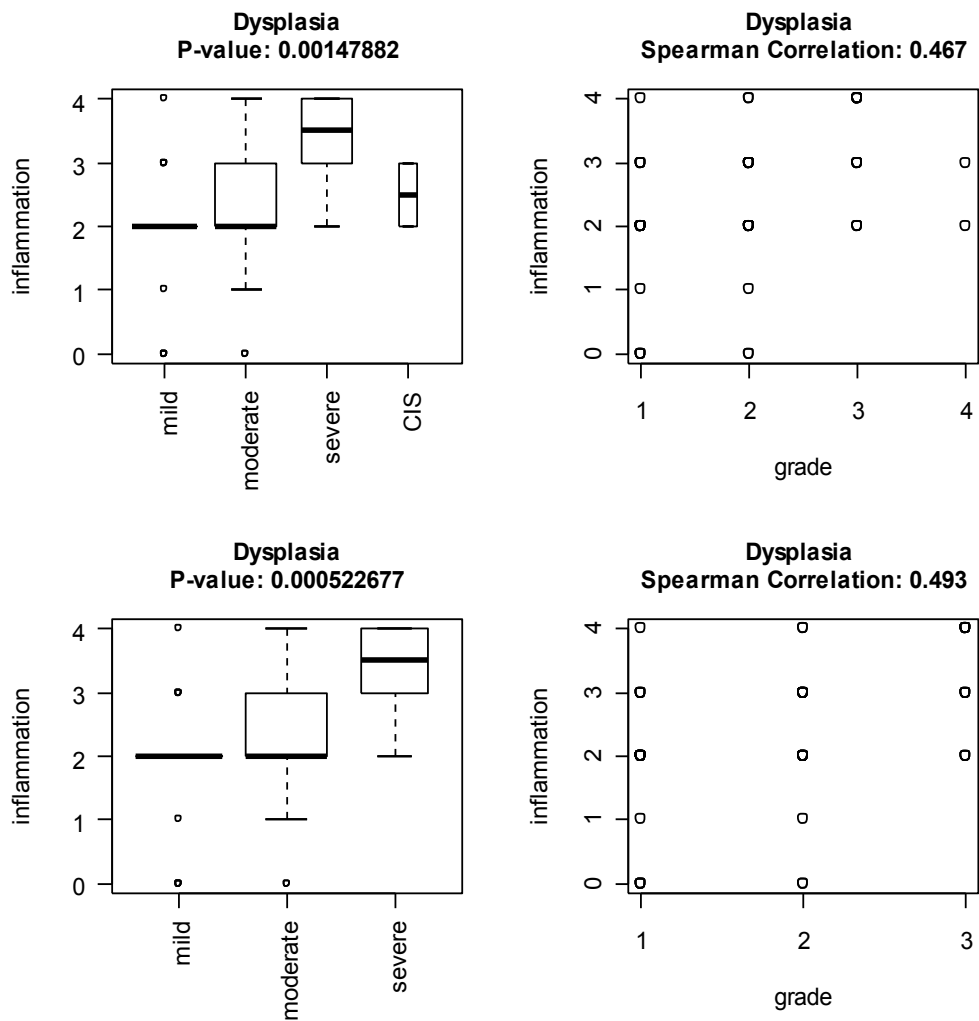


Figure 1.4. The boxplots are derived from the Kruskal Wallis rank sum test, testing for differences in inflammatory infiltrate within the dysplasia group at increasing severity of dysplasia. The top 2 figures and corresponding statistics consider all dysplasia samples while the bottom 2 figures/statistics exclude the 2 CIS cases. Note that the significance and correlation increases when the CIS samples are excluded.

The correlation between grade severity and inflammation level is positive, as expected.

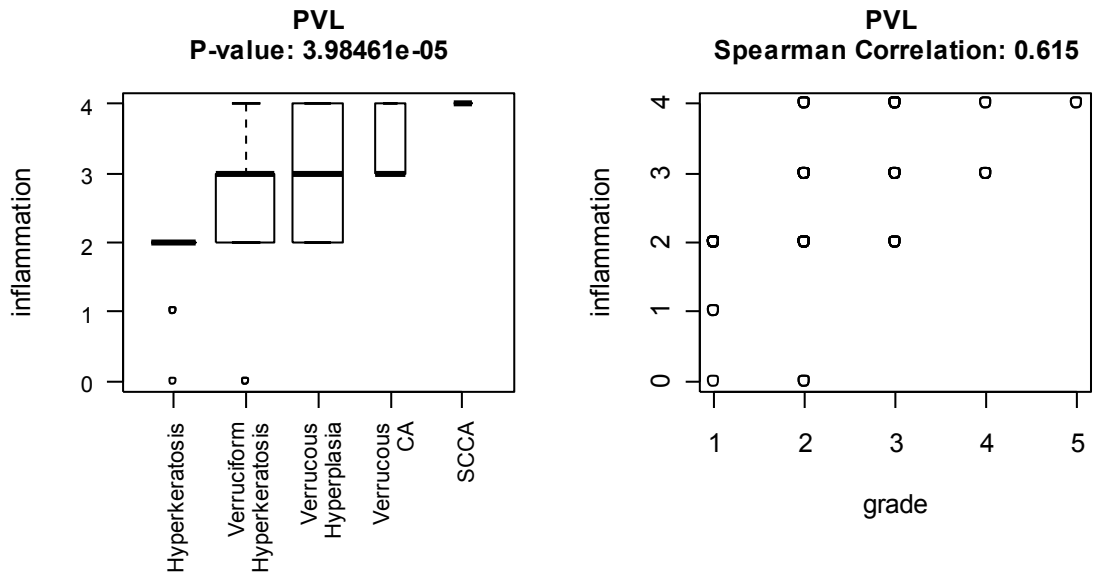


Figure 1.5. The p-values below are boxplots from Kruskal Wallis rank sum tests. There is significant association of inflammation with grade within PVLs and they have a positive correlation.

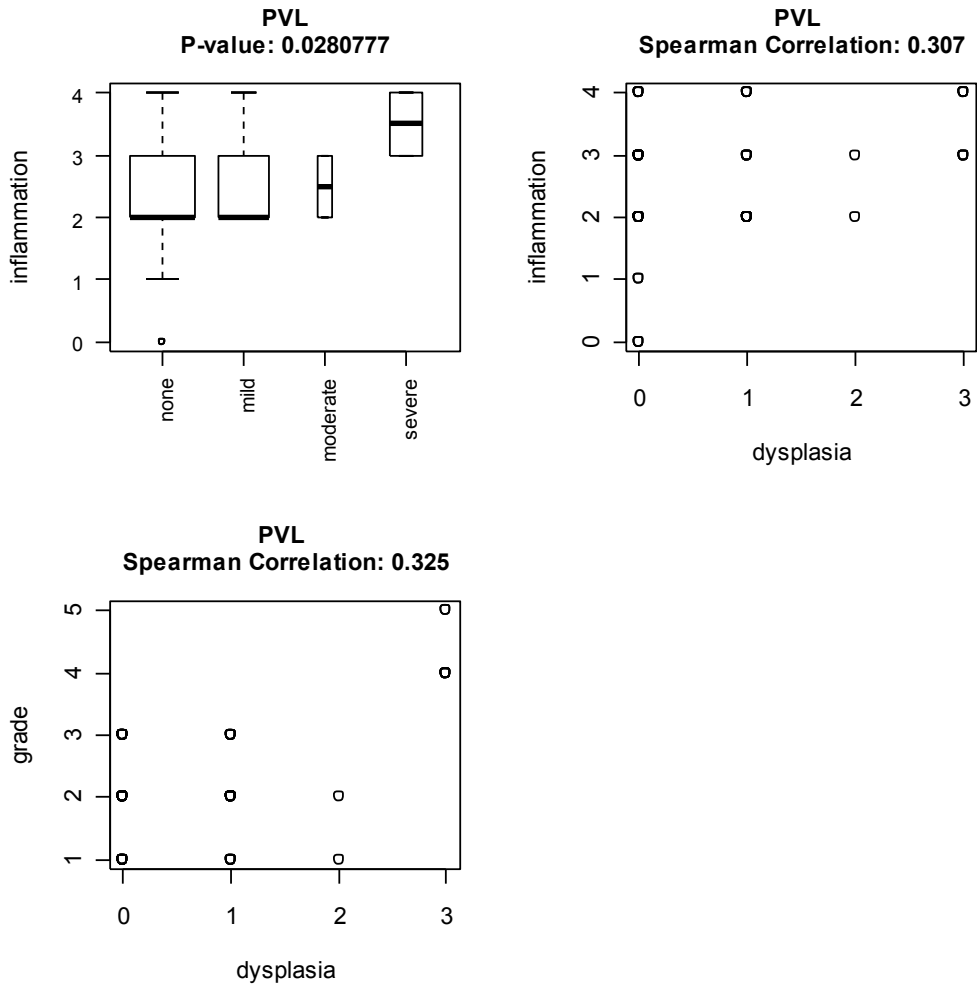


Figure 1.6. The p-values below are from Kruskal Wallis rank sum tests. Among PVLs, there is significant association of inflammation with dysplasia but the association is less significant than that between inflammation and grade.

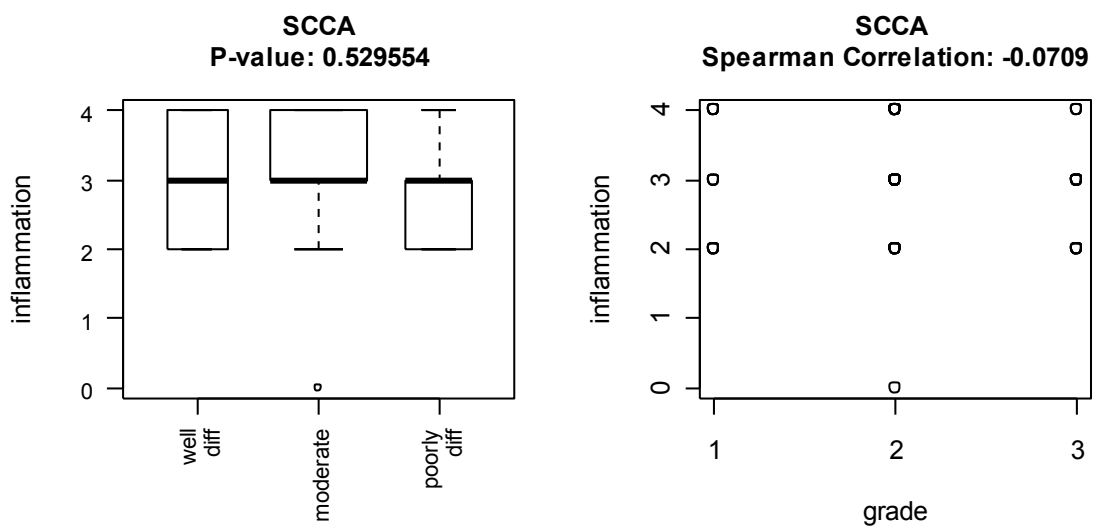


Figure 1.7. There is no significant association of inflammation with grade within Oral SCCs.

Discussion.

The data presented in this chapter are consistent with the previously described characteristics of PVL in that the majority of the patients in the chart review were females and the even distribution of sites confirms a multifocal lesion with the high number of pathology reports associated with a previous biopsy suggesting a highly recurrent lesion. Such characteristics suggest a dysfunction not necessarily of the epithelial cells but elements of the stroma, this is in contrast to OED, which typically develops in one location and has a relatively low recurrence rate after excision, indicating that removal of the dysfunctional epithelium is the critical step, whereas in PVL this is usually not sufficient to obtain a cure, signaling a problem with the soil rather than just the seed^{11,12}. Further, analogous to lichen planus where there is an underlying dysfunction of the immune response producing a multifocal recurrent lesion of varied clinical presentation (from white lacey superficial lesions to red angry erosive lesions), PVL may also represent a similar abnormality of the underlying stromal processes. The results of this chapter, which demonstrate that as the grade of PVL lesion increases (hyperkeratosis, verruciform hyperkeratosis, verrucous hyperplasia *etc.*) the level of the inflammatory infiltrate increases are in agreement with this hypothesis and might indicate a dysfunction of the immune system as being the underlying pathological driver.

This relationship between the lesion and stromal infiltrate, however, is also present in OED, as the severity of dysplasia increases from mild, moderate, to

severe so does the level of infiltrate. OED has a much different clinical presentation than PVL, as stated it occurs in males of late-middle age with a strong history of smoking and drinking and has a much lower transformation rate of around 16%. Thus, it is difficult to conclude that the pathogenesis of PVL is exactly analogous to lichen planus given that both types of lesions, PVL and OED are associated with increasingly severe inflammatory infiltrates. The opposing possibility is that the lesion, itself, is solely responsible for attracting a normally functioning inflammatory infiltrate to an unaltered stroma and as a the PVL becomes increasingly severe it produces more chemotactic/stimulatory mediators drawing in more inflammatory cells in the manner characteristic of a normal immune response to antigenic stimulation. There are tumor antigens specific to Oral SCC, the MAGE cancer testis antigens, which could be responsible for such an immune response¹³. Alternatively, as a combination of the individual epithelial and stromal pathogenic mechanisms, there may be a reciprocal, co-evolving relationship that exists between the preneoplasia and the associated stroma and depending on how this interaction evolves, will dictate the aggressiveness of a specific lesion. Work by several authors supports such a proposal, where the stroma actually develops a specific phenotype or polarization in the presence of a lesion and that stromal phenotypes can become polarized to be either tumor rejecting or tumor promoting depending on the mediators produced in the tumor microenvironment¹⁴. Further, the stromal phenotype is a reflection of the phenotype of the cellular constituents including lymphocytes, macrophages, and mast cells.

Previous authors have investigated the relationship of the inflammatory infiltrate with varying severities of oral lesions. Similar to our study results, Gannot *et al.* observed an increasing level of infiltrate in the series of lesions they studied from hyperkeratosis, OED to Oral SCC¹⁵. The cell types included T helper cells, T cytotoxic cells, monocytes/macrophages, B cells and other antigen presenting cells, which all displayed increased numbers as the severity of the lesions worsened. A specific characterization of cell type and phenotypic polarization (as mentioned above) in the specimens examined in our series of PVL lesions may help to clarify which cells are more important in guiding the progression of a preneoplasia and the surrounding microenvironment.

Lastly, The literature that investigates the role of the infiltrate in carcinoma development and progression seems to largely ignore the role of the cell type that is the central controller of the stroma, the fibroblast. The influence the fibroblast has on the stroma is clear when one examines the mechanisms of wound healing and observes that fibroblast defects greatly affect this process¹⁶. The subject of the following chapters will investigate the role of the fibroblast and its tumor associated counterpart the carcinoma-associated fibroblast (CAF) and how this central stromal controller influences the cancer microenvironment.

Chapter 2: Derivation of Oral Fibroblast Strains from Human Surgical Specimens.

Introduction.

The 5-year survival rate for oral squamous cell carcinoma has remained at less than 50% for decades now despite surgical and scientific advances. It is well established that oral squamous cell carcinoma is the result of oncologic genetic alterations within the epithelial layers of the oral mucosa¹⁷. However, it is becoming increasingly evident, even from the early dysplastic stage that the underlying stroma has an important role to play in tumorigenesis^{18,19}. Through reciprocal interactions between tumour and tumour stroma, a carcinoma-associated microenvironment (CAM) is generated with cellular, extra-cellular components and signalling systems having the effect of phenotypically altering the CAM to be either tumour promoting or tumour inhibiting, as suggested in the previous chapter. Thus it becomes important to understand the elements of the CAM and how their individual phenotypes can contribute to the global phenotype. One approach is to develop primary cell cultures of the cell types found in the tumour microenvironment to allow for specific cell characterization and functional analysis.

The tumour and CAM consists of many cell types. Including resident elements such as tumour cells, fibroblasts, endothelial cells, mesenchymal cells, neuronal elements, lymphatic elements, mast cells, eosinophils and other antigen presenting cells such as Langerhans's cells, additionally, there are transient, invading elements such as T and B lymphocytes, neutrophils and macrophages as well as bone marrow-derived stem cells. Many of these cell types have been shown to exist in varying phenotypic states in the CAM, which itself has been shown to be either tumour promoting or inhibiting. Studies of tumour-associated

macrophages illustrate the interconnectedness between the tumour and stromal elements. Tumours and their CAMs produce chemokines such as MCP, M-CSF and VEGF, which serve to recruit macrophages and promote their survival and TGF β , which promotes macrophage differentiation. The macrophage in turn produces growth factors, TNF, nitric oxide, matrix metalloproteinases, TGF β , VEGF, FGF2 which increase tumour cell proliferation and survival, progression and metastasis, matrix remodelling and angiogenesis²⁰. The most generic classification of the polarized macrophage is between the M1 macrophages which develops in the presence of IFN- γ , LPS and the M2 macrophages which arise due to CSF-1, IL-4, IL-13, IL-10 and immunocomplexes associated with either IL-1R or TLR ligands. The M1 macrophage is an inflammatory actor producing reactive oxygen species, IL-1, TNF, IL-6, presents MHC I on the surface and is polarized towards the affect of tumour eradication. Conversely, the M2 macrophage is a tissue reparative cell type, making polyamine, TGF β , IL-10 and presenting MHC II on the cells surface, contributing to its protumoral characteristics²¹. A similar phenotypic delineation is emerging for the carcinoma-associated fibroblast (CAF). The CAF is an activated fibroblast analogous to the myofibroblast, which is a central player in the wound healing process. Both are characterized by expression of α -smooth muscle actin (α -SMA). The presence of α -SMA expressing fibroblasts in the CAM is positively correlated to poor clinical outcomes in a variety of tumour types, including oral squamous cell carcinoma^{22,23}. Despite this, our understanding of CAF biology is limited, especially regarding the existence of either protumoral or antitumoral subgroups as has been described for the macrophage. Thus, it is important to be

able to isolate and propagate individual fibroblast cell strains in order to understand their influence on the CAM and tumorogenesis more completely.

Isolating animal cells and propagating them outside of the body was first credited to Roux in 1885. In 1961, Hayflick and Moorhead reported that a cell type called a fibroblast divides only a finite number of times when removed from the body and placed in a cell culture system²⁴. More contemporary investigators have gone on to describe the successful cultivation of not only fibroblast cell cultures but also keratinocyte and tumour cell cultures. The purpose of this chapter is to detail the techniques our laboratory used to derive the cellular components that principally comprise the epidermis and dermis, the keratinocyte and fibroblast, respectively. Further, this chapter will analyse the success rates of each individual attempted cell strain based on cell type, anatomic site, age, sex and technician experience. It is hoped that this knowledge will increase the success rates of cell strain derivation in the future for studies investigating the effect of the CAFs on tumorogenesis. An additional application of this information is apparent based on the relatively recent advent of tissue engineering used to repair oral defects that arise as a result of the surgical treatment of oral squamous cell carcinoma. Utilization of this knowledge may contribute to more physiologically compatible organogenesis and the generation of functional tissue that have a greater chance of being able to more faithfully restore a patient's original anatomy.

Methods.

Establishment of primary keratinocyte and fibroblast cell cultures

Human oral tissues were obtained from patients undergoing routine oral surgical procedures at the University of California San Francisco Dental Clinic, the Oral Surgery Department at the Veteran's Affairs Medical Center in San Francisco and the Oncologic Service at the University of California San Francisco Department of Oral and Maxillofacial Surgery. Patients were consented and ranged in age from 17 to 85. Each tissue specimen was given an anonymous code for sample identification purposes and a patient specific identifier. A clinical information database was created and stored at an encrypted, password protected server location.

Generally, the anatomic derivation and the tissue type of the specimens depended on the primary procedure and are as follows. Normal gingival samples were taken from non-cancer patients undergoing routine dentoalveolar procedures, most often tooth extractions. Gingival tissues were harvested immediately adjacent to the extraction site and included all of the tissue from the base of the gingival sulcus, the free gingiva or marginal gingiva, the attached keratinized gingiva and varying amounts of un-attached gingiva past the mucogingival junction. The entire thickness of the tissue was harvested. In cases where a completely impacted third molar was extracted then the tissue immediately adjacent and distal to the second molar was taken. Gingival samples were also taken from patients undergoing carcinoma resections. In those cases, carcinoma-associated gingiva was harvested immediately adjacent to and often including the primary tumour and clinically normal gingival tissue was

harvested from the same patient at a site away from the primary tumour. Tongue samples were most often derived from patients undergoing carcinoma resection. As with the gingival samples, a specimen was taken from tissue immediately adjacent to and/or containing the tongue tumour and one taken from a clinically normal area at some distance away from the tumour. Two tongue samples not associated with a carcinoma resection were the source of the fibroblast (OF) and keratinocyte (OK) strains 107 and 118 (OF/OK107 and OF/OK118). The first (OF/OK107) included tissue from the dorsal tongue and the second (OF/OK118) was from the lateral tongue. Buccal and floor-of-mouth mucosal specimens were submitted with the majority originating from patients undergoing mandibular vestibuloplasties, a procedure designed to lower the floor-of-mouth and buccal vestibule to assist in prosthesis fabrication. There were also buccal and floor-of-mouth specimens that were derived from carcinoma resections. As with the tongue and gingival samples, tissue was taken from the center of a tumour and normal tissue was taken from a clinically normal site away from the primary tumour.

Once harvested, tissue specimens were transported from the operatory suite in a 15 ml tube with 10 ml of media containing standard DME H-16 with gentamycin (50 µg/ml) or a Pen/Strep solution containing 100 units/ml of penicillin and 100 µg/ml of streptomycin and fungizone (2.5 µg/ml). All antimicrobials were obtained from the University of California San Francisco Cell Culture Facility. Once in the laboratory, tissue specimens were placed at 4° C until further processing. The time period from patient to laboratory was variable but

averaged approximately 3 hours, with the minimum time being 1 hour and the maximal time approaching 5 hours.

Further processing of the tissues then proceeded as follows. Oral tissues were incubated in 5 ml of 70% ethanol for five minutes, and then rinsed in 5 ml Hank's balanced salt solution (University of California San Francisco Cell Culture Facility). Using a #11 scalpel, the tissue was cut into small pieces (~ 0.25 cm²) and placed in 4 ml of dispase solution (4.8 mg/ml in PBS, Roche) supplemented with gentamycin (50 µg/ml). After an overnight incubation at 4° C, the epidermis was separated from the dermis by holding the dermis in place in a sterile dish using one scalpel and sliding the epidermis off using another scalpel.

Epidermal tissue was minced and incubated in 3 ml 0.25% trypsin in 0.02% EDTA at 37° C for five minutes, after which time 10 ml of a soy bean trypsin inhibitor solution (250 mg/L, Roche) in PBS was added. To further dissociate the cells, the mixture was pipetted up and down vigorously approximately 20 times using a glass pipette. The epidermal keratinocytes were collected by centrifugation at 1000 rpm for 3 minutes in a 15 ml tube and ~50-200 µl of cells were placed in a T75 flask containing 10 ml of keratinocyte serum-free media (KSFM, Gibco, Invitrogen) supplemented with gentamycin (50 µg/ml) or Pen/Strep (100 units/ml and 100 µg/ml, respectively) and fungizone (2.5 µg/ml). Keratinocyte culture media was replaced every other day.

Antimicrobials were eventually omitted from the culture media by reducing the concentrations by one-half for each medium change over the course of 3-4 media changes.

Dermal tissue was minced and placed in 3 ml of collagenase type IA (Sigma) solution (1 mg/ml in DMEM) supplemented with gentamycin (50 µg/ml). After incubation overnight at room temperature, 20 ml of DME H-16 (University of California Cell Culture Facility) supplemented with 10% fetal calf serum (Gibco) was added and the mixture was pipetted up and down a number of times to further dissociate the cells. Fibroblasts were collected by centrifugation at 1500 rpm for 3 minutes and ~50-200 µl of cells were placed in a T75 flask containing 10 ml of DME H-16 supplemented with 10% fetal calf serum and gentamycin (50 µg/ml) or Pen/Strep (100 units/ml and 100 µg/ml, respectively) and fungizone (2.5 µg/ml). As with the keratinocyte cultures the antimicrobials were eventually omitted from the culture media by reducing the concentrations by one-half for each medium change over the course of 3-4 media changes.

Oral squamous cell carcinoma tissue was minced and a small piece (~0.25 cm²) was placed in each well of a 6-well plate with 1 ml of either keratinocyte serum-free media or 1 ml of DME H-16 supplemented with 10% fetal calf serum and gentamycin (50 µg/ml) or Pen/Strep and fungizone (2.5 µg/ml). The tissue was monitored on a daily basis and when a well had become populated with fibroblasts, 0.5 ml of 0.25 % trypsin in 0.02% EDTA (University of California San Francisco Cell Culture Facility) was added to the well which was placed in the incubator for five minutes to allow cells to detach and then 2 ml of DME H-16 supplemented with 10% fetal calf serum was added and centrifuged at 1000 rpm for 3 minutes in a 15 ml tube and ~50-200 µl of cells were placed in a T75 flask containing 10 ml of DME H-16 supplemented with 10% fetal calf serum and gentamycin (50 µg/ml) or Pen/Strep (100 units/ml and 100 µg/ml,

respectively) and fungizone (2.5 µg/ml). As with the keratinocyte cultures the antimicrobials were eventually omitted from the culture media by reducing the concentrations by one-half for each medium change over the course of 3-4 media changes.

Cell strains were maintained under normal culture conditions as described above. For passaging or freezing the cells, a 4 ml volume of 0.05% (for keratinocytes) or 0.25% trypsin (for fibroblasts) with 0.02% EDTA was placed in a T75 containing an adherent cell strain and put in the incubator for 5 minutes to allow cells to detach and then 6 ml of keratinocyte serum-free media or DME supplemented with 10% fetal calf serum was added. The cell suspensions were transferred from the T75 to a 15 ml tube and centrifuged at 1000 rpm for 3 minutes and then either the cells were placed back in additional T75 flasks with 10 ml of keratinocyte serum-free media or DME supplemented with 10% fetal calf serum for passaging or frozen in a 1 ml cryogenic vial (Corning) using 1 ml of cell culture preservation media (10% fetal calf serum and 10% DMSO) or keratinocyte serum-free preservation media (University of California San Francisco Cell Culture Facility). Cells were either temporarily stored at -80°C or more permanently stored in liquid nitrogen. To unfreeze a cell strain, a cryogenic vial containing the desired cell strain was thawed in a 37°C bath, the cell suspension was then placed in a 15 ml tube with 5 ml of keratinocyte serum-free media or DME supplemented with 10% fetal calf serum and spun down at 1000 rpm for 3 minutes, then ~50-200 µl of cells were placed in a T75 flask containing 10 ml of medium and cultured as appropriate for keratinocytes or fibroblasts as described above.

Results and Discussion.

Derivation of Human Oral Cavity Primary Keratinocyte and Fibroblast Cell Strains

Tissue specimens from volunteer patients undergoing oral surgical procedures were collected over a three-year time span. There were two categories of patients who participated in the study. The first were those who were undergoing an oncological resection of a primary oral cavity squamous cell carcinoma and the second, mainly were undergoing a tooth extraction or pre-prosthetic surgery. From the cancer resection group there was generally harvested a piece of the tumour itself, which was unimportant for either diagnostic or prognostic purposes or the evaluation of resection margins and a piece of anatomically equivalent, histologically non-tumour bearing tissue taken as far away from the primary tumour as surgically feasible. So, if for instance, a tongue squamous cell carcinoma was being resected, then a section of the resected tumor would be donated along with a piece of normal tongue tissue from the contralateral side, in the ideal situation. The non-ideal situation, such as in the case where there is a resection of a very large tumour with a complicated reconstructive plan, may preclude the harvesting of normal tissue at a significant distance from the margin of the tumour. From the tooth extraction group there was generally harvested a small piece of clinically normal tissue adjacent to the surgical site, the size and location of which the individual surgeon had determined would have no effect on normal post-operative healing. In the case of the tumour tissue, for all specimens an attempt was made to culture both the tumour cells and the fibroblasts from the tumour stroma. For the normal tissue from both patients with cancer and those undergoing tooth extractions, an

attempt was made to culture the keratinocytes from the mucosal layer and the fibroblasts from the dermal layer. Table 2.1 lists in detail the entirety of the cell strains that were attempted and the associated clinical, anatomical and histological information.

There was a total of 52 patients who participated in the study with approximately equal participation of males and females with their ages ranging from as young as 11 to as old as 85 with the median age being 61 (Table 2.2). Further, a total of 23 cancer patients and 28 tooth extraction patients donated tissue for which a total of 155 unique primary cell cultures were attempted from the tumour, tumour stroma, epidermal or dermal compartments. Of the 155 attempted cell cultures, 67 were successfully established and 88 were not successfully established. In this case, successfully established means that the cells under culture were able to grow to near confluency and have the ability to survive through multiple passages, although in future chapters low passage number cells were exclusively used. For the cell strains that were not successfully established, the cells either failed to grow, in which case they were classified as died, or they grew to some extent but the culture became dominated by microbes, despite the use of antimicrobials, and the cultures had to be discarded, these were classified as contaminated. Overall, in the cell strains which were unsuccessfully established, it was much more common that the failure was due to death or failure to establish a growing population of the cells rather than the issue being a problem with contamination. The reason for this is most likely the use of the cocktail of the three antimicrobials added to the media throughout the initial stages of the culture preparation. Further, for the cell

cultures that failed and were classified as died or dead there could be multiple reasons that led to such a result. One reason is the length of time the tissue specimen spends after resection or excision from the patient until it is placed in the collection media. If this time is extended then the tissue may dry out or become hypoxic and the cells within the specimen may simply die. This variable was mostly surgeon and situation dependent. For instance, cancer resections can be long procedures and obvious attention has to be paid to the surgical procedure at hand, which at times may result in a tissue specimen that has been separated from the patient and not placed in the collection media in a timely manner, resulting in decreased viability. On the other hand, in a relatively short tooth extraction procedure, the time from the patient to collection media is often less, presumably, resulting in greater viability. Other variables that may affect cell viability and culturability will be discussed below and in the following sections.

One of those possible variables that may affect the outcome of an attempted cell culture is the sex of the patient from which the tissue was derived. The results of the comparison of the male/female ratios of the cell strains that were successfully established versus those that were not (Figure 2.1 and Table 2.3) demonstrate that there was no statistically significant differences found within each group, leading to the conclusion that sex-dependent variables (hormones etc.) do not seem to contribute to the successful establishment of a primary cell strain.

Table 2.1 Characterization of the attempted primary human oral cavity cell strains. Each attempted cell strain is assigned a cell type identification (OF1, OK1...etc) based on cell type (keratinocyte versus fibroblast) and general order of tissue collection. A unique identification number was assigned to each patient to preserve patient confidentiality. Note that the patient identification number is often associated with multiple cell type identification numbers depending on the location of tissue specimens submitted. Tissue origin is the anatomical structure where the specimen was obtained and tissue site is the anatomical location, i.e. maxillary gingiva or mandibular gingiva. The histology column refers to the histological status of the specimen as verified by pathology report or clinical information. Age and sex of the patient associated with the attempted cell strain is listed. The procedure column describes the specific primary procedure performed allowing for the secondary donation of the tissue specimen. The established column simply lists whether the attempted cell strain was successfully established or not. If the cell strain was not successfully established, then the failure column describes why the culture did not succeed, either it died or was contaminated. The last two columns provide the percentage of vimentin and pancytokeratin staining in fibroblast cell strains using immunofluorescence, the fibroblasts which were not characterized in this manner are identified with a "na" – not available.

Cell Type	Patient ID#	Tissue origin	Site	Histology	Age	Sex	Procedure	Established?	Failure	Vimentin %	Pancytokeratin %
Tongue Fibroblasts	OF1	A001	TONGUE	ADJACENT TO MODERATE DYSPLASIA	43	M	SURGICAL RESECTION	YES		100	1.4
	OF6	B0031	TONGUE	ADJACENT TO SCC	63	M	SURGICAL RESECTION	YES		100	0.3
	OF7	B0044	TONGUE	ADJACENT TO SCC	76	M	SURGICAL RESECTION	NO	DIED		
	OF8	B0042	TONGUE	ADJACENT TO SCC	37	M	SURGICAL RESECTION	YES		100	0.4
	OF51	B000A	TONGUE	ADJACENT TO SCC	56	M	SURGICAL RESECTION	YES		100	0
	OF54	B000B	TONGUE	ADJACENT TO SCC	30	M	SURGICAL RESECTION	NO	CONTAM		
	OF56	B000C	TONGUE	ADJACENT TO SCC	56	M	SURGICAL RESECTION	NO	DIED		
	OF59	B000D	TONGUE	ADJACENT TO SCC	24	M	SURGICAL RESECTION	YES		100	0
	OF78	B0072	TONGUE	ADJACENT TO SCC	60	F	SURGICAL RESECTION	YES		100	1.6
	OF82	B0074	TONGUE	ADJACENT TO SCC	66	F	SURGICAL RESECTION	YES		100	0
	OF84	B0077	TONGUE	ADJACENT TO SCC	71	F	SURGICAL RESECTION	YES		100	0
	OF100	B0082	TONGUE	ADJACENT TO SCC	65	F	SURGICAL RESECTION	YES		100	0
	OF107	T002	TONGUE	NORMAL	61	M	SURGICAL EXCISION	YES		100	2.44
	OF113	B0089	TONGUE	ADJACENT TO SCC	85	F	SURGICAL EXCISION	NO	DIED		
	OF115	B0090	TONGUE	ADJACENT TO SCC	54	M	SURGICAL EXCISION	YES		100	0
	OF117	SW001	TONGUE	ADJACENT TO SCC	61	M	SURGICAL EXCISION	YES		100	na
	OF118	T031	TONGUE	NORMAL	63	M	BIOPSY	NO	DIED		
	Tongue Keratinocytes	OK1	A001	TONGUE	ADJACENT TO MODERATE DYSPLASIA	43	M	SURGICAL RESECTION	YES		
OK6		B0031	TONGUE	ADJACENT TO SCC	63	M	SURGICAL RESECTION	YES			
OF7		B0044	TONGUE	ADJACENT TO SCC	76	M	SURGICAL RESECTION	NO	DIED		
OK8		B0042	TONGUE	ADJACENT TO SCC	37	M	SURGICAL RESECTION	NO	CONTAM		
OK51		B000A	TONGUE	ADJACENT TO SCC	56	M	SURGICAL RESECTION	NO	CONTAM		
OK54		B000B	TONGUE	ADJACENT TO SCC	30	M	SURGICAL RESECTION	NO	DIED		
OK56		B000C	TONGUE	ADJACENT TO SCC	56	M	SURGICAL RESECTION	NO	DIED		
OK59		B000D	TONGUE	ADJACENT TO SCC	24	M	SURGICAL RESECTION	NO	DIED		
OK78		B0072	TONGUE	ADJACENT TO SCC	60	F	SURGICAL RESECTION	NO	DIED		
OK82		B0074	TONGUE	ADJACENT TO SCC	66	F	SURGICAL RESECTION	NO	DIED		

OK84	B0077	TONGUE	TONGUE	ADJACENT TO SCC	71	F	SURGICAL RESECTION	NO	DIED
OK100	B0082	TONGUE	TONGUE	ADJACENT TO SCC	65	F	SURGICAL RESECTION	NO	DIED
OK107	T002	TONGUE	TONGUE	NORMAL	61	M	SURGICAL EXCISION	NO	DIED
OK113	B0089	TONGUE	TONGUE	ADJACENT TO SCC	85	F	SURGICAL EXCISION	NO	DIED
OK115	B0090	TONGUE	TONGUE	ADJACENT TO SCC	54	M	SURGICAL EXCISION	NO	DIED
OK117	SW001	TONGUE	TONGUE	ADJACENT TO SCC	61	M	SURGICAL EXCISION	YES	
OK118	T031	TONGUE	TONGUE	NORMAL	63	M	BIOPSY	YES	
OF2	A002	GINGIVA	MAXILLA	NORMAL	27	M	WISDOM TOOTH EXTRACTION	YES	na
OF3	A003	GINGIVA	MANDIBLE	NORMAL	29	F	WISDOM TOOTH EXTRACTION	NO	DIED
OF5R	A005	GINGIVA	MANDIBLE	PVL	62	M	PVL EXCISION	NO	DIED
OF5L	A005	GINGIVA	MANDIBLE	PVL	62	M	PVL EXCISION	NO	DIED
OF35	T004	GINGIVA	MAXILLA	NORMAL	29	F	WISDOM TOOTH EXTRACTION	YES	100
OF37	T006	GINGIVA	MANDIBLE	NORMAL	37	M	WISDOM TOOTH EXTRACTION	YES	na
OF38	T007	GINGIVA	MANDIBLE	NORMAL	21	F	WISDOM TOOTH EXTRACTION	NO	DIED
OF39	T008	GINGIVA	MAXILLA	NORMAL	11	F	WISDOM TOOTH EXTRACTION	NO	CONTAM
OF40	T009	GINGIVA	MANDIBLE	NORMAL	41	F	WISDOM TOOTH EXTRACTION	YES	100
OF41	T010	GINGIVA	MAXILLA	NORMAL	61	F	WISDOM TOOTH EXTRACTION	NO	DIED
OF42	T011	GINGIVA	MAXILLA	NORMAL	85	M	TOOTH EXTRACTIONS	YES	na
OF43A	T012	A-GINGIVA	MANDIBLE	NORMAL	31	F	WISDOM TOOTH EXTRACTION	NO	DIED
OF43B	T012	UN-GINGIVA	MANDIBLE	NORMAL	31	F	WISDOM TOOTH EXTRACTION	NO	DIED
OF44	T014	GINGIVA	MANDIBLE	NORMAL	34	F	WISDOM TOOTH EXTRACTION	YES	100
OF45	T015	GINGIVA	MANDIBLE	NORMAL	82	F	IMPLANT UNCOVERING	NO	DIED
OF46	T016	GINGIVA	MANDIBLE	NORMAL	68	M	TOOTH EXTRACTION #18	NO	DIED
OF47	T017	GINGIVA	MAXILLA	NORMAL	26	M	WISDOM TOOTH EXTRACTION	YES	100
OF47	T017	GINGIVA	MAXILLA	ADJACENT TO PVL	71	F	PVL EXCISION	NO	DIED
HN110	B0001	GINGIVA	MANDIBLE	ADJACENT TO SCC	63	M	SURGICAL RESECTION	YES	100
OF5gingiva	B0031	GINGIVA	MAXILLA	NORMAL	53	F	EXTRACTION MAXILLARY MOLAR	YES	100
OF49	T018	GINGIVA	MAXILLA	NORMAL	68	M	WISDOM TOOTH EXTRACTION	YES	100
OF50	T019	GINGIVA	MAXILLA	NORMAL	78	M	FULL MOUTH EXTRACTION	YES	na
OF63	T029	GINGIVA	MAXILLA	ADJACENT TO SCC	84	F	SURGICAL RESECTION	YES	100
OF66	B0058	GINGIVA	MAXILLA	ADJACENT TO SCC	64	M	TOOTH EXTRACTION #30	YES	na
OF105	T001	GINGIVA	MANDIBLE	NORMAL	64	M	TOOTH EXTRACTION #2	YES	na
OF106	T001	GINGIVA	MAXILLA	NORMAL	64	M	TOOTH EXTRACTION #2	YES	na
OF110	T003	GINGIVA	MANDIBLE	NORMAL	72	M	TOOTH EXTRACTION #14	YES	na
OK2	A002	GINGIVA	MAXILLA	NORMAL	27	M	WISDOM TOOTH EXTRACTION	YES	
OK3	A003	GINGIVA	MANDIBLE	NORMAL	29	F	WISDOM TOOTH EXTRACTION	NO	DIED
OK5R	A005	GINGIVA	MANDIBLE	PVL	62	M	PVL EXCISION	NO	DIED

Gingival

Fibroblasts

Gingival

Keratinocytes

OK5L	A005	GINGIVA	MANDIBLE	PVL	62	M		PVL EXCISION	NO	DIED
OK35	T004	GINGIVA	MAXILLA	NORMAL	29	F		WISDOM TOOTH EXTRACTION	NO	DIED
OK37	T006	GINGIVA	MANDIBLE	NORMAL	37	M		WISDOM TOOTH EXTRACTION	NO	DIED
OK38	T007	GINGIVA	MANDIBLE	NORMAL	21	F		WISDOM TOOTH EXTRACTION	YES	
OK39	T008	GINGIVA	MAXILLA	NORMAL	11	F		WISDOM TOOTH EXTRACTION	NO	CONTAM
OK40	T009	GINGIVA	MANDIBLE	NORMAL	41	F		WISDOM TOOTH EXTRACTION	NO	DIED
OK41	T010	GINGIVA	MAXILLA	NORMAL	61	F		WISDOM TOOTH EXTRACTION	NO	DIED
OK42	T011	GINGIVA	MAXILLA	NORMAL	85	M		TOOTH EXTRACTIONS	NO	CONTAM
OK43A	T012	A-GINGIVA	MANDIBLE	NORMAL	31	F		WISDOM TOOTH EXTRACTION	NO	DIED
OK43B	T012	UN-GINGIVA	MANDIBLE	NORMAL	31	F		WISDOM TOOTH EXTRACTION	NO	DIED
OK44	T014	GINGIVA	MANDIBLE	NORMAL	34	F		WISDOM TOOTH EXTRACTION	NO	DIED
OK45	T015	GINGIVA	MANDIBLE	NORMAL	82	F		IMPLANT UNCOVERING	NO	DIED
OK46	T016	GINGIVA	MANDIBLE	NORMAL	68	M		TOOTH EXTRACTION #2	YES	
OK47	T017	GINGIVA	MAXILLA	NORMAL	26	M		WISDOM TOOTH EXTRACTION	NO	DIED
HN110	B0001	GINGIVA	MAXILLA	ADJACENT TO PVL	71	F		PVL EXCISION	NO	DIED
OK49	T018	GINGIVA	MAXILLA	NORMAL	53	F		EXTRACTION MAXILLARY MOLAR	NO	DIED
OK50	T019	GINGIVA	MAXILLA	NORMAL	68	M		WISDOM TOOTH EXTRACTION	YES	
OKgingiva	B0031	GINGIVA	MANDIBLE	ADJACENT TO SCC	63	M		SURGICAL RESECTION	YES	
OK63	T029	GINGIVA	MAXILLA	NORMAL	78	M		FULL MOUTH EXTRACTION	NO	DIED
OK66	B0058	GINGIVA	MAXILLA	ADJACENT TO SCC	84	F		SURGICAL RESECTION	NO	DIED
OK105	T001	GINGIVA	MANDIBLE	NORMAL	64	M		TOOTH EXTRACTION #30	NO	CONTAM
OK106	T001	GINGIVA	MAXILLA	NORMAL	64	M		TOOTH EXTRACTION #2	NO	CONTAM
OK110	T003	GINGIVA	MANDIBLE	NORMAL	72	M		TOOTH EXTRACTION #14	NO	DIED
Of4B	A004	BUCCAL	BUCCAL	DYSPLASIA	49	M		SURGICAL RESECTION	NO	DIED
Of4S	A004	BUCCAL	BUCCAL	DYSPLASIA	49	M		SURGICAL RESECTION	NO	DIED
Of36	T005	BUCCAL	MAXILLA	NORMAL	17	M		ORTHOGNATHIC SURGERY	YES	na
Of48	B0043	BUCCAL	MAXILLA	SCAR	47	M		SCAR REVISION	YES	na
Of48A	B0043	BUCCAL	MAXILLA	ADJACENT TO SCAR	47	M		SCAR REVISION	YES	na
Of58	T026	BUCCAL	BUCCAL	NORMAL	83	M		VESTIBULOPLASTY	NO	DIED
Of62	T028	BUCCAL	BUCCAL	NORMAL	62	M		VESTIBULOPLASTY	NO	DIED
Of64	T029	BUCCAL	BUCCAL	NORMAL	78	M		VESTIBULOPLASTY	YES	na
Of6buccal	B0031	BUCCAL	MANDIBLE	ADJACENT TO SCC	63	M		SURGICAL RESECTION	NO	DIED
Of69	B0064	BUCCAL	BUCCAL	PVL	80	F		SURGICAL RESECTION	NO	DIED
Of70	B0064	BUCCAL	BUCCAL	ADJACENT TO PVL	80	F		SURGICAL RESECTION	NO	DIED
Of74	B0065	BUCCAL	BUCCAL	ADJACENT TO SCC	76	F		SURGICAL RESECTION	NO	DIED
Of75	B0070	BUCCAL	BUCCAL	ADJACENT TO SCC	60	F		SURGICAL RESECTION	YES	na

**Buccal
Fibroblasts**

OF80	B0073	BUCCAL	BUCCAL	BUCCAL	BUCCAL	ADJACENT TO SCC	63	M	SURGICAL RESECTION	YES	na	na
OF98	B0081	BUCCAL	BUCCAL	BUCCAL	BUCCAL	ADJACENT TO SCC	84	F	SURGICAL RESECTION	YES	na	na
OF102	B0084	BUCCAL	BUCCAL	BUCCAL	BUCCAL	ADJACENT TO SCC	66	M	SURGICAL RESECTION	YES	100	1.2
OF104	B0085	BUCCAL	BUCCAL	BUCCAL	BUCCAL	ADJACENT TO SCC	53	F	SURGICAL RESECTION	YES	100	na
OF109	B0087	BUCCAL	BUCCAL	BUCCAL	BUCCAL	ADJACENT TO SCC	58	F	SURGICAL RESECTION	YES	100	0
OF111	T003	BUCCAL	BUCCAL	BUCCAL	BUCCAL	NORMAL	72	M	TOOTH EXTRACTION	YES	100	0
OK4B	A004	BUCCAL	BUCCAL	BUCCAL	BUCCAL	DYSPLASIA	49	M	SURGICAL RESECTION	YES		
OK4S	A004	BUCCAL	BUCCAL	BUCCAL	BUCCAL	DYSPLASIA	49	M	SURGICAL RESECTION	NO	DIED	
OK36	T005	BUCCAL	BUCCAL	MAXILLA	BUCCAL	NORMAL	17	M	ORTHOGNATHIC SURGERY	NO	DIED	
OK6buccal	B0031	BUCCAL	BUCCAL	MANDIBLE	BUCCAL	ADJACENT TO SCC	63	M	SURGICAL RESECTION	YES		
OK48	B0043	BUCCAL	BUCCAL	MAXILLA	BUCCAL	SCAR	47	M	SCAR REVISION	YES		
OK48A	B0043	BUCCAL	BUCCAL	MAXILLA	BUCCAL	ADJACENT TO SCAR	47	M	SCAR REVISION	YES		
OK58	T026	BUCCAL	BUCCAL	BUCCAL	BUCCAL	NORMAL	83	M	VESTIBULOPLASTY	NO	DIED	
OK62	T028	BUCCAL	BUCCAL	BUCCAL	BUCCAL	NORMAL	62	M	VESTIBULOPLASTY	NO	DIED	
OK64	T029	BUCCAL	BUCCAL	BUCCAL	BUCCAL	NORMAL	78	M	VESTIBULOPLASTY	NO	DIED	
OK69	B0064	BUCCAL	BUCCAL	BUCCAL	BUCCAL	PVL	80	F	SURGICAL RESECTION	NO	DIED	
OK70	B0064	BUCCAL	BUCCAL	BUCCAL	BUCCAL	ADJACENT TO PVL	80	F	SURGICAL RESECTION	NO	DIED	
OK74	B0065	BUCCAL	BUCCAL	BUCCAL	BUCCAL	ADJACENT TO SCC	76	F	SURGICAL RESECTION	NO	DIED	
OK75	B0070	BUCCAL	BUCCAL	BUCCAL	BUCCAL	ADJACENT TO SCC	60	F	SURGICAL RESECTION	NO	DIED	
OK80	B0073	BUCCAL	BUCCAL	BUCCAL	BUCCAL	ADJACENT TO SCC	63	M	SURGICAL RESECTION	NO	DIED	
OK98	B0081	BUCCAL	BUCCAL	BUCCAL	BUCCAL	ADJACENT TO SCC	84	F	SURGICAL RESECTION	NO	DIED	
OK102	B0084	BUCCAL	BUCCAL	BUCCAL	BUCCAL	ADJACENT TO SCC	66	M	SURGICAL RESECTION	NO	DIED	
OK104	B0085	BUCCAL	BUCCAL	BUCCAL	BUCCAL	ADJACENT TO SCC	53	F	SURGICAL RESECTION	NO	DIED	
OK109	B0087	BUCCAL	BUCCAL	BUCCAL	BUCCAL	ADJACENT TO SCC	58	F	SURGICAL RESECTION	NO	DIED	
OK111	T003	BUCCAL	BUCCAL	BUCCAL	BUCCAL	NORMAL	72	M	TOOTH EXTRACTION	NO	DIED	
OF57	T026	FOM	FOM	FOM	FOM	NORMAL	83	M	VESTIBULOPLASTY	YES	na	na
OF61	T028	FOM	FOM	FOM	FOM	NORMAL	62	M	VESTIBULOPLASTY	YES	na	na
OF65	T029	FOM	FOM	FOM	FOM	NORMAL	78	M	VESTIBULOPLASTY	NO	DIED	
OK57	T026	FOM	FOM	FOM	FOM	NORMAL	83	M	VESTIBULOPLASTY	NO	DIED	
OK61	T028	FOM	FOM	FOM	FOM	NORMAL	62	M	VESTIBULOPLASTY	NO	DIED	
OK65	T029	FOM	FOM	FOM	FOM	NORMAL	78	M	VESTIBULOPLASTY	NO	DIED	
HN112	B0001	GINGIVA	GINGIVA	MANDIBLE	BUCCAL	SCC	71	F	SURGICAL RESECTION	YES	100	1
OF6caf	B0031	TONGUE	TONGUE	TONGUE	BUCCAL	SCC	63	M	SURGICAL RESECTION	YES	100	0
OF7caf	B0044	TONGUE	TONGUE	TONGUE	BUCCAL	SCC	76	M	SURGICAL RESECTION	NO	DIED	
OF8caf	B0042	TONGUE	TONGUE	TONGUE	BUCCAL	SCC	37	M	SURGICAL RESECTION	NO	DIED	
OF52	B000A	TONGUE	TONGUE	TONGUE	BUCCAL	SCC	56	M	SURGICAL RESECTION	YES	100	3.2

Buccal

Keratinocytes

FOM

Fibroblasts

FOM

Keratinocytes

Carcinoma-

Associated

Fibroblasts

OF53	B000A	TONGUE	TONGUE	SCC	56	M	SURGICAL RESECTION	NO	CONTAM
OF55	B000C	TONGUE	TONGUE	SCC	56	M	SURGICAL RESECTION	NO	CONTAM
OF60	B000D	TONGUE	TONGUE	SCC	24	M	SURGICAL RESECTION	NO	DIED
OF68	B0058	GINGIVA	MAXILLA	SCC	84	F	SURGICAL RESECTION	YES	100
OF73	B0065	GINGIVA	MANDIBLE	SCC	76	F	SURGICAL RESECTION	NO	DIED
OF76	B0070	GINGIVA	MANDIBLE	SCC	60	F	SURGICAL RESECTION	YES	100
OF77	B0072	TONGUE	TONGUE	SCC	60	F	SURGICAL RESECTION	YES	100
OF79	B0073	GINGIVA	MAXILLA	SCC	63	M	SURGICAL RESECTION	YES	100
OF81	B0074	TONGUE	TONGUE	SCC	66	F	SURGICAL RESECTION	YES	100
OF83	B0077	TONGUE	TONGUE	SCC	71	F	SURGICAL RESECTION	YES	100
OF97	B0081	FOM	FOM	SCC	84	F	SURGICAL RESECTION	YES	10.1
OF99	B0082	TONGUE	TONGUE	SCC	65	F	SURGICAL RESECTION	YES	100
OF101	B0084	GINGIVA	MANDIBLE	SCC	66	M	SURGICAL RESECTION	NO	DIED
OF103	B0085	GINGIVA	MANDIBLE	SCC	53	F	SURGICAL RESECTION	NO	DIED
OF108	B0087	GINGIVA	MANDIBLE	SCC	58	F	SURGICAL RESECTION	YES	100
OF112	B0089	TONGUE	TONGUE	SCC	85	F	SURGICAL RESECTION	YES	100
OF114	B0090	TONGUE	TONGUE	SCC	54	M	SURGICAL RESECTION	NO	DIED
OF116	SW001	TONGUE	TONGUE	SCC	61	M	SURGICAL RESECTION	YES	100
HN111(F)	B0001	GINGIVA	MAXILLA	PVL	71	F	SURGICAL RESECTION	YES	na
HN111(K)	B0001	GINGIVA	MAXILLA	PVL	71	F	SURGICAL RESECTION	NO	CONTAM

PVL
Associated
fib/ker

Establishment of Primary Cell Strains by Cell Type and Anatomic Subset

As stated, attempts at primary cell strain creation were undertaken with the tumour, tumour stroma, epidermal and dermal components. Thus, there are three cell types for which primary cell strains were ultimately established; normal keratinocytes (NK) from the epidermal layer and normal fibroblasts (NF) from the dermal layer of normal tissue from the tooth extraction patients and the normal tissue taken from the cancer resection patients, and carcinoma-associated fibroblasts (CAF) derived from the tumour stroma of a particular carcinoma specimen. All attempts (n=155) at developing primary cell strains of carcinoma were unsuccessful and these were not included in the analysis.

Figure 3.2 demonstrates the success rate between the various cell types. There was a significantly higher percentage of normal fibroblast and carcinoma-associated fibroblast cell strain development (66% and 61%, respectively) when compared to the success rate of the normal keratinocyte cell strain formation (19%). This is consistent with prior studies^{25,26} and may reflect the overall differentiation of each cell type in its respective compartment. The epidermal layer consists of keratinocytes which follow a very well-defined differentiation pattern with the basal layer being least differentiated and even containing a population of epidermal stem cells which would be most amenable to propagation and as the keratinocytes become more differentiated towards the surface their ability to divide decreases in order to form a structure that is a physical barrier to the outside world. This would result in a relatively small number of cells, which could readily divide

and populate a culture dish. In contrast, throughout the literature fibroblasts have proven to be relatively easy to cultivate^{27,28}. As the main cellular component of the dermal compartment, the fibroblasts do not have the same differentiation pattern as found in the epidermal layer and indeed one of the main functions of the fibroblast is to be able to divide and coordinate a general tissue response such as the actions found in wound healing. Thus, the overall result of a decreased success rate of cell strain establishment in normal keratinocytes is not surprising given the inherent physiologic functions of each cell type.

Another variable that may affect the outcome of an attempt to create a primary cell strain is the anatomic derivation of the tissue specimen. The four anatomic locations in the oral cavity from which the specimens were derived are buccal mucosa, floor-of-mouth, gingiva and tongue. It is possible given each area's unique embryologic formation and physiologic functioning that there may exist differences in success rates of cell strains attempted from each area. Table 2.4 lists in detail the cell type (NF, NK and CAF) and the anatomic subset (tongue, buccal, floor-of-mouth, gingiva) of each cell strain attempted and lists whether or not they were successfully established. Figures 2.3 a, b and c graphically demonstrate that there were no significant differences in cell strain establishment rates found comparing the various anatomical subsets within each cell type (NF, NK and CAF groups). Further, there was no significant affect of sex on establishment of cultures with tissue from different anatomic subsets within each cell type, (figure 2.4 a, b, and c). However, when comparing the success rates across each cell type, significantly fewer

keratinocyte cultures were successfully derived from females than males as compared to normal fibroblasts and carcinoma-associated fibroblasts. In fact, no keratinocyte cell strain was successfully derived from a female donor. This difference, however, may be due to the small sample size.

Table 2.2. Study Population Characteristics.

	#	Median age	Range
Total patients	52	61	11 to 85
Female patients	23	60	11 to 85
Male patients	29	61	17 to 85

Table 2.3. Success of Primary Cell Strain Cultures.

	Total attempted	Established	Died
Total	155	67	88
Males	91	42	49
Females	64	25	39

Table 2.4. Cell Strain Survival by Cell Type and Anatomic Subset.

Cell type	Anatomic subset	Attempted (no.)	Established (no.)	Died (no.)	Contaminated (no.)
Normal keratinocytes (n=59)	NK Buccal	15	2	13	0
	NK Floor-of-mouth	3	0	3	0
	NK Gingiva	24	5	15	4
	NK Tongue	17	4	11	2
	Total	59	11	42	6
Normal fibroblast (n=59)	NF Buccal	15	10	5	0
	NF Floor-of-mouth	3	2	1	0
	NF Gingiva	24	15	8	1
	NF Tongue	17	12	4	1
	Total	59	39	18	2
Carcinoma-associated fibroblast (n=23)	CAF Buccal	0	0	0	0
	CAF Floor-of-mouth	1	1	0	0
	CAF Gingiva	8	5	3	0
	CAF Tongue	14	8	4	2
	Total	23	14	7	2
Other (PVL, Dysplasia, Scar) (n=14)	Buccal fibroblasts (PVL)	1	0	1	0
	Buccal keratinocytes (PVL)	1	0	1	0
	Buccal fibroblasts (Dysplasia)	2	0	2	0
	Buccal keratinocytes (Dysplasia)	2	1	1	0
	Buccal fibroblasts (Scar)	1	1	0	0
	Buccal keratinocytes (Scar)	1	1	0	0
	Gingival fibroblasts (PVL)	3	0	2	1
	Gingival keratinocytes (PVL)	3	1	2	0
	Total	14	4	9	1

Success of Primary Cell Strain Establishment Based On Age

One obvious contributor to the successful establishment of a cell strain may be the age of the individual from whom the tissue specimen originated. This supposition comes mainly from the observation that as individuals age, cells and fibroblasts specifically, change and can undergo senescence where their replicative abilities are reduced²⁹. However, as demonstrated in figures 2.5 a, b and c there were no significant differences found within the cell types based on age, where three age groups were defined as less than or equal to 30, between 31 and 60, and older than 60.

Overall Male/Female Ratios

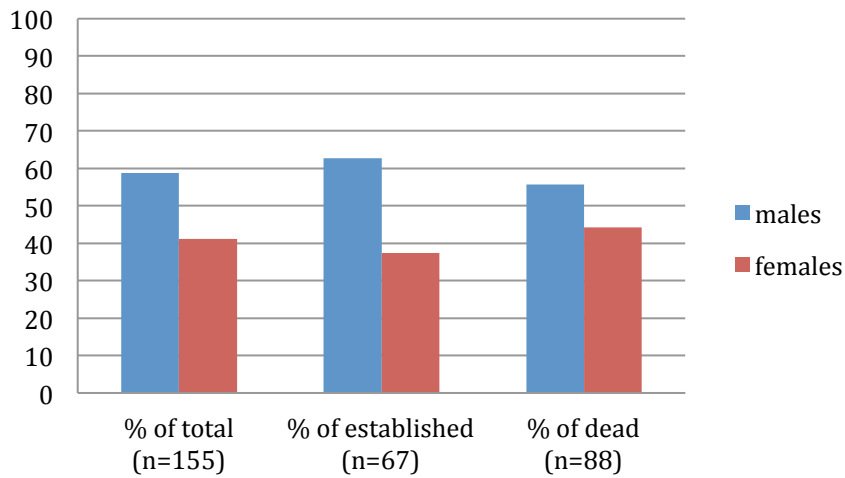


Figure 2.1. Success of culturing according to sex of tissue donor. Shown is the male/female makeup of the overall attempted cell strains, then according to the cell strains that were established or died. There were no significant differences in the number of males and females between the established and dead groups. In this analysis dead includes both died and contaminated classifications.

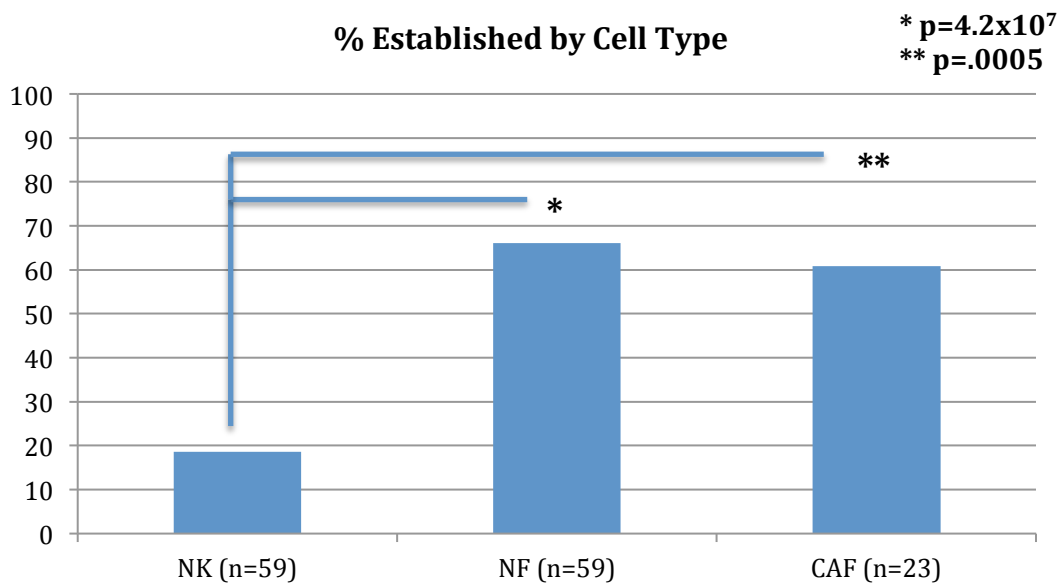


Figure 2.2. Success of cell strain establishment in the normal keratinocyte, normal fibroblast or carcinoma-associated fibroblast groups. The survival rate for normal keratinocytes is significantly lower compared to normal fibroblasts and carcinoma-

associated fibroblasts and there is no significant difference in the success rate between the normal fibroblast group and the carcinoma-associated fibroblast group.

Figure 2.3a.

NK Culture Results by Anatomic Site

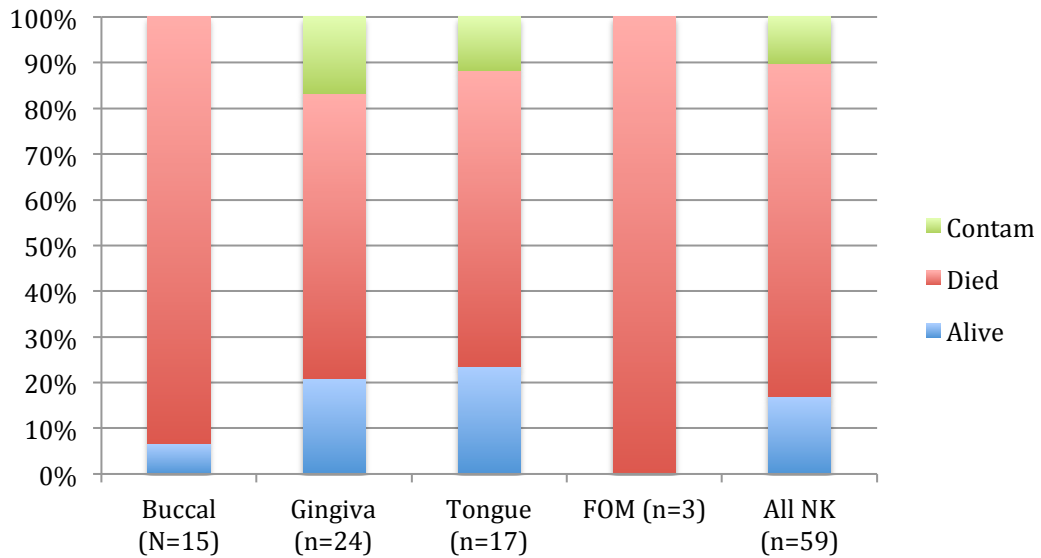


Figure 2.3b.

NF Culture Results by Anatomic Site

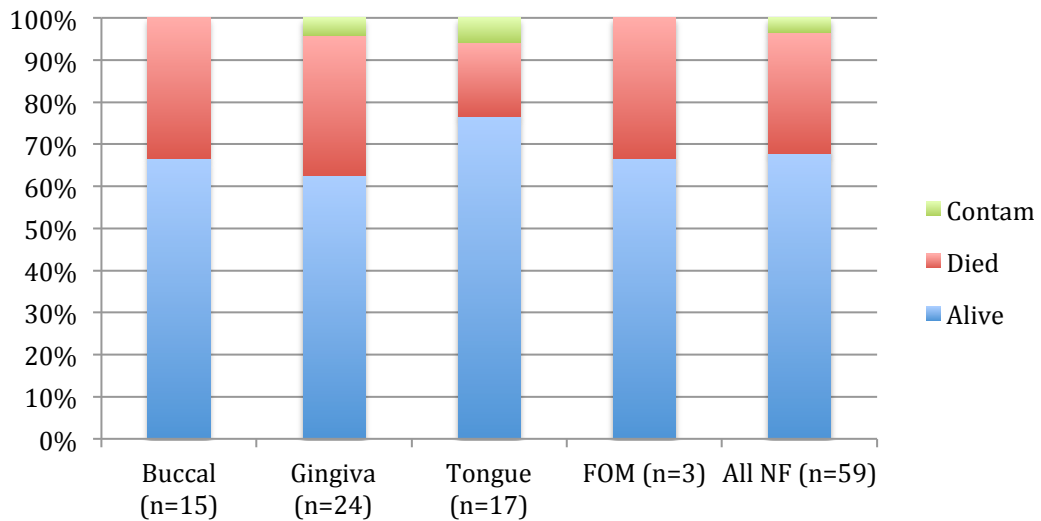


Figure 2.3c.

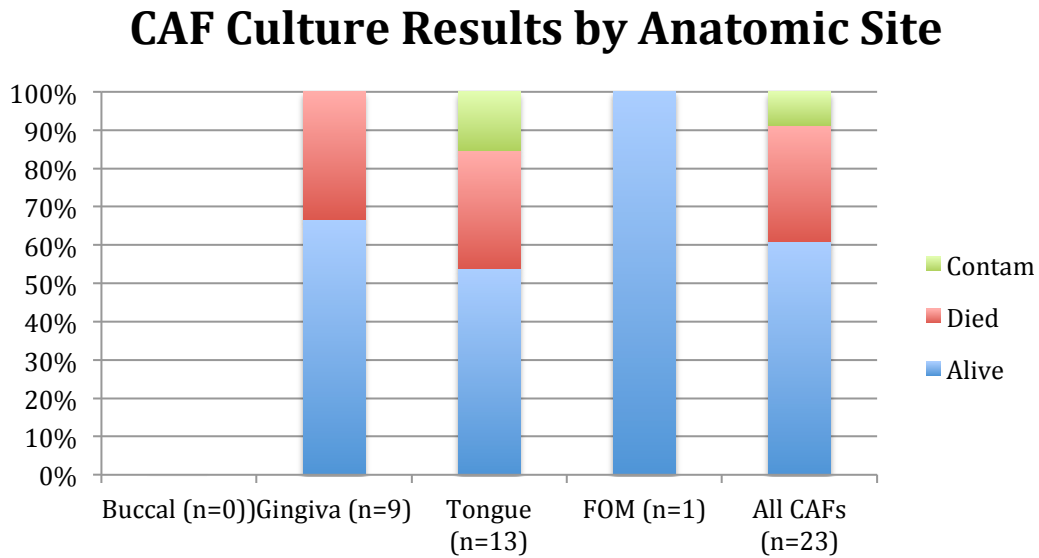


Figure 2.3. Cell strain survival according to cell type and tissue of origin. The percentage of established cell strains according to anatomic subsite is shown for normal keratinocytes (a), normal fibroblasts (b) and carcinoma associated fibroblasts (c). There were no significant differences found in the rates of culture survival between the anatomic subsites.

Figure 2.4a.

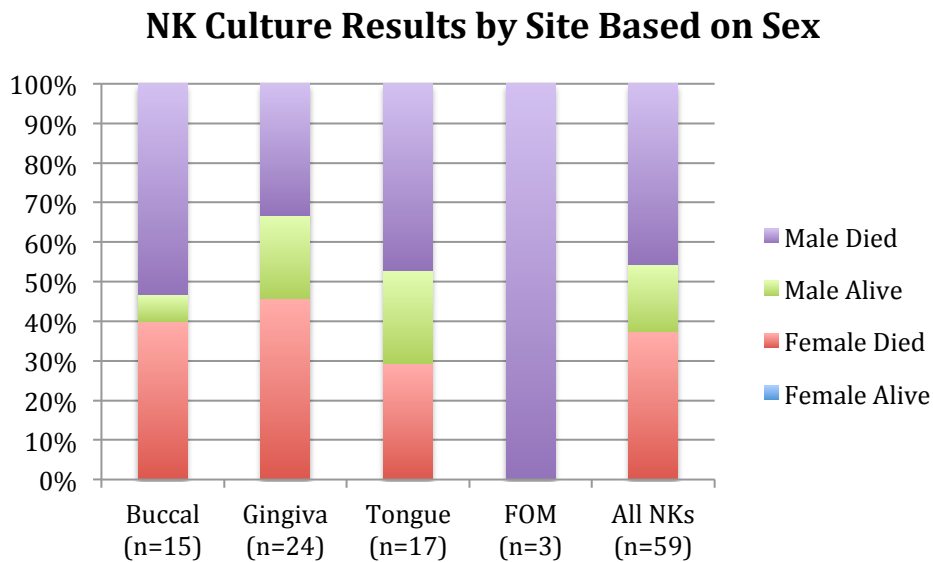


Figure 2.4b.

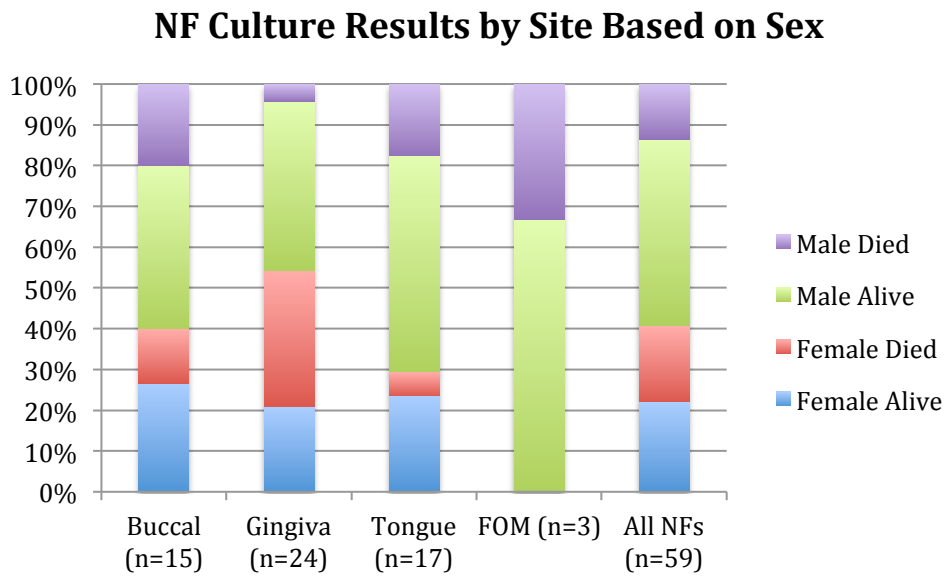


Figure 2.4c.

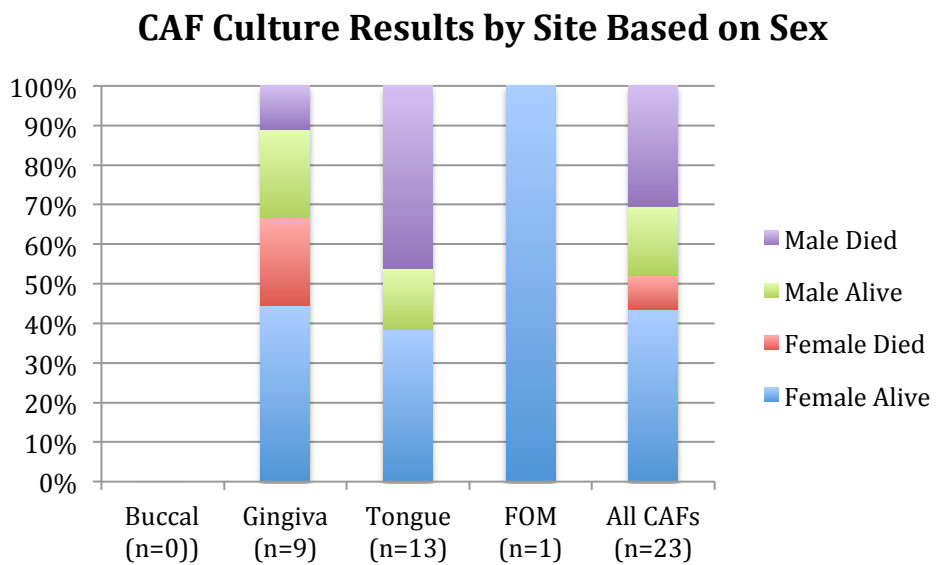


Figure 2.4d.

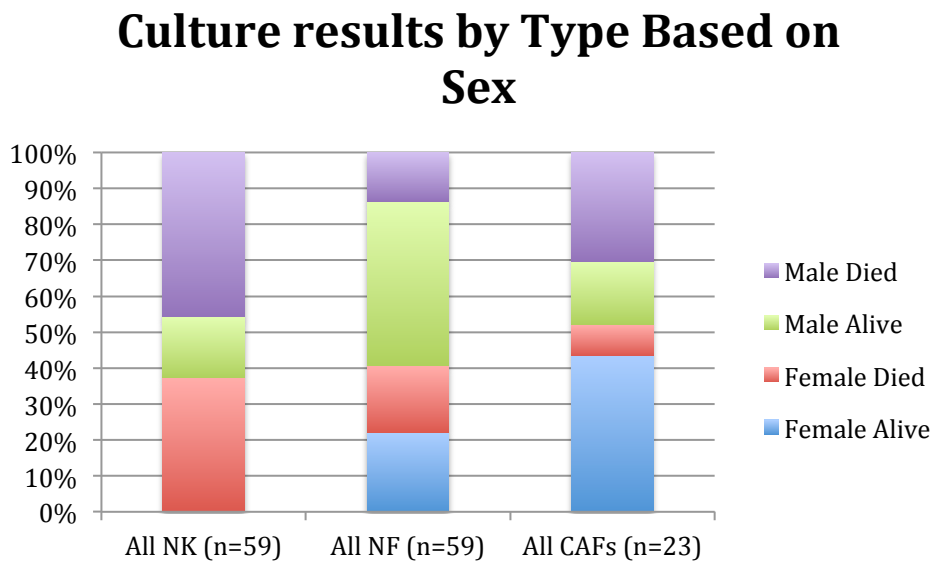


Figure 2.4. Culture success according to sex of the tissue donor. Percentage of established cell strains from males versus females is shown for normal keratinocytes (a), normal fibroblasts (b) and carcinoma associated fibroblasts (c). There were no significant differences found in the rates of culture survival between the anatomic subsites based on sex of tissue donor. The percentage of established cell strains from males versus females by anatomic site across the three cell types (d) did show a significant difference in the survival rates of cultures derived from female versus male patients for normal fibroblasts and carcinoma-associated fibroblasts and normal keratinocytes ($p=0.046$ and $p=0.0005$ respectively, Fisher Exact Test). There were no significant differences between the normal fibroblast and carcinoma-associated fibroblast group.

Figure 2.5a.

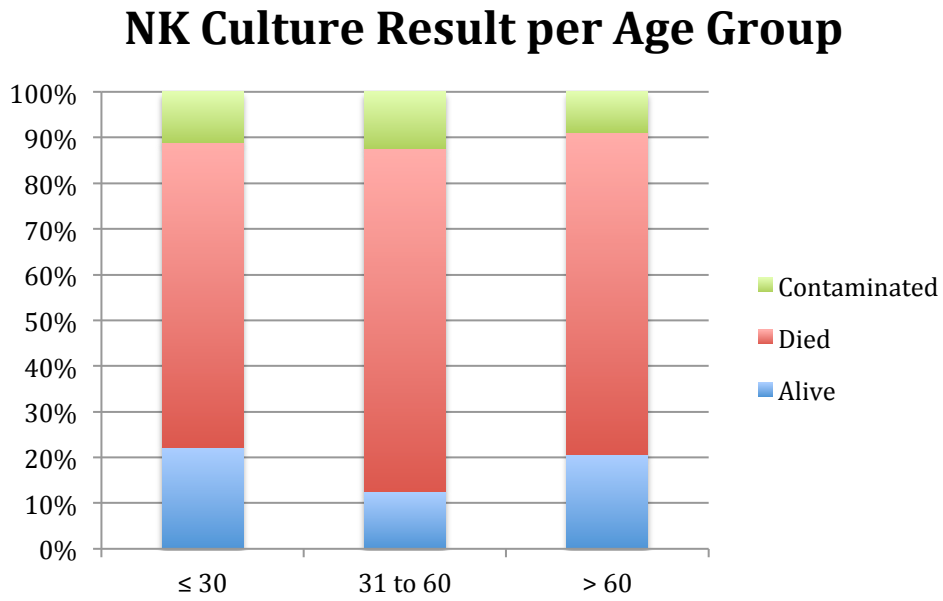


Figure 2.5b.

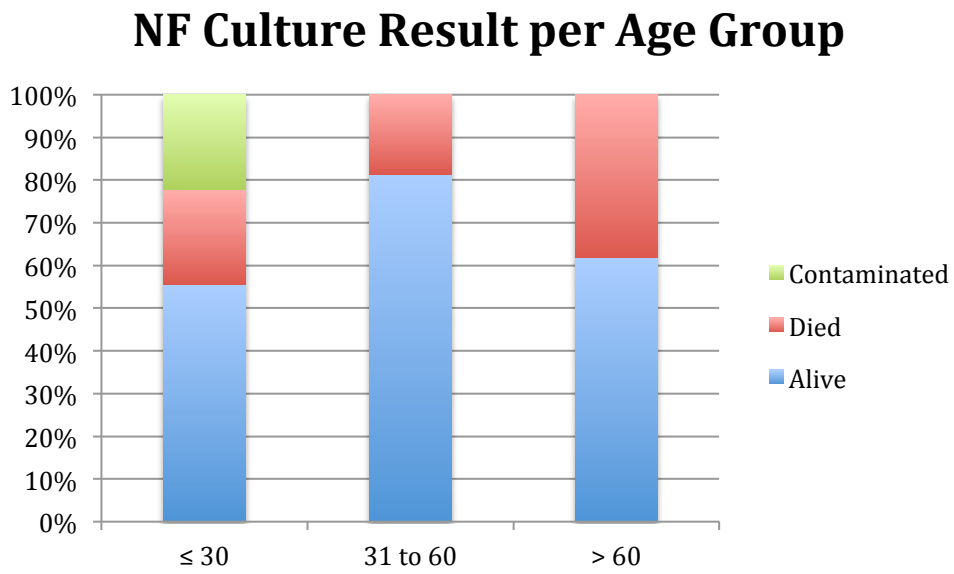


Figure 2.5c.

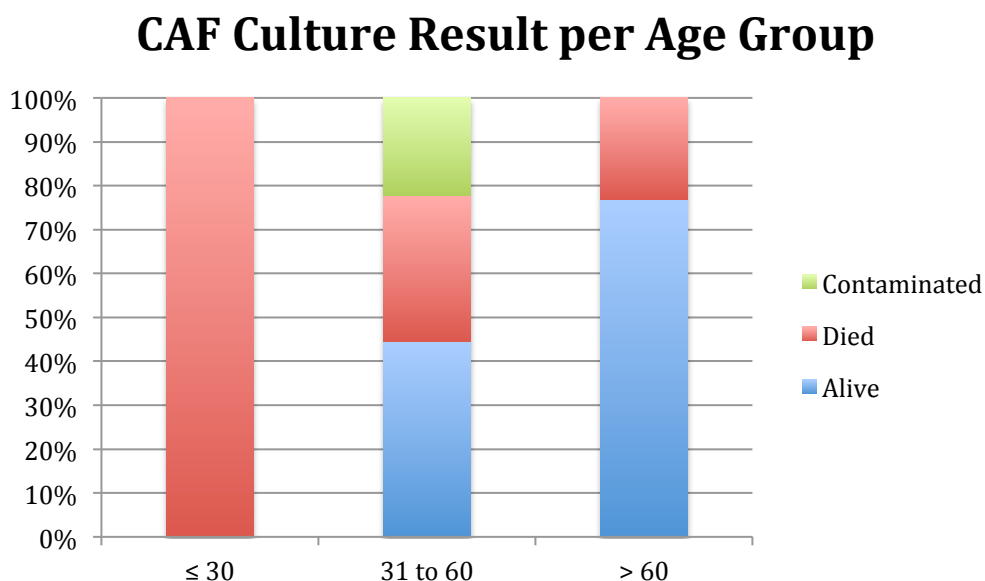


Figure 2.5. Success of cell strain establishment by age group. Percentage of established cell strains from the three age groups, Group A: 1-30 (n=9), Group B:31-60 (n=16) and Group C 61 and older (n=34), is shown for normal keratinocytes (a) and normal fibroblasts (b) and in Group A: 1-30 (n=1), Group B:31-60 (n=9) and Group C 61 and older (n=13) for the carcinoma associated fibroblasts. There were no significant differences found in the rates of culture between the anatomic subsites based on age group.

Success of Primary Cell Strain Establishment Based on Researcher Experience

One variable that is outside the physiologic realm of possibilities affecting the successful establishment of a primary cell strain is the experience of the person attempting to cultivate the various cellular components from the tissue specimen. To investigate this question, the three year time period over which this study was carried out was divided into three time groups that consisted of the first 15 months (early in time), 16-30 months (middle time), and more than or equal to 31 months

to present (recent time). In comparing the results within the three cell types, experience appears to not significantly contribute to survival rates in normal fibroblasts or carcinoma associated fibroblasts. However, in the normal keratinocyte group it does appear that experience contributed to the successful outcome of cell strain cultivation with the most recent time period having a significant increase in success rates (Figure 2.6). Interestingly, this corresponded to a change in the supplier of the primary keratinocyte media, which is the only variable that was altered at the beginning of this time-period as the personnel performing the cultivation did not change.

Figure 2.6a.

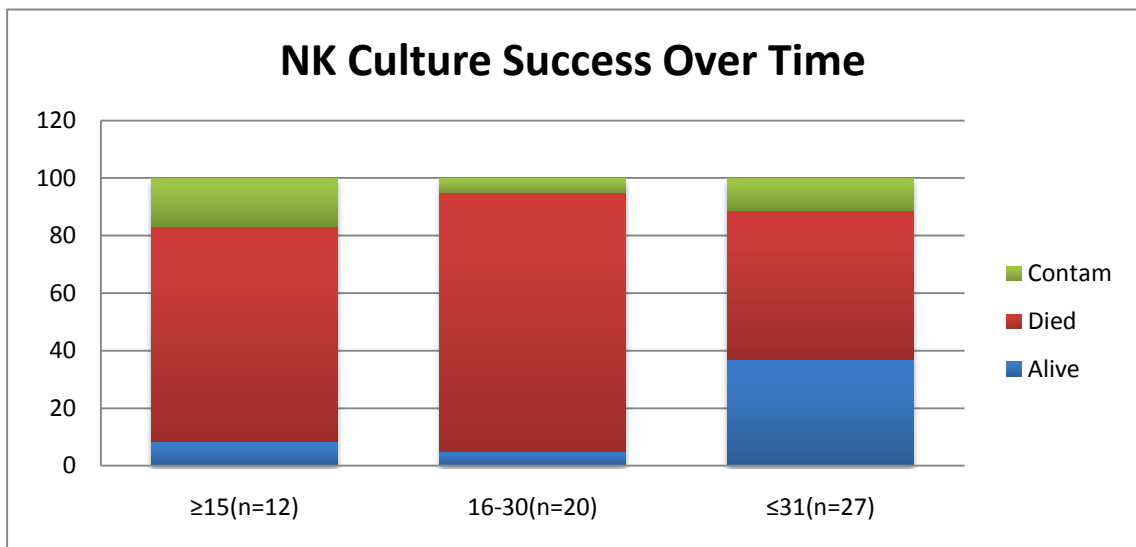


Figure 2.6b.

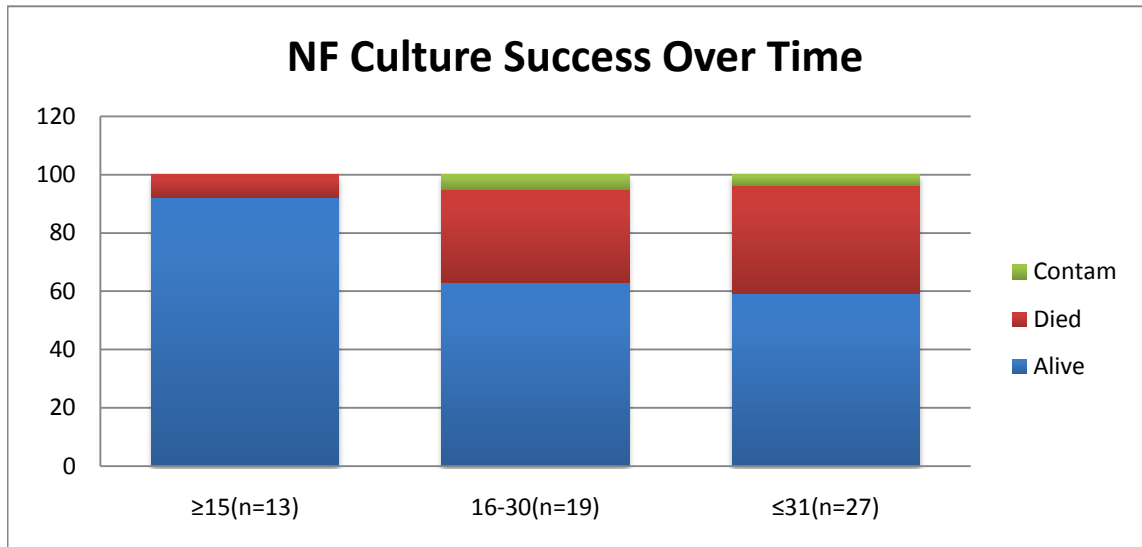


Figure 2.6c.

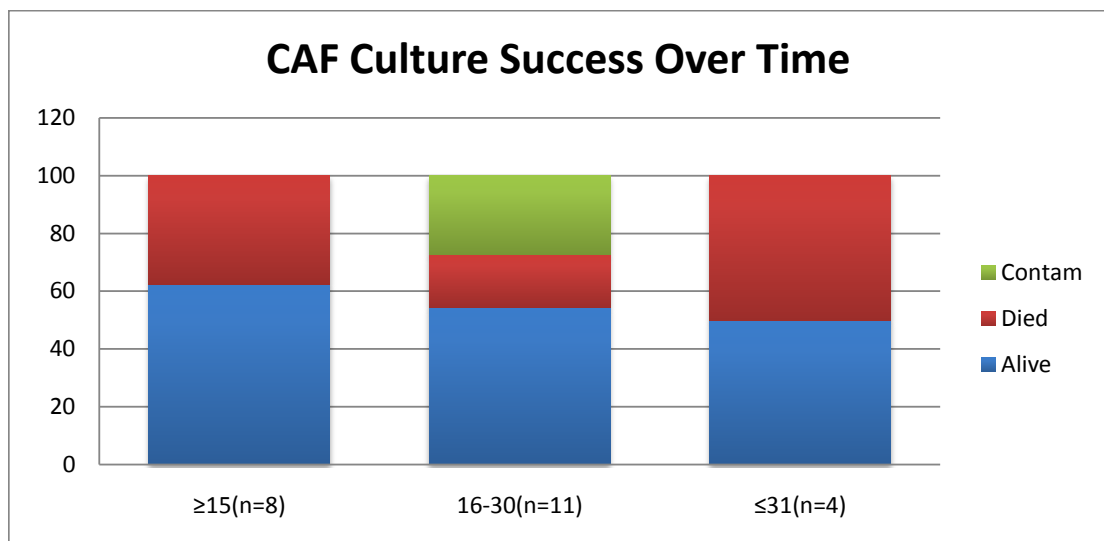


Figure 2.6. Success of cell strain establishment over time. Percentage of established cell strains from the three year study was divided into three time periods, early: 0 to 15 months, middle: 16 to 30 months, recent: 31 months to present is shown for normal keratinocytes (a), normal fibroblasts (b) and carcinoma associated fibroblasts (c). The success rate of normal keratinocyte cell culture significantly improves over time with the

last time period being more productive than the initial two time periods ($p=0.015$ and 0.014 , Fisher Exact Test), whereas the success rate of normal fibroblasts and carcinoma associated fibroblasts had no significant relationship to the time periods.

Survival of Maxillary versus Mandibular Gingival Primary Cell Cultures

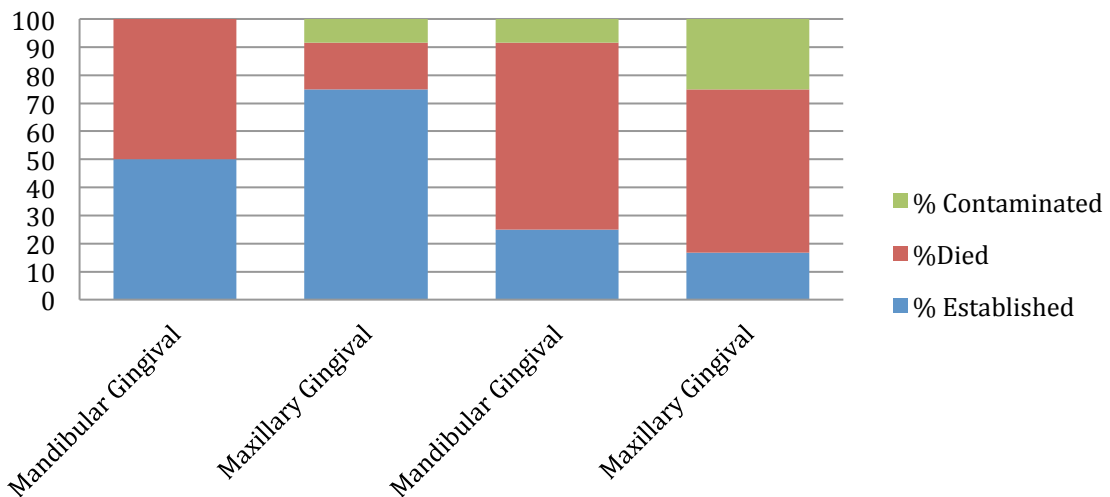


Figure 2.7. The survival rate of gingival fibroblasts and keratinocytes from maxillary versus mandibular donor sites is shown. There is no significant difference in survival rates of primary cell strains between maxillary or mandibular gingival donor sites.

Chapter summary and future directions

We have shown that sex and age of the donor as well as anatomic subsite do not seem to have a major influence on the successful derivation of any one specific cell strain. However, we have demonstrated higher success rates for normal fibroblasts and carcinoma associated fibroblasts than for keratinocytes overall and specifically, we have found that it very difficult to generate keratinocytes from female donors. Additionally, with experience the success rate for generating keratinocyte cultures increases, which is consistent with the overall difficulty and low percentage of

successfully generating keratinocyte cultures, in general, compared to normal fibroblasts and carcinoma associated fibroblasts.

In the future, we hope to expand our current “library” of cell strains to include more examples from other anatomic sites such as the floor-of-mouth and buccal mucosa. This may potentially lead to further insights regarding the innate differences that exist between both the normal fibroblasts and carcinoma associated fibroblasts from different anatomic sites. Further, having cell strains from these different sites may allow us to address unresolved questions such as the cell of origin of the carcinoma associated fibroblasts, whether there are subsets of carcinoma associated fibroblasts and whether they have differential influences on a particular carcinoma that may be responsible for the typical clinical behaviour observed from tumours arising from the varied anatomic locations. In the following chapters, we will begin to address the questions of anatomic variability in fibroblast biology (Chapter 3) and then further investigate the question of carcinoma associated fibroblast subsets and cellular origin (Chapter 4) utilizing a portion of the cell strains we have described here.

**Chapter 3: Anatomic Variation in Oral Fibroblast Response to TGF β or TGF β -
Mediated Stimulation.**

Introduction.

Despite years of effort, our understanding of the development and progression of oral squamous cell carcinoma remains limited. This is reflected by the fact that oral cancer is associated with one of the poorest 5-year survival rates (40%) of any malignancy in the body. The current treatment strategies of surgery and radiotherapy result in considerable morbidity and often fail, resulting in loco-regional recurrence and distant metastatic spread. Clinically, it has been observed that some areas of the oral cavity develop carcinomas more frequently than others and even rates of invasion and metastasis differ between the different subsites³⁰. Nevertheless, differences in genomic alterations in tumors from different oral subsites have not been revealed by genomic DNA copy number analysis³¹. It has been previously suggested that the stroma surrounding these lesions can have a profound influence on their genesis and progression and these observations raise the possibility that inherent differences in the stroma from different sites contribute to the clinical characteristics observed in patients with oral squamous cell carcinoma. Thus, it becomes important to better understand the influence of the stroma on these mechanisms.

Carcinoma/stromal interaction

In recent years a significant amount of literature has been devoted to exploring the reciprocal relationship between cancer and the surrounding stroma. Much of this

interest has been focused on the contributions of the inflammatory system³². Many types of tissues exposed to chronic inflammation have a higher risk of developing cancer and interestingly, non-steroidal anti-inflammatories have been shown to reduce this risk ref. Further, as discussed in Chapter 1, inflammatory cells and their associated mediators are a major feature of the microenvironment of most tumors and often increased cell numbers of certain lymphocytic populations can be a poor prognostic indicator.

However, the microenvironment surrounding tumors consists of more than just the inflammatory infiltrate; there are also endothelial cells, adipocytes, neuronal elements, extracellular matrix and fibroblasts. Interestingly, the fibroblasts located in the stroma adjacent to the invasive front of carcinomas often acquire an altered phenotype and become what some have termed “carcinoma associated fibroblasts” (CAFs). These CAFs are analogous to the activated fibroblasts or myofibroblasts seen in normal wound healing and interact with the microenvironment in several ways. First, in the process of becoming CAFs the fibroblasts in the surrounding stroma respond to signals generated by the cancer cells and transdifferentiate from a resting fibroblast phenotype to an active myofibroblast phenotype, the hallmark of which is the production of the highly contractile protein α -smooth muscle actin (SMA, *ACTA2*). Importantly, it seems that this is a process only observed in malignancy and not dysplastic precancerous conditions³³. Secondly, as part of the desmoplastic response, the fibroblasts also up regulate production of connective

tissue growth factor (*CTGF*) which is a member of a multi-functional family of proteins that play a role in regulating angiogenesis, cell adhesion, migration and differentiation³⁴. Thirdly, the fibroblasts alter the relationship and the structure of the extracellular matrix (ECM) by mechanisms other than production of SMA, including increasing the number and strength of cellular-ECM adhesions, increasing the production of ECM components, production of matrix metalloproteinases, tissue inhibitors of metalloproteinase, and by the elaboration of a myriad of cytokines and chemokines³⁵. Lastly, as the carcinoma progresses, the stromal environment created by the smooth muscle actin expressing myofibroblasts becomes increasingly permissive to cancer cell growth and invasion. Recent evidence demonstrates that isolated myofibroblasts and CAFs can directly convey invasive capacity upon cancer cells^{36,37}. In fact, in a study of tongue squamous cell carcinomas by Kellermann et al. the increased presence of myofibroblasts and positive smooth muscle actin staining was significantly correlated with a greater likelihood of lymph node metastasis, extracapsular lymph node infiltration, vascular and neural invasion, and an overall decreased survival rate when compared to those lesions with a scarcity of myofibroblasts and SMA staining³⁸. Similar results were seen in a study by the same authors of oral squamous cell carcinoma where it was found that nearly 60% of oral SCCs contained myofibroblasts in the tumor stroma and again they found a significant correlation between N stage, disease stage, regional recurrence and proliferation of tumor cells³⁹. This same study demonstrated that carcinoma cells were able to transdifferentiate normal oral fibroblasts into myofibroblasts in a TGF-

β dependent manner in co-culture. In a study on ductal breast cancer⁴⁰ the authors observed the most numerous transformed fibroblasts in the most advanced cases. Additionally, in a mouse model, CAFs were generated from a mammary carcinoma and implanted into the backs of syngeneic mice, which gave rise to sarcomatoid tumors whose characteristics shared many similarities to the stroma seen in wound repair and carcinogenesis⁴¹. Thus the evidence demonstrates that the cancer/stroma interaction is analogous to wound healing where the fibroblasts create an environment for the wound to contract and give the opportunity for the keratinocytes to migrate and re-epithelialize the wound. One could imagine that the carcinoma cells use these mechanisms to their advantage to proliferate, invade and populate the resident tissues. Further, keep in mind that unlike the normal wound healing processes where the activated fibroblasts either become phenotypically quiescent fibroblasts or apoptose, carcinomas are essentially “wounds that do not heal”⁴² and the desmoplastic reaction persists with continued myofibroblast activation and promotion of a pro-carcinogenic environment.

TGF- β , Endothelin-1, Connective Tissue Growth Factor

There are three major signaling mechanisms that drive the desmoplastic response. These are the TGF- β pathway, the endothelin pathway, CTGF (connective tissue growth factor) pathway as well as mechanical stress generated from interactions of the fibroblasts with the extracellular matrix fibers.

TGF-β

TGF-β is one of the major cytokines induced during the wound healing process⁴³. It stimulates fibroblasts to make and contract ECM⁴⁴. In TGF-β signaling, there are three TGF-β isoforms synthesized as latent precursors that form a complex with latent TGF-β proteins, which are later removed by proteolysis. Once this happens, TGF-β is in its active form and can bind a heterotrimeric receptor made up of one TGF-β type I receptor and one TGF-β type II receptor. The remainder of the canonical pathway involves phosphorylation of the receptor activated SMADs (SMAD2 and 3) which go on to bind with SMAD4 enabling the entire complex to translocate into the nucleus and affect transcriptional regulation of fibrotic mediators. There are at least three other non-canonical signaling mechanisms induced by TGF-β stimulation and include the ras/MEK/ERK, p38 and JNK pathways⁴⁵. There is long standing evidence that demonstrates that TGF-β is important in inducing desmoplasia. Mesenchymal cells exposed to TGF-β are transdifferentiated into myofibroblasts that make as well as contract ECM and this situation remains as long as TGF-β is present⁴⁶. TGF-β has the effect of enhancing deposition of ECM when injected subcutaneously or into surgically implanted metal chambers⁴⁷ and in animal models of wound repair, incisions treated with anti-TGF-β antibodies or anti-sense oligonucleotides show a drastic reduction in scarring and synthesis of ECM⁴⁸. Recent evidence from our laboratory using an organotypic co-culture model has demonstrated that under the influence of *GLI2* over-expressing

keratinocytes, foreskin fibroblasts can be induced to transdifferentiate into myofibroblasts and produce a desmoplastic stroma. Further, it was found that specific TGF- β receptor II inhibition strongly attenuated this response, providing evidence that the production of desmoplasia in this model is mainly a TGF- β mediated event³³.

Endothelin-1

Although it seems as though TGF- β is the most potent mediator of the desmoplastic reaction in the stroma during normal wound healing and carcinogenesis, there are other pathways that may have an important influence on the threshold of the response that fibroblasts have to TGF- β signaling or may even act independently or in concert with TGF- β . One of these pathways is the Endothelin pathway.

Endothelin-1 (ET-1, *EDN1*), the major isoform in humans, is made by a wide variety of cell types including endothelial cells, epithelial cells, mast cells, macrophages and fibroblasts⁴⁹. Its expression is increased in hypoxic states, low shear stress, and by cytokines including TGF- β ^{50,51}. Endothelin-1 is made as the precursor prepro-ET-1 which is enzymatically cut twice to produce an active molecule⁵² that can then stimulate either of the G-protein-coupled receptors EDNRA or EDNRB. Different cell populations can express varying levels of EDNRA or EDNRB and these receptor levels and sensitivities can be further altered in disease states. Aberrant EDN1 expression and signaling may play a role in pathologies such as cancer, congenital

heart disease, pulmonary hypertension and fibrosis⁵³⁻⁵⁵. Current evidence suggests that in fibroblasts derived from lung tissue in scleroderma patients, EDN1 can act synergistically with TGF- β to cause fibroblasts to increase production of ECM and exert contractile forces and that the EDNRA receptor seems most responsible for SMA synthesis and contraction of the ECM, while both receptors appear to be needed for ECM production^{56,57}. Induction of EDN1 by TGF- β in normal lung fibroblasts in an ALK5/JNK dependent manner leads to much of the desmoplastic response attributable to TGF- β , including SMA and CTGF production as well as contraction of the ECM⁵⁸. In diseased fibroblasts, such as those derived from scleroderma patients, general antagonism of the ET-1 receptors with bosentan results in reduced SMA, CTGF and type I collagen expression, as well as decreased ECM contraction⁵⁹. Thus, it appears as though endothelin and TGF- β together play major roles in the desmoplastic response.

In addition to contributing to the desmoplastic response, endothelin also seems to play a major role in neovascularization in tumor development and progression⁶⁰. Endothelin has been shown to stimulate a dose-dependent increase in VEGF expression in cultured ovarian cancer cells through endothelin receptor A⁶¹. Endothelin receptor A antagonism with ABT-627 significantly reduced VEGF secretion⁶² however, in endothelial cell lines VEGF and endothelin receptor B induced increased migration and invasiveness⁶³. Thus, the evidence suggests that

endothelin-1 plays an important role in promoting angiogenesis in association with VEGF.

Connective Tissue Growth Factor (CTGF)

CTGF is a protein that belongs to the CCN family of modular matricellular proteins, which are adhesive molecules that alter signaling responses to external signals like ECM and growth factors, thus the receptor is an integrin^{64,65}. Induction of CTGF is through stimulation by TGF- β , SMADs, EDN1, protein kinase C and ras/MEK/ERK^{66,67}. In rodents, CTGF and TGF- β work together to promote a prolonged desmoplastic response⁴⁷. Mouse embryonic fibroblasts lacking CTGF are able to respond to TGF- β stimulation via the SMAD pathway but they have attenuated stimulation of adhesive signaling⁶⁸ lending support to the notion that the CTGF receptors are indeed integrins and that CTGF is a cofactor of TGF- β . Lastly, anti-sense oligonucleotides to CTGF suppress fibrosis in several animal models^{69,70}. So, the evidence supports a role for all three molecules in the desmoplastic response or stromal transdifferentiation in, at the least, diseased fibrotic states and normal wound healing but maybe also in carcinogenesis.

Anatomic variation

The major line of evidence that generated one of the underlying hypothesis of this chapter originated from previous observations made in our laboratory that *GLI2* over-expressing keratinocytes stimulate a desmoplastic response in the fibroblast layer in three-dimensional organotypic reconstructs³³. *GLI2* is a member of the *GLI* family of transcription factors that are downstream mediators of hedgehog signaling. This pathway is activated in as many as 25% of oral SCCs and it has been demonstrated that *GLI2* transcriptional targets may promote tumor formation, including suppression of contact inhibition and differentiation. It was our observation that *GLI2* over-expressing keratinocytes in organotypic co-culture with fibroblasts induced cancer associated characteristics in the epithelium and stroma, both recapitulating known features and predicting previously unappreciated aspects of *GLI2* amplifying tumors. One of the interesting findings was that the desmoplastic response, measured as enhanced SMA and collagen IV staining by immunohistochemistry and immunofluoresence, was produced only when foreskin or tongue fibroblasts were used in co-culture with *GLI2* overexpressing keratinocytes and not gingival fibroblasts. This observed difference generated the obvious question why?

There is longstanding evidence that supports the idea that fibroblasts derived from different anatomical sites display phenotypic variability. For example, fibroblasts

derived from one area of the body that support one characteristic epithelial cell type will continue to generate that specific epithelial type as separate transplants⁷¹.

When gene expression programs from fibroblasts are evaluated, it is observed that there are large-scale differences between fibroblasts populations. The differences were so striking that there was just as much variation between diverse populations of fibroblasts as there was between fibroblasts and hematopoietic cells⁷². Further, these differences in gene expression programs followed anatomic divisions including anterior-posterior, proximal-distal, and dermal versus non-dermal patterns. Also, fibroblasts in these different cell populations maintained their unique embryologic HOX gene expression patterns. There are other examples of phenotypic variability among fibroblasts derived from different tissues in the body. When oral fibroblasts were compared to skin fibroblasts in wound contraction models, it was found that oral fibroblasts accelerated collagen gel contraction, produced more KGF and HGF, but expressed lower levels of SMA than their dermal counterparts in the same model system⁷³. In another wound contraction model focusing on ECM reorganization, significant differences in collagen lattice contraction was found in oral fibroblasts versus skin fibroblasts⁷⁴. Phenotypic differences are seen in different fibroblast populations even within the oral cavity. Irwin et al. found that fibroblasts derived from the papillary tips of the gingiva behaved like fetal fibroblasts with cell density migration measures and migration stimulating factor levels significantly higher than the more adult-like fibroblasts derived from deeper reticular tissue of the gingiva and that these phenotypic differences had implications

for wound healing in the oral cavity⁷⁵. When HGF and KGF production was compared in fibroblasts derived from periodontal ligament (PDL) versus those from buccal mucosa, it was observed that PDL fibroblasts constitutively make more of these cytokines⁷⁶. Thus, the literature is replete with examples illustrating the differences between regionally distinct fibroblasts.

If one looks for reasons why the fibroblast should display such distinct phenotypes based on regional location, three major influences must be considered. These factors are (a) embryologic origin, (b) the characteristics of the surrounding ECM and associated cells/tissue types and (c) functional differences.

During embryonic development, the primitive oral cavity is lined with both ectoderm and endoderm. From the ectoderm arises the anterior two thirds of the tongue and all of the hard palate, whereas the endoderm generates the posterior third of the tongue, the floor of mouth, the palato-glossal folds, and the soft palate⁷⁷. Thus, it follows that the ectomesenchyme develops from neural crest cells from the midbrain and anterior rhombomeres and the tongue mesenchyme derives from occipital somites⁷⁸. The epithelial structures further differentiate with varying levels of keratinization, development of teeth, taste buds and salivary glands. So, embryologic origin is one obvious reason for differences between fibroblast subtypes within the oral cavity and as discussed above these fibroblasts maintain their homeobox expression profiles, which were uniquely established during

development. Interestingly, the gene expression profiles are preserved when primary cultures are made of regionally distinct fibroblasts and it has been demonstrated that the profile characteristics are maintained for many passages⁷⁹.

Another reason for regional variation in fibroblasts is that they affect and react to other cell types as well as the ECM in the environment and their phenotypes can be either maintained or altered as a result. This is best demonstrated by observations based on three dimensional tissue reconstruction models and animal tissue transfer models as discussed here and above. In heterotypically recombined scenarios, it is observed that keratinocytes from one anatomic location can influence fibroblasts from a separate location to phenotypically resemble fibroblasts from the tissue source of the keratinocytes⁸⁰. The same is true in the opposite direction; foreign fibroblasts can influence the development of native keratinocytes to more closely resemble keratinocytes derived from the original foreign fibroblasts⁸¹.

Lastly, the fibroblasts in the oral cavity are exposed to varying functional demands that contribute to their phenotype. The oral cavity is a complex environment with correspondingly complex anatomy. For example, if one just draws a comparison between gingiva and tongue, the gingiva consists of keratinized (attached) and non-keratinized (unattached) mucosa and is generally a non-mobile structure, whereas the tongue is completely keratinized and is a highly mobile structure. This should have implications for the types of stresses and ECM organization the fibroblasts are

exposed to and this would be reflected in the phenotypic differences between the two populations. Further, these phenotypic differences influenced by the different anatomic environments may lead to gene expression profiles that may explain why one type of stroma has a higher propensity to transdifferentiate than another.

Whether this difference is due to alterations in receptor levels, to the varying levels of responsiveness in down stream events, or with changes in integrin signaling within the fibroblasts remains to be determined. Clinically, this is important because it is the differences in the ability of one stroma to transdifferentiate over another that we are interested in investigating because of the implication that a transformed stroma has a positive influence on the development and progression of carcinomas.

In this chapter we hypothesize that fibroblasts from different anatomic sites have varying thresholds to stimulation by TGF- β as measured by the secretion of fibrotic products such as SMA. It is important to better understand how these influences interact to produce an altered stroma, which is more permissive to oral cancer progression

Methods.

Cell Culture

HaCaT cells transfected with pBABE-puro or pBABE-puro-GLI2 were cultured in the presence of puromycin (1 µg/ml, Sigma-Aldrich, St. Louis, MO). Double stable inducible HaCaT GLI2 cells expressing 6xHis-GLI2ΔN in pcDNA4/TO and the tetracycline repressor in pcDNA6/TR were grown in the presence of 25 µg/ml zeocin and 8 µg/ml blasticidin-S (Sigma-Aldrich, St. Louis, MO). GLI2 protein expression was induced by adding 1 µg/ml doxycycline to the culture media. Control HaCaT Tet Cells, stably expressing only the tetracycline repressor, were grown in the presence of 8 µg/ml blasticidin-S.

Organotypic Cultures

Dermal equivalents were prepared by adding 1 ml of acellular collagen mixture, consisting of bovine collagen type I (0.78-1.0 mg/ml, Organogenesis, Canton, MA), Minimal Essential Medium with Earle's Salts (Cambrex, East Rutherford, NJ), 1.7 mM L-glutamine, 10% fetal calf serum (Hyclone, Thermo Scientific, Hudson, NH) and 0.15% sodium bicarbonate to each well of a 6-well tissue reconstruct tray (Organogenesis, Canton, MA). The tray was incubated at 37°C for 15-30 minutes, and then 3 ml of a second layer of collagen mixture, supplemented with 7.5×10^4 primary fibroblasts, was added to each well. After the tray was incubated at 37°C for 45 minutes to completely polymerize the cellular collagen layer, 10 ml of the

fibroblast growth media (DMEM H-16 supplemented with 10% FCS) was placed underneath and 2 ml on top of each insert. After seven days, the fibroblasts had contracted the collagen layer forming a mesa shaped plateau. The tissue reconstruct tray was washed twice for 30 minutes each with a mixture of DMEM and F-12 media (3:1). After removing the media, 50 μ l of DMEM and F-12 media (3:1) containing 5×10^5 HaCaT cells or primary foreskin, tongue or gingiva derived keratinocytes were placed on the plateau. Trays were incubated at 37°C for 30-60 minutes after which time 10 ml of media I [DMEM and F-12 media (3:1) supplemented with 4 mM L-glutamine, 1.48 μ M hydrocortisone, 1xITES (insulin, transferrin, ethanolamine, selenium (BioWhittaker, Lonza, Walkersville, MD)), 0.1 mM o-phosphorylethanolamine, 0.18 mM adenine, 2.4 mM CaCl_2 , 4 pM progesterone, 20 pM triiodothyronine and 0.1% chelated newborn calf serum] were placed underneath and 2 ml on top of each insert. Two days later, media was replaced with media II (media I with non-chelated newborn calf serum at 0.1%). Doxycycline (1 μ g/ml, Sigma-Aldrich, St. Louis, MO) was added to media II and media III in control HaCaT Tet reconstructs or to induce GLI2 in reconstructs containing HaCaT GLI2 cells. After two days, the media underneath each insert was replaced with 7.5 ml of media III (media I with DMEM and F-12 media 1:1, no progesterone and 2% non-chelated newborn calf serum). No media was placed on top to allow epidermalization of the keratinocytes. Media underneath the inserts was replaced every other day for six days. Reconstructs were removed, cut in half, fixed overnight in 10% buffered formalin and processed for routine paraffin embedding. Sections of

each reconstruct were stained with H&E and evaluated using a light microscope. For the TGF- β inhibitor studies, 2 μ M of the TGF- β receptor I/II kinase inhibitor LY2109761 or control, dimethyl sulfoxide was added to the organotypic cultures and then harvested in the same manner as above.

Immunohistochemistry (IHC) and immunofluorescence (IF)

Sections were deparafinized in three separate xylene washes of 5 minutes each. Slides were washed two times for 5 minutes each in 100%, 95% and 75% ethanol and then placed in dH₂O. Different antigen (AG) retrieval methods were used (Table 3.1). After antigen retrieval, sections were washed in dH₂O followed by PBS/0.05% Tween20 for 5 minutes each and endogenous peroxidase activity was blocked in 3% H₂O₂ in PBS for 15 min. Sections were washed three times for 3 minutes each in PBS/0.05% Tween20 after which sections will be blocked in a solution containing 3% BSA in 4x SSC for 30 minutes at room temperature. Sections were incubated with the primary antibody for 60 minutes in Antibody Diluent Solution with background reducing agents (DAKO). Sections were washed three times for 5 minutes each in PBS/0.05% Tween20 after which sections were incubated with appropriately labeled secondary antibodies (e.g. Alexa 488, Alexa 594) for 45 minutes at a 1:1000 dilution in Antibody Diluent Solution with background reducing agents (DAKO). Sections were washed three times for 5 minutes each in PBS/0.05% Tween20 and mounted or counterstained with Vectashield mounting media containing DAPI.

Table 3.1 Antibodies used for immunofluorescence and immunohistochemistry.

IF	Vendor	Cat#	Dilution	AG retrieval
Ki67	DAKO	N1633	prediluted	Citrate pressure cook
GFP	ABCAM	AB290	1 -250	Citrate pressure cook
ITGB4	ABCAM	AB6136	1-100	EDTA steam
SMA	DAKO	M0851	1-100	0.01 M TRIS pressure cook
IHC	Vendor	Cat#	Dilution	AG retrieval
Ki67	DAKO	M720	1-100	Trypsin & Citrate MW
Involucrin	ABCAM	AB20202	1-15000	Citrate MW
		PRB-		
Loricrin	COVANCE	145P	1-200	Non
COL IV	ABCAM	AB6311	1-200	Citrate pressure cook
ITGB4	ABCAM	AB6136	1-100	Steam
Vimentin	Zymed	18-0052	1-400	None
SMA	DAKO	M0851	1=100	Target retrieval solution MW

TGF- β Dose Response Curve

Foreskin and oral fibroblast cell strains were grown to approximately 80% confluence in 10 ml of DMEM H16 with 10% FBS and were released from T75 culture flasks (Corning, NY) using 4ml of 0.25% trypsin, pelleted by centrifugation at 1 g for 3 minutes and suspended in 3 ml of DMEM with 10% FBS. A haemocytometer (Reichert, Buffalo, NY) was used to determine the fibroblast concentration per ml so that 1×10^4 cells were plated onto a flat bottom 96-well plate (Corning, Corning, NY) in a 150 μ l volume of DMEM H16 with 10% FBS. These cells

were allowed to attach overnight. The next day the media was removed and DME H-16 without supplementation was added to the wells in order to provide for a serum starvation period of 24 hours to cease active proliferation of the fibroblasts. At the end of the 24 hour period the serum free media was removed and DME H-16 supplemented with 5% fetal bovine serum containing TGF- β (R&D Systems) in the following concentrations 0, 0.1, 1, 5, 10, 20 ng/ml was added for 72 hours. At the end of that period the medium was removed and cells washed with cold PBS. Next, mRNA extraction was performed using an in-well extraction protocol (ABI, Life Technologies, Carlsbad, CA) Briefly, a lysis buffer is added to the wells for 5 minutes with a DNase treatment, this is followed by a stop buffer, which halts the reaction. The lysate is then added to an RT master mix, and a thermal cycler (ABI, Carlsbad, CA) was used to incubate and then inactivate the RT enzyme. Then an ABI real-time PCR instrument (ABI, Carlsbad, CA) was used to carryout the remainder of the Taqman[®] Gene Expression assay to include an UDG incubation period and an enzyme activation period followed by PCR cycling. The following mRNA gene expression levels were measured using assays from Taqman[®] Gene Expression Assays-on-Demand (ABI, Life Technologies, Carlsbad, CA), they included ACTA2 (smooth muscle actin, Cat# HS00426835_G1), CTGF (CCN2, connective tissue growth factor, Cat# HS01026927_G1), ET-1 (EDN1, endothelin-1, Cat# HS00174961_M1), EDNRA (Endothelin Receptor type A, Cat# HS00609865_M1), and EDNRB (Endothelin Receptor type B, Cat# HS00934968_G1).

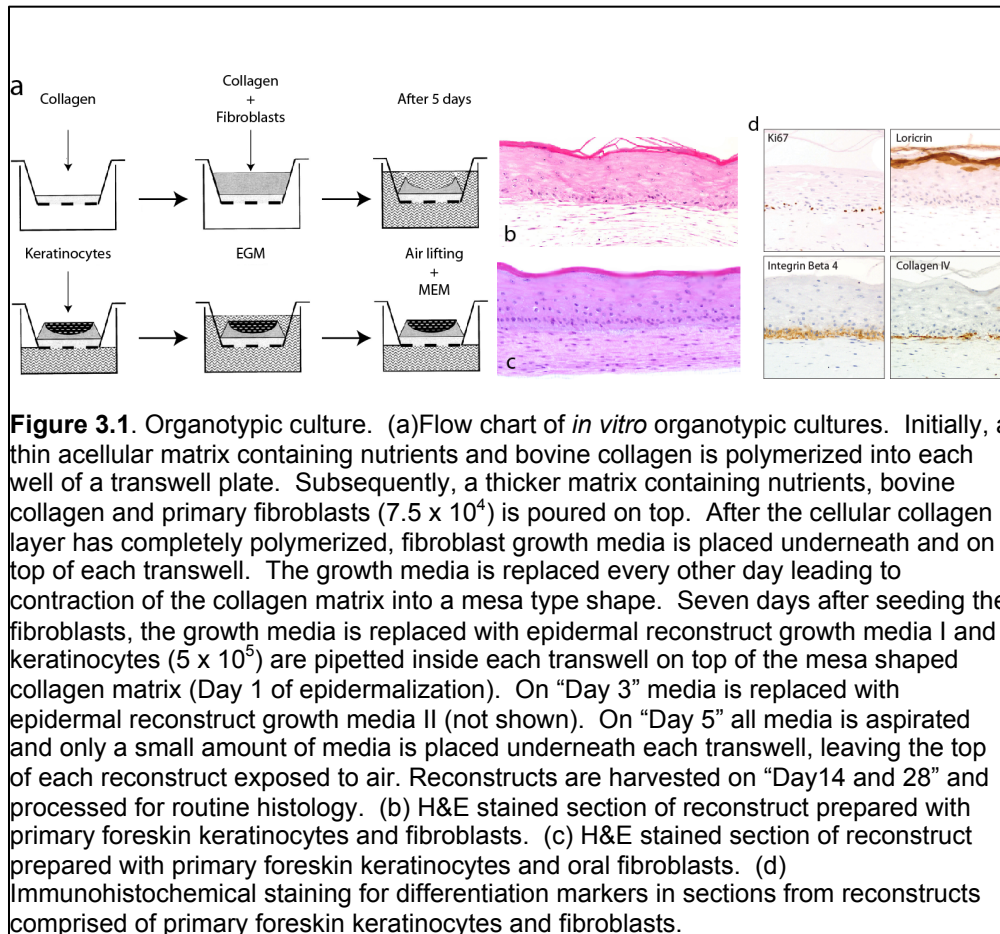
Results.

Disclosure: The first section in the results section was taken from a previously published report by Snijders *et al*, to which the author of this thesis made a minor contribution as indicated in the acknowledgements page.

Over-expression of GLI2, a gene amplified in oral SCC, blocks differentiation and induces transdifferentiation of fibroblasts into myofibroblasts.

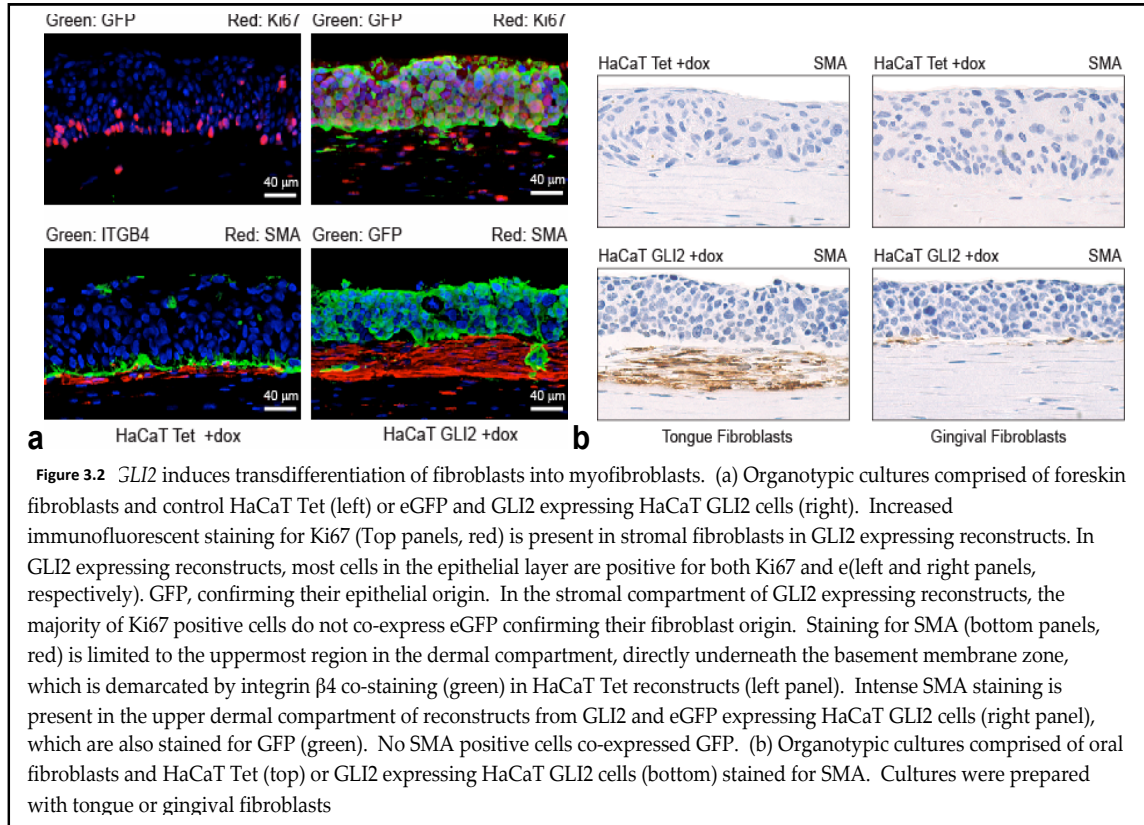
Oral SCC typically amplifies narrow regions of the genome. These genomic alterations identify genes likely to contribute to development or progression of this disease when over-expressed. To investigate the oncogenic functions of *GLI2*, a gene amplified in oral SCC, we have generated organotypic co-cultures using *GLI2* over-expressing HaCaT cells or normal HaCaT cells for the epithelial component with foreskin, tongue and gingival fibroblasts for the dermal component. The normal epithelial/dermal relationship is recapitulated in organotypic cultures. The preparation of these cultures is summarized in Figure 3.1a. In this model system, fibroblasts are initially cultured for a week in collagen gels submerged in tissue culture medium. Growth of the fibroblasts results in contraction of the collagen gel to form a cup. Keratinocytes are then added on top of the collagen/fibroblast layer and the co-cultures further propagated for four days, before exposure to air. Within three weeks, a stratified and differentiated epithelium is formed that recapitulates the phenotype of the tissue source of the cells. For example, when normal keratinocytes are cultured with foreskin fibroblasts they form a stratified epithelium with basal layers and differentiated layers including a stratum

granulosum and orthokeratotic stratum corneum. On the other hand, when cultures are prepared with oral fibroblasts a parakeratotic stratum corneum is present consistent with the normal differentiation of oral epithelia (Figures 3.1b and c). Immunohistochemical staining of differentiation markers shows appropriate expression of basal and suprabasal markers (Figure 3.1d).

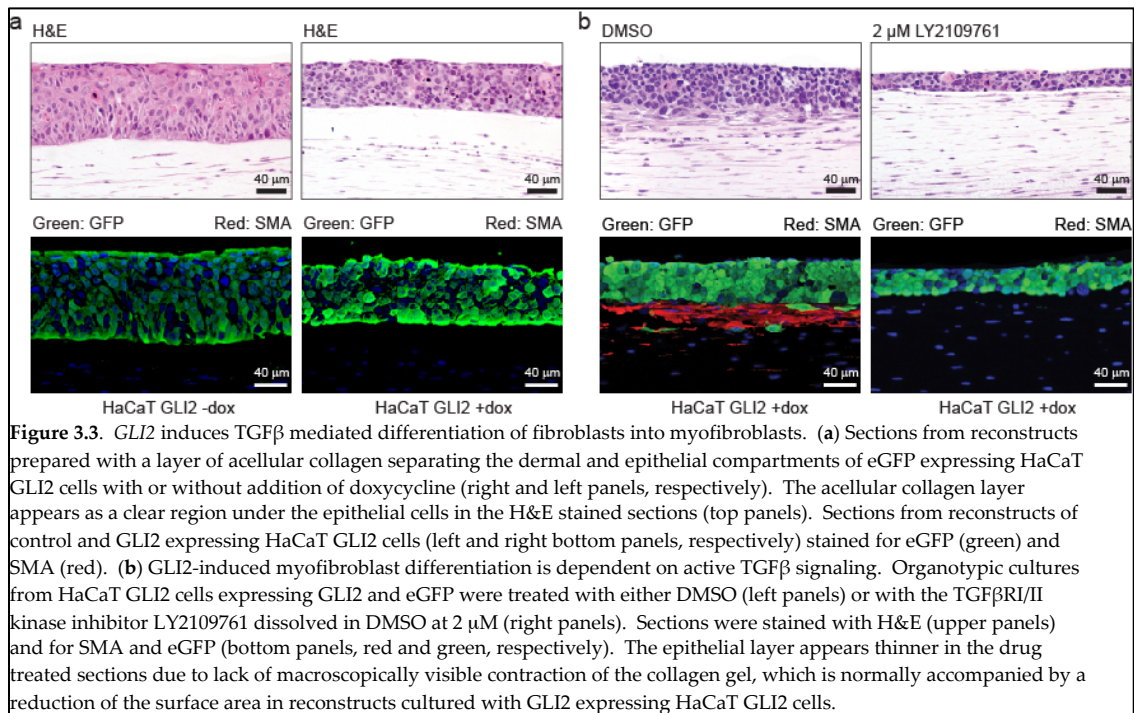


By contrast, in our experiments, we have observed that the *GLI2* over-expressing cells do not differentiate properly. They also are able to stimulate a desmoplastic response in a TGF- β dependent manner in the dermal compartment composed of foreskin and tongue fibroblasts. However, when gingival fibroblasts are used under

the same conditions there is no resultant desmoplastic reaction in the dermal compartment (Figure 3.2).



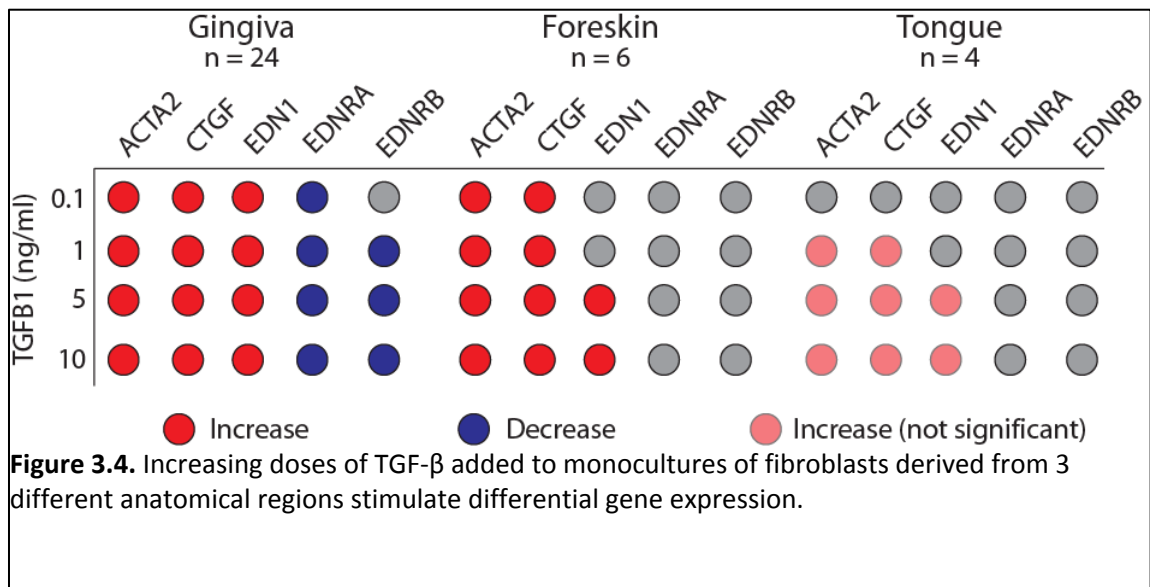
We have shown this response is TGF- β dependent, because it can be significantly attenuated by a specific TGF- β receptor II inhibitor (LY2109761) and by introduction of a dominant negative TGF- β receptor II construct lacking the kinase domain. Additionally, we have shown that this desmoplastic response is stimulated by the close proximity of the *GLI2* over-expressing keratinocytes because when a collagen layer separates the two compartments again the desmoplastic response is significantly reduced (Figure 3.3).



TGF- β dose response curves demonstrate differential responses in fibroblasts derived from anatomically diverse areas of the oral cavity.

In order to further explore the differential desmoplastic response between gingival and tongue fibroblasts to the presence of *GLI2* over-expressing cells, we have completed the TGF- β dose response curve for 26 separate primary cell strains in two-dimensional culture (Figure 3.4). Our observations comparing foreskin fibroblasts (n=6) with tongue (n=3) and gingival fibroblasts (n=10) show that the initial mRNA levels of SMA and CTGF are equivalent in magnitude. Endothelin-1 initial mRNA levels are lower for gingival fibroblasts compared to tongue and foreskin fibroblasts, which are equivalent. Opposite results are seen for the endothelin receptors, the initial mRNA levels of endothelin receptor type A are

lowest in tongue fibroblasts compared to gingival fibroblasts and foreskin fibroblasts which have the highest initial levels. However, for the endothelin receptor type B the lowest initial levels are seen in the foreskin fibroblasts compared to gingival and tongue fibroblasts, which demonstrated the highest initial levels of mRNA expression.



For the TGF-β dose response curves it appears that the maximal induction of SMA, CTGF and EDN1 occurred at the 1 ng/ml dose, but the EDN1 mRNA expression levels over the entire curve were lowest in gingival fibroblasts compared to foreskin and tongue fibroblasts which showed equivalent levels. There were opposing values seen in the dose-response curve results for the endothelin receptors. In response to increasing levels of TGF-β the EDNRA mRNA levels were overall higher in foreskin fibroblasts compared to tongue fibroblasts but the opposite was true for the EDNRB

mRNA levels which show that the tongue fibroblasts have overall higher levels compared to foreskin fibroblasts. However, for both the EDNRA and EDNRB the mRNA expression levels in the gingival fibroblasts significantly decreased through the increasing doses of TGF- β , whereas in tongue and foreskin fibroblast the mRNA expression levels increased.

When examining the mRNA expression levels in response to the initial induction dose of 0.1 ng/ml we observed that SMA and CTGF expression was highest in foreskin fibroblasts, next highest in gingival fibroblasts and lowest in tongue fibroblasts. For EDN1, EDNRB, EDNRA expression levels were higher in the gingival fibroblasts compared to foreskin and tongue fibroblasts, which were equivalent.

Discussion.

In an organotypic co- culture system, keratinocyte overexpression of GLI2 results in a TGF β 1 dependent differential desmoplastic response in tongue vs. gingival fibroblasts

This chapter has demonstrated that as a pleiotropic oncogene, *GLI2* overexpression in HaCaT cells in an organotypic culture system produces many of the hallmarks of an epidermal cancer and results in a differential response of fibroblasts derived from unique anatomical locations in the oral cavity (tongue vs. gingiva). Further, this differential response is TGF β 1 mediated as evidenced by the reduction in fibroblast α -SMA production with the addition of the TGF β receptor I/II kinase inhibitor, LY2109761. These observations suggest that there may be differential

intrinsic capabilities of the anatomically diverse fibroblasts to respond to TGF β 1 and indeed, we demonstrate differential expression of desmoplastic mediators in the TGF β 1 dose response curves.

The differential results of the TGF β 1 dose response curve are consistent with anatomic variations of the stromal fibroblasts derived from different areas of the oral cavity

Of the mediators whose mRNA expression levels were measured, α -SMA, CTGF and EDN1 seem to be universally elevated but, importantly, there were significant differences seen in the level of TGF β 1 required to increase expression of EDN1 to a level of significance. In particular, the gingival fibroblasts increased expression of EDN1 at a lower concentration of TGF β 1 compared to foreskin and tongue fibroblasts. This result would be consistent with the proposed role of EDN1 to act synergistically with TGF β 1 to up-regulate the production of ECM components in fibrotic disease states and it is also consistent given the specific functional demands placed on gingival tissue as compared to foreskin and tongue tissue. Gingival tissue is situated so as to receive nearly direct masticatory force and thus, one would expect the gingival fibroblasts that are responsible for making the ECM have an intrinsic ability to make ECM that is appropriate to withstand the forces placed upon it. So, in gingival fibroblasts, a smaller amount of TGF β 1, compared to foreskin and tongue fibroblasts, is required to up-regulate EDN1, its synergistic partner, resulting in a more exuberant production of fibrotic components through a feed-forward loop. Further, our result showing that there is a down-regulation of EDNR

(A and B) mRNA as a result of TGF β 1 stimulation, is entirely consistent with this theory and represents the feedback loop that is in place to ensure that the fibrosis is not overly exuberant by lowering the cells' responsiveness to EDN1 and essentially putting the brakes on the feed forward loop. Both the feed forward and feed back signaling mechanisms are in place to ensure the underlying dermis has an appropriate level of fibrosis to meet the site-specific functional demands. Not observing this relationship in tongue and foreskin fibroblasts does indicate that there maybe underlying site-specific differences in the stroma that explain the differences in the clinical characteristics of tumors which arise from varied locations in the oral cavity and that this is merely one example.

Future directions

In future chapters we will extend our characterization of the mRNA levels of just a few genes to profiling the entirety of the expressed mRNA and comparing a much larger set of tongue fibroblasts and gingival fibroblasts. We will be profiling carcinoma associated fibroblasts and, where possible, paired normal fibroblasts. If one believes the literature, that states that oral squamous cell carcinoma is associated with high levels of TGF β 1 compared to normal tissues⁸², by comparing CAFs with NFs we will be repeating the above experiment but on a larger scale. This will hopefully provide us with a larger picture of the TGF β 1 related signaling mechanisms and downstream mediators that contribute to the development of a carcinoma-associated microenvironment.

**Chapter 4: Immunofluorescence Study Seeking to Identify Carcinoma-
Associated Fibroblast Subsets and Cell-of-Origin.**

Introduction

The previous chapter discussed in detail the inherent differences in fibroblast biology based on anatomic site and that may contribute to the varied influences the CAFs have on the microenvironment surrounding a carcinoma. The potential influences are diverse, in a comprehensive review by Rasanen *et al.*, CAFs have been shown to have multiple pro-tumorigenic effects such as being a source of classical growth factors (EGF, TGF β and HGF) serving to directly stimulate tumor cell growth, having direct pro-metastatic effects possibly through the chemokine CCL5, maintaining homeostasis of the tumor microenvironment by serving as a buffer for the highly metabolic cancer cells, the recruitment and transformation of pro-tumorigenic inflammatory cells and even as a modifier of sensitivity of cancer cells to chemo or radiotherapy⁸³. It is noted that this research is largely based on defining a CAF via classic markers, namely, α SMA, vimentin and collagen I. However, recent literature suggests there are at least two subsets of CAFs, one is fibroblast specific protein-1 (FSP1) positive and negative for neuron-glia antigen-2 (NG2), α -SMA and platelet derived growth factor receptor beta (PDGFR β), the other group is just the opposite, positive for NG2, α -SMA and PDGFR β and negative for FSP1^{84,85}. Fibroblast activated protein (FAP) has also been used as a CAF marker and depending on the CAF population under study displays overlap with the above markers⁸⁶.

In addition to subset identification, different cells of origin for the CAFs have been proposed. The genesis of CAFs from the local fibroblast population was the original supposition⁸⁷ but evidence suggests that they may also arise from epithelium via

epithelial-to-mesenchymal transition⁸⁸, endothelium⁸⁹ and bone marrow stem cells⁹⁰. This all suggests that CAFs are actually a very heterogeneous population of cells with potentially different origins and functions. Having the ability to identify the different subsets and study their specific genetic expression profiles would lead to an increased understanding of how they contribute to tumor progression.

Further, verification that unique CAF subsets exist, may completely alter how we think about CAF influences on tumorigenesis. Thus, that is what we attempt to do in this chapter, we use immunofluorescence to label each of the fibroblast strains with antibodies specific for the above mentioned markers to attempt to identify subsets of CAFs and potentially their tissue of origin.

Methods

Fibroblast cell strains were grown to approximately 80% confluence in 10 ml of DMEM H16 with 10% FBS and were released from T75 culture flasks (Corning, NY) using 4ml of 0.25% trypsin, pelleted by centrifugation at 1 g for 3 minutes and re-suspended in 3ml of DMEM with 10% FBS. A haemocytometer (Reichert, Buffalo, NY) was used to determine the fibroblast concentration per ml so that 1×10^4 cells were plated in a volume of 2 ml of DME H-16 with 10% FCS on sterile glass cover slips in 6 well plates and allowed to attach overnight. Medium was aspirated and cells were washed with PBS for 3 minutes. Cells were fixed with acetone-methanol-formaldehyde (19:19:2, Sigma, St. Louis, MO) for 3 minutes and fixative was aspirated. Cells were washed twice with PBS Tween (1Liter PBS with 0.5 mL Tween

20, Sigma, St. Louis, MO) for 3 minutes each, and wash solution aspirated. Cells were incubated in 3% bovine serum albumin (BSA) for 30 minutes to block non-specific binding sites following which BSA was aspirated off. Cells were incubated in 50 μ L of primary antibody (1:100 dilution, see Table I) at RT for 2 hours. Primary antibody was washed off with 3 washes of PBS Tween with agitation for 5 minutes. Cells were incubated with 50 μ L secondary antibody (1:500 or 1:1000 dilution, see Table 4.I) for 30 minutes in the dark. Secondary antibody was washed off with 3 washes of PBS Tween with agitation for 5 minutes. Cover slips with attached cells were mounted in Vectastain DAPI (Vector Labs, Burlingame, CA), transferred to slides and imaged.

Table 4.1: The antibodies used to label the specific protein markers are listed along with their clonality, species host, species reactivity, the dilution it was used at and the associated catalogue number.

Primary Antibody	Clonality	Host	Species-reactivity	Dilution	Catalogue #	Company
α -Smooth Muscle Actin	Monoclonal (1A4)	Mouse	Human	1-100	M0851	Dako, Glostrup, Denmark
Fibroblast Activated Protein	Polyclonal	Rabbit	Human	1-100	ab53066	Abcam, Cambridge, MA
Fibroblast Specific Protein-1	Polyclonal	Rabbit	Human	1-100	ab40722	Abcam, Cambridge, MA
Neruon-glia Antigen 2	Monoclonal (9.2.27)	Mouse	Human	1-100	ab78284	Abcam, Cambridge, MA
Platelet Derived Growth Factor Receptor β	Monoclonal (Y92)	Rabbit	Human	1-100	ab32570	Abcam, Cambridge, MA
Vimentin	Monoclonal	Mouse	Human	1-100	129001	Invitrogen, Life Technologies, Carlsbad, CA
pan Cytokeratin	Monoclonal (AE1/AE3)	Mouse	Human	1-100	MAB3412	Millipore, Billerica, MA
	Monoclonal (CAM 5.2)	Mouse	Human	1-100	347653	BD Biosciences, San Jose CA
Secondary Antibody DyLight [®] 488	Polyclonal	Goat	Mouse	1-500	ab96879	Abcam, Cambridge, MA
Alexa Fluor [®] 488	Poylclonal	Goat	Rabbit	1-1000	A11008	Invitrogen, Life Technologies, Carlsbad, CA

Results

The immunofluorescence results verify the mesenchymal origins of the fibroblast strains with the majority having less than 1% of the cells positive for pancytokeratin whereas there was universal positivity for vimentin. (Table 4.2). There were two cell lines, which had approximately 10% of the cells positive for pancytokeratin100(OF77 and OF97). Figure 4.1 demonstrates the typical immunofluorescent pattern observed in the positive control cells, the immortalized keratinocyte line, HaCaTs (upper left panel), in contrast to the typically negative fibroblast strain

(upper right panel).The figure also shows that HaCaTs are negative for vimentin (lower left panel) whereas the filament-like cytosolic staining in the fibroblast strains (lower right panel) was always strongly positive.

Table 4.2: The table lists the fibroblast cell strains used, including tissue of origin, whether it was from normal tissue or carcinoma, the patient identification number (5/6 of the tongue pairs and 1/6 of the gingival pairs came from the same patient), the passage number and the percentage of cells that were positive for pancytokeratin and vimentin.

Name of sample	Tissue Type	NF/CAF?	Patient	Passage #	PK%	VM%
OF78	TONGUE	NF	B00072	5	1.6	100
OF77	TONGUE	CAF	B00072	5	9.8	100
OF82	TONGUE	NF	B00074	4	0	100
OF81	TONGUE	CAF	B00074	5	0	100
OF84	TONGUE	NF	B00077	4	0	100
OF83	TONGUE	CAF	B00077	4	0	100
OF100	TONGUE	NF	B00082	4	0	100
OF99	TONGUE	CAF	B00082	4	0	100
OF117	TONGUE	NF	K0083	3	0	100
OF116	TONGUE	CAF	K0083	3	0	100
OF6 TONGUE	TONGUE	NF	B00031	4	0.3	100
OF107	TONGUE	NF	T00010	3	0	100
OF 108	GINGIVA	CAF	B00087	3	1.8	100
OF35	GINGIVA	NF	T004	3	.7	100
OF6 GINGIVA	GINGIVA	NF	B00031	3	1.1	100
OF6 CAF	GINGIVA	CAF	B00031	3	0	100
OF40	GINGIVA	NF	T009	4	0	100
HN112	GINGIVA	CAF	B0001	4	1	100
OF50	GINGIVA	NF	T019	4	13	100
OF79	GINGIVA	CAF	B00073	5	0	100
OF49	GINGIVA	NF	T018	4	2.7	100
OF97	GINGIVA	CAF	B00081	4	10.1	100
OF47	GINGIVA	NF	T017	4	0.58	100
OF76	GINGIVA	CAF	B00070	4	3.3	100

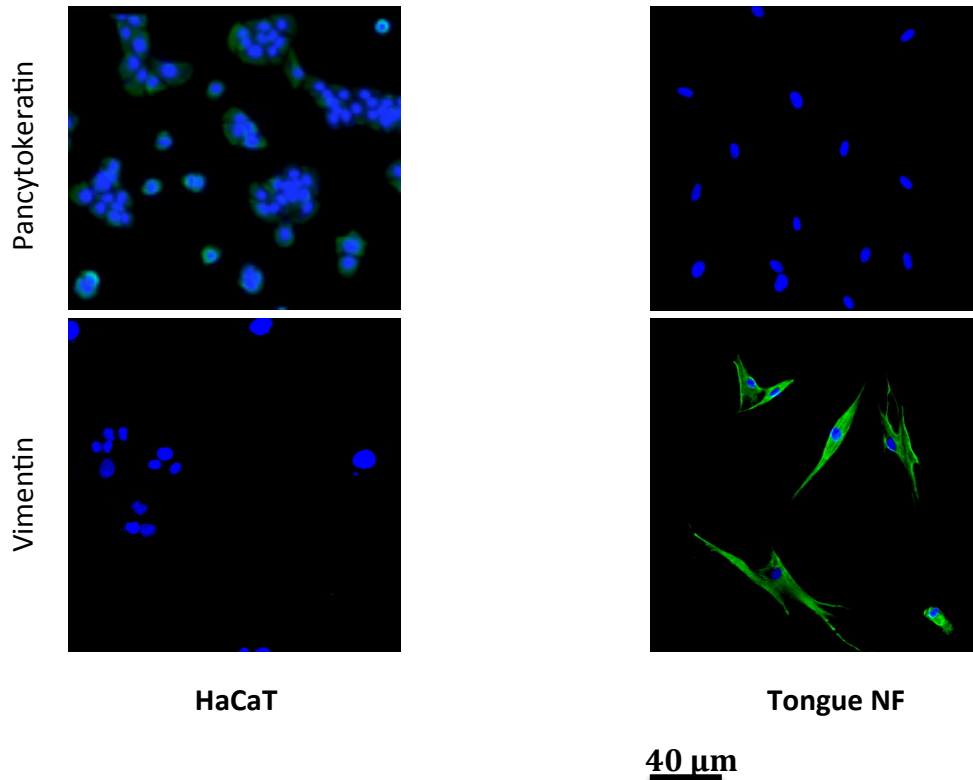


Figure 4.1: Upper left and upper right panels are pancytokeratin fluorescence in HaCaTs and tongue normal fibroblasts, respectively and the lower left and lower right panels are vimentin staining in HaCaTs, and tongue normal fibroblasts, respectively.

In order to investigate the possible origins of the various fibroblast strains and potentially identify subgroups of carcinoma-associated fibroblasts, additional primary antibodies were tested. (α -SMA, FSP-1, PDGFR β , FAP and NG2. Figure 4.2 and 3 demonstrate the typical immunofluorescent patterns for each of these antibodies in a strongly positive and weakly positive cell line (HaCaT) or fibroblast strain. α -SMA positivity is the hallmark of the “activated” fibroblast or carcinoma-associated fibroblast and appears as long intra-cytosolic fibers traversing the length of the cell (Figure 4.2 upper right panel). FSP-1 is located more diffusely within the cytosol but can have intense nuclear staining (Figure 4.2 lower right panel)

consistent with its known nuclear translocation upon activation. PDGFR β generally showed a bright punctate pattern (Figure 4.3 upper right panel), reflecting its role as a receptor located at the cell surface and the cytoplasm, NG2 typically demonstrated a diffuse pattern as well (Figure 4.3 lower right panel), however as seen in melanoma cell line, A375, there was a tendency for the signal to be much more intense at a leading edge. Finally, although several antibodies for FAP were tried, we failed to identify one that was reproducible, thus we were unable to characterize the fibroblast strains for this protein.

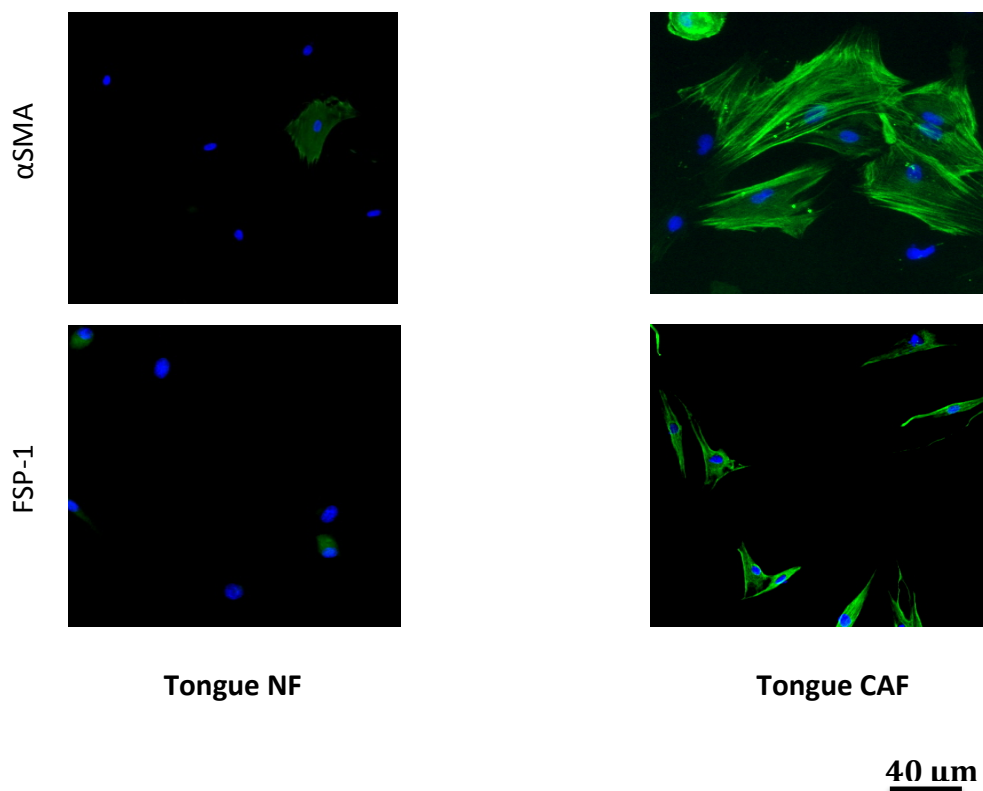


Figure 4.2: Upper left and upper right panels are α SMA fluorescence in tongue normal fibroblasts and carcinoma-associated fibroblasts, respectively and the lower left and lower right panels are FSP-1 staining in tongue normal fibroblasts and carcinoma-associated fibroblasts, respectively.

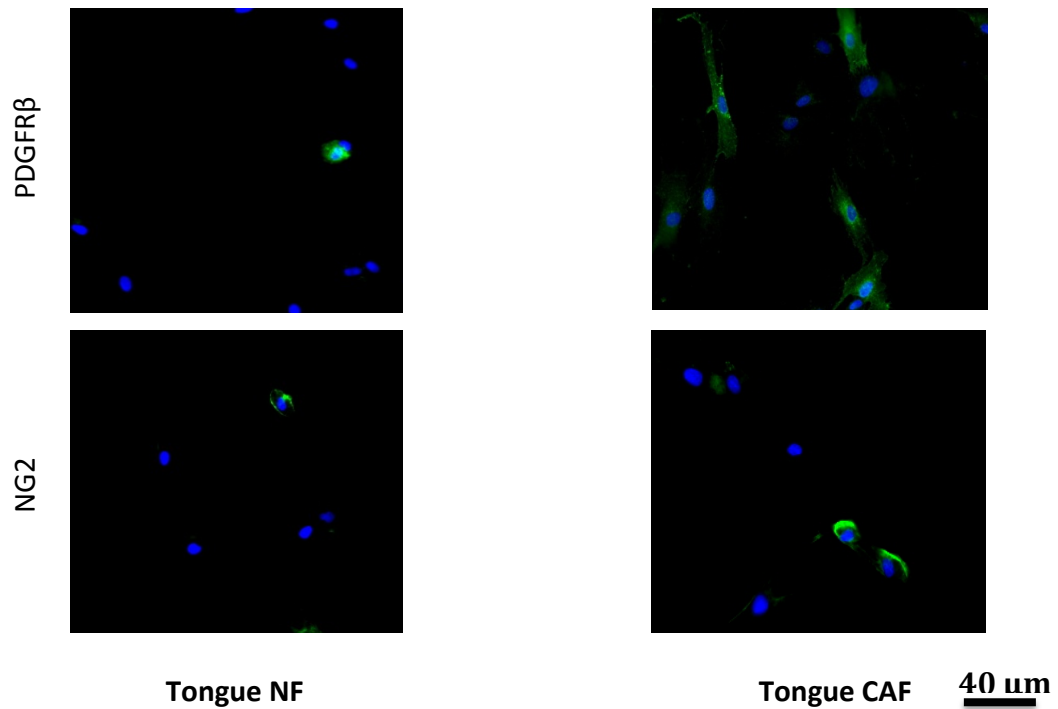


Figure 4.3: Upper left and upper right panels are PDGFR β fluorescence in tongue normal fibroblasts and carcinoma-associated fibroblasts, respectively and the lower left and lower right panels are NG2 staining in tongue normal fibroblasts and carcinoma-associated fibroblasts, respectively.

Analysis of the immunofluorescence for each of the 24 cells strains separated into tongue and gingival CAF groups versus NF groups reveals that there is a statistically significant difference in the α -SMA positivity in the gingival CAF strains compared to the gingival NF strains (32 ± 5 vs. 6 ± 2 , $p=0.0006$, student's t-test, Table 4.3 and Figure 4.4). Although there was a trend towards higher α -SMA staining in the tongue CAF group compared to the tongue NF group, there appeared to be too much variation in the data and thus significance was not reached (29 ± 11 vs. 13 ± 10 , N.S., Table 4.3 and Figure 4.4). Of the other three antibodies tested only NG2 seemed to have a trend towards significance in both the tongue and gingival CAF versus NF

comparisons (20±10 vs. 12±4 and 21±11 vs. 12±4, N.S., respectively Table3). Both FSP1 and PDGFRβ displayed roughly equivocal staining across the groups.

Table 4.3 Table 3 demonstrates the mean percentage ± standard error representing the positive fluorescence for each of the individual markers for each anatomic subgroup (n for each group is listed in Figure 4).

Immunofluorescence Results

	Tongue (mean%)			Gingiva (mean%)		
	CAF	NF	p	CAF	NF	p
αSMA	29±11	13±10	N.S.	32±5	6±2	p=0.0006
FSP1	58±16	72±4	N.S.	76±12	78±7	N.S.
NG2	20±10	12±4	N.S.	21±11	12±4	N.S.
PDGFRB	45±11	39±5	N.S.	32±9	25±10	N.S.
FAP	No suitable antibody available					

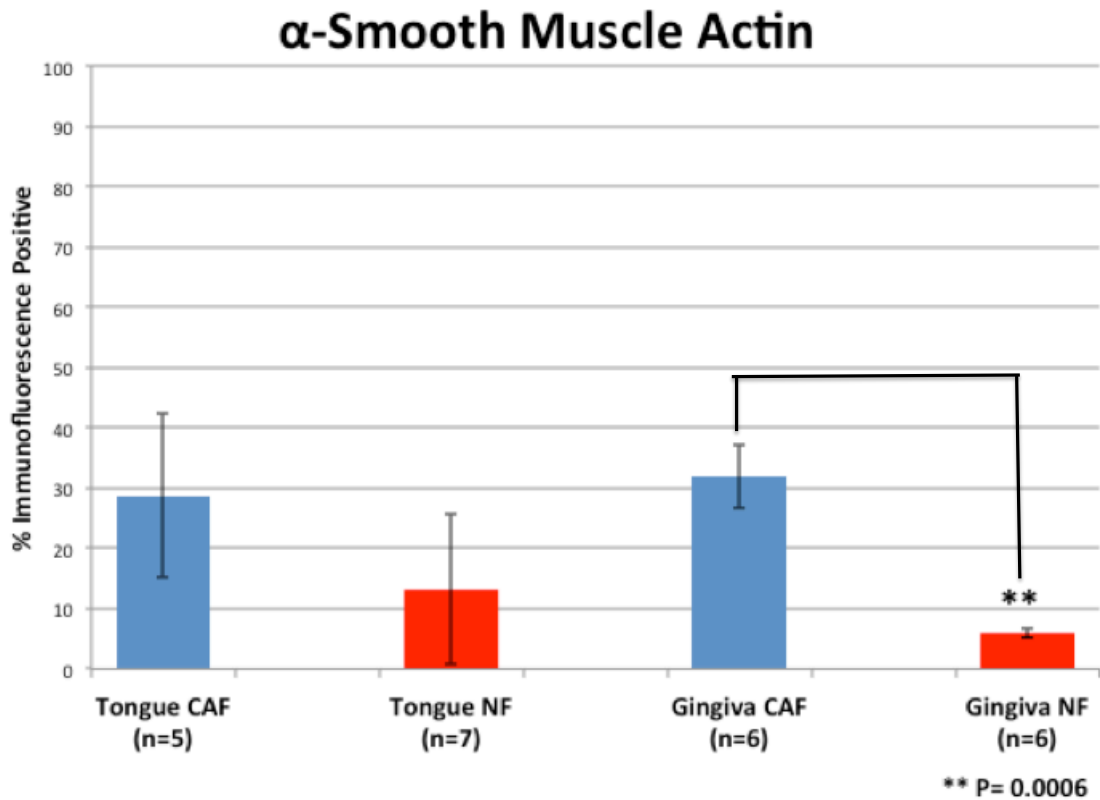


Figure 4.4 The figure represents the average percentage and standard error of α-SMA positive cells for each of the anatomic subgroups. The connecting bars represent a statistically significant difference between the gingival carcinoma-associated fibroblasts and gingival normal fibroblast populations.

Discussion

αSMA positively identifies CAF populations in the gingival subgroup

We have verified that αSMA is a reliable CAF marker in the gingival anatomic subgroup and there was a trend towards this in the tongue subgroup. The other markers assessed did not reach significance. Among the reasons for this is that despite labeling one of the largest collections of CAFs and NFs existing, the n is still

relatively small and variation in just one or two strains is enough to increase the standard deviation to the point where the differences no longer reach statistical significance. Additionally, although a low passage number was preferentially used in this study (between passage 3 and 5), cell culture is unavoidably artificial in the sense that the fibroblasts are grown from harvested tissue, removing them from the chemical milieu and forces they are normally exposed to. This may result in a certain number of the CAFs that were activated (positive α SMA), switching phenotypes to the inactivated form (negative α SMA) or also there could be a preferential selection for fast growing and dividing cells which may favor a larger number of non-activated fibroblasts in the strain population. There are additional concerns in tongue group, in which 5/6 of the CAF/NF pairs were same patient pairs, whereas there was only one such pair in the gingival group, where it becomes problematic to verify that the tissue of origin for the tongue NFs was from true “normal” tongue. CAFs are derived from tissue taken from the center of a cancer specimen and the NFs are grown from a piece of tissue taken from a site away from the tumor in clinically and histologically normal tissue. The problem is that unlike gingiva where one can obtain normal tissue from a truly distant site such as the contralateral side of the oral cavity, the tongue is more or less a tubular organ and it is difficult to get far enough away from the lesion to be sure you are in an unaffected zone, anatomy limits this. Secondly, and this is true for the gingiva as well, tumors secrete a wide variety of messengers such as cytokines and chemokines which may be intended to act locally but might also have distant effects. Additionally, cancers

also elaborate more exotic characters such as small RNA species, microRNA⁹¹, and exosomes, which have been detected in patients blood and saliva⁹² and recent work has implicating them in prepping distant sites to receive metastatic islands for propagation⁹³. So, there is a question as to what extent NFs are affected by these systemic influences elaborated by the tumor and whether or not they become more like CAFs in the process, thus, making it difficult to determine differences between the two populations. Despite all this, it is reassuring that we are able to identify differences between CAFs and NFs, in a statistically significant manor, in the gingival subgroup using α SMA as a marker. This indicates that although there maybe other markers of CAFs, α SMA is the most robust and perhaps the most suitable marker to use to delineate cells into a specific population, which gives more meaning to the molecular characterization of CAFs going forward. In fact, in the next chapter we use mRNA expression profiling to further characterize the differences between CAFS and NFs.

**Chapter 5: mRNA Expression Profiling of Carcinoma-Associated and Normal
Fibroblasts.**

Introduction.

For some time now, investigators have been measuring single genes, panels of genes and more recently, entire transcriptomes in order to discover the critical drivers of carcinomas. The majority of this work has focused on measuring RNA derived from either whole tumors or cultured tumor cell lines, which has left the stromal specific gene expression characteristics largely unknown. However, recent work has begun to investigate the gene expression characteristics of stroma as well as stromal CAFs and the results so far have been promising. One such study examined the gene expression patterns of the micro-dissected stroma of the well-characterized neoplastic progression of Barrett's esophagus to dysplasia and then finally, esophageal adenocarcinoma. These authors were able to identify stromal genes that discriminated pre-invasive disease from invasive disease and found that they were predictive of outcome⁹⁴. Still others have isolated fibroblast populations by primary cell culture from the carcinoma-associated microenvironment and compared them to normal fibroblasts and have reported results similar to ours, described in Chapter 4, namely that fibroblast populations are heterogeneous in nature with variability between individuals and even within the same individuals⁹⁵. Yet, despite this heterogeneity, other authors have gone on to draw useful conclusions from fibroblast gene expression data, including one group that demonstrated a correlation between the fibroblast gene expression profile and the genomic stability and stage of tumor progression of the associated oral squamous cell carcinoma⁹⁶.

Still others have used expression data in concert with functional studies to elucidate important gene signaling networks and mechanisms⁹⁷.

In this chapter we utilize the Affymetrix Human 1.0 ST Exon Array to develop an expression profile of each of the fibroblast cell strains we describe in Chapter 4. Using these data, we will attempt to identify differentially expressed genes that differentiate a CAF from an NF as well as tongue fibroblasts from gingival fibroblasts. With this information we will then be able to further describe the genes and their functions that are important in the tumor/stromal interaction and neoplastic progression.

Methods.

Fibroblast cell strains were grown to approximately 80% confluence in 10 ml of DMEM H16 with 10% FBS and were released from T75 culture flasks (Corning, NY) using 4ml of 0.25% trypsin, pelleted by centrifugation at 1 g for 3 minutes. The supernatant was aspirated and 2.5 ml of Trizol (Invitrogen, Life Technologies, Carlsbad, CA) was added with repeat pipetting to lyse the cells. Next, 1.25 ml of the Trizol cell lysis solution was placed in a 2 ml tube and then 0.25 ml of chloroform (Sigma, St. Louis, MO) was added, followed by 15 seconds of vigorous shaking and then a 3 minute incubation period at room temperature. The samples were centrifuged at 12,000 g for 15 minutes at 4°C to achieve phase separation. The aqueous phase containing the RNA was then pipetted into a new 2 ml tube into which 0.625 ml of isopropyl alcohol was introduced and then a 10-minute

incubation period at room temperature was followed by centrifugation at 12,000 g for 10 minutes at 4°C to precipitate the RNA into a gel-like pellet. The supernatant was then removed. The RNA pellet was washed with a 1.25 ml volume of 70% ethanol followed by centrifugation at 7,500 g for 5 minutes at 4°C. The supernatant was removed and the RNA pellet was allowed to briefly dry for 10 minutes. The RNA was then re-dissolved in 15-30 µl of water. All samples were then subjected to an RNA “clean-up” procedure utilizing an RNeasy® Mini Kit (Qiagen, Life Technologies, Carlsbad, CA) following the manufacturer’s recommendations which included an in-column DNase treatment. Next, the quality of the mRNA samples was evaluated using an Agilent Bioanalyzer (Wilmington, DE) and the concentration was measured using a Nanodrop instrument (Thermoscientific, Wilmington, DE). Samples that had A260/A280 and A260/A230 ratios above 1.8, total RNA (28S/18S) ratios above 1.6 and RNA integrity numbers (RIN) above 7 (Table I) were considered suitable for expression analysis using the Affymetrix Human ST 1.0 Exon Arrays. Analyses were carried out with 24 fibroblast strains by the Gladstone Institute’s Genome Core (Gladstone Institute, San Francisco, CA) following the manufacturer’s recommendations. Briefly, 100 ng of total RNA is aliquoted in a RNase free tube and added to that was the diluted poly A control, which was prepared by making serial dilutions of the GenChip PolyA controls using the polyA dilution buffer supplied with the kit, to a final concentration of 1:50,000 of the original stock. Next, a master mix composing of 1 µl ribominus probe and 30 µl of the betaine buffer is added and incubated at 70°C for 5 minutes and then placed on ice. Then 50 µl of the

resuspended bead solution is placed into a fresh tube with 50 μ l of RNase-free water added and spun down, the supernatant was aspirated and discarded and the process was repeated. The beads were then resuspended in the hybridization buffer with the betaine solution, followed by centrifugation and resuspension of the beads in

Table 5.1. Characteristics of the CAF/NF strains and the quality control measurements of the associated total RNA as measured by the Nanodrop and Bioanalyzer instruments.

Name of sample	Tissue Type	NF/ CAF?	Patient ID	Passage #	Concentration of	Vol of	A_{260}/A_{280} ratio	RIN of
					Total RNA (ng)	Total RNA (ul)	of Total RNA	Total RNA
OF78	TONGUE	NF	B00072	5	98 ng/ul	30 ul	2.1	9.9
OF77	TONGUE	CAF	B00072	5	224 ng/ul	30 ul	1.99	9.5
OF82	TONGUE	NF	B00074	4	29 ng/ul	30 ul	2.11	9.6
OF81	TONGUE	CAF	B00074	5	30 ng/ul	30 ul	2.1	9.9
OF84	TONGUE	NF	B00077	4	214 ng/ul	30 ul	1.98	9
OF83	TONGUE	CAF	B00077	4	117 ng/ul	30 ul	2.08	9.1
OF100	TONGUE	NF	B00082	4	76 ng/ul	30 ul	1.86	7.8
OF99	TONGUE	CAF	B00082	4	77 ng/ul	30 ul	1.93	8.8
OF117	TONGUE	NF	K0083	3	382 ng/ul	30 ul	2.08	9.5
OF116	TONGUE	CAF	K0083	3	372 ng/ul	30 ul	2.06	9.7
OF6 TONGUE	TONGUE	NF	B00031	4	119 ng/ul	30 ul	1.88	8.9
OF107	TONGUE	NF	T00010	3	259 ng/ul	30 ul	2.09	9.6
OF 108	GINGIVA	CAF	B00087	3	54 ng/ul	30 ul	2.14	9.7
OF35	GINGIVA	NF	T004	3	469 ng/ul	30 ul	2.06	9.9
OF6 GINGIVA	GINGIVA	NF	B00031	3	98 ng/ul	30 ul	1.82	9.4
OF6 CAF	GINGIVA	CAF	B00031	3	39 ng/ul	30 ul	1.57	7.1
OF40	GINGIVA	NF	T009	4	87 ng/ul	30 ul	1.88	8.9
HN112	GINGIVA	CAF	B0001	4	51 ng/ul	30 ul	n/a	9.4
OF50	GINGIVA	NF	T019	4	79 ng/ul	30 ul	1.76	9.5
OF79	GINGIVA	CAF	B00073	5	98 ng/ul	30 ul	2.04	9.4
OF49	GINGIVA	NF	T018	4	80 ng/ul	30 ul	1.87	n/a
OF97	GINGIVA	CAF	B00081	4	160 ng/ul	30 ul	2.06	8.5
OF47	GINGIVA	NF	T017	4	93 ng/ul	30 ul	1.84	8.7
OF76	GINGIVA	CAF	B00070	4	127 ng/ul	30 ul	1.98	9.4

20 µl of hybridization buffer with betaine and incubated at 37°C for 10 minutes mixing once during the incubation. Next, the master mix is combined with the bead suspension and incubated at 37°C for 10 minutes, this is then transferred to a fresh tube as the rRNA reduced sample. Then 350 µl of cRNA binding buffer from the GenChip IVT cRNA cleanup kit is added to each rRNA reduced sample, vortexed and 250 µl of 100% ethanol is added and run through the IVT cRNA cleanup column, centrifuged at 15s at 8,000xg, a wash buffer is then added followed by another 15 s centrifugation, the same process is followed with 80% ethanol. Lastly, 11 µl of RNase-free water is added directly to the membrane, spun at 20,000x for 1 minute to elute the rRNA reduced total RNA/PolyA RNA control mix. Then we checked the samples on a bioanalyzer to ensure that the ribosomal peaks are reduced, there should be greater than 80% reduction followed this.

For synthesis of labeled cDNA a dilution of the supplied t7-(N)₆ primers was added to the rRNA reduced total RNA/Poly A RNA control mix, spun down, and incubated for 5 minutes at 70°C followed by 2 minutes at 4°C and then placed on ice. The double-stranded cDNA was prepared using the GeneChip WT cDNA synthesis kit as per the manufacturer's protocol, which is converted to complimentary RNA by *in vitro* transcription using the GeneChip WT cDNA amplification kit as per the manufacture's protocol, this typically yielded 1.5 to 3 µg of cRNA. The cRNA is then reverse transcribed back to cDNA using random primers and a 10 mM nucleotide mix containing dNTP and dUTP, which is fragmented using Uracil DNA glycolase and human apurinic/apyrimidine endonuclease fragmenting the cDNA reproducibly at

locations where dUTP is incorporated and this is labeled using terminal deoxynucleotide transferase (TdT) and the kit supplied DNA labeling reagent that is linked to biotin. Lastly, the labeled cDNA is mixed with 20x eukaryotic hybridization controls, denatured and hybridized to Human Exon 1.0 ST arrays as recommended in the kit and after 18 hours of hybridization the arrays are subjected to a fluidics protocol that washes and stains the array with streptavidin phycoerythrin. The arrays are then scanned in a GeneChip 3000G scanner and data is exported as CEL files.

The 24 samples were hybridized to the Affymetrix GeneChip Human Gene 1.0 ST Array. Each of the 28,869 genes on the array is represented by approximately 26 probes dispersed across the length of the gene. Only perfect match probes are included on the array. Gene-level and exon-level expression summaries were derived using the Robust Multichip Average (RMA) method⁹⁸. The RMA method was utilized through the Affymetrix Power Tool software suite. In particular, the program apt-probeset-summarize program was used. All arrays passed quality control cutoffs.

The 10% of genes (2887) with the highest variance were clustered. Traditional hierarchical agglomerative clustering of both samples and genes was utilized. In this form of clustering, every object (sample or gene) begins as its own cluster. The two closest objects are clustered, and this process is repeated iteratively until all objects are in a single cluster. A dendrogram describes the order in which samples clustered and a heat map shows the patterns of the expression values in the

clustering. The distance metric used was one minus correlation and the linkage method was Ward's method. A cluster of genes that had particularly strong expression was examined for over-representation of gene themes using DAVID⁹⁹. The samples were taken either from tongue or gingiva and were either cancer-associated fibroblasts (CAFs) or normal fibroblasts (NFs). There were 5 tongue CAFs, 7 tongue NFs, 5 gingiva CAFs, and 6 gingiva NFs. Because all the tongue CAFs were paired with tongue NFs, differences in expression between CAFs and NFs for the tongue samples were assessed in a paired manner. The gingiva samples of CAFs and NFs were unpaired so an unpaired analysis was undertaken. For CAF samples, differences were identified between the tongue and gingiva, and a similar analysis was performed for the NF samples. These comparisons were unpaired.

The Limma method¹⁰⁰ was used for all the differential expression analyses. This test is based on the moderated t-statistic. In this statistic, the standard error is calculated by borrowing strength across genes. This can be helpful for small sample sizes for which it can be difficult to properly estimate it for every gene. The cutoff for significance was a p-value less than 0.001. With nearly 30,000 genes, approximately 30 genes would be expected to be significant even if there was no signal in the data.

For the validation study, the total RNA used for the mRNA expression profiling was assayed using the Qiagen (SABiosciences, Frederick, MD) RT² Profiler Custom PCR array in a 384-well format; the genes selected for validation are shown in Table 2. The quality of the total RNA was assessed as described above for the expression

arrays as well as run with the RT² Profiler QC PCR array to ensure appropriate performance of the RNA with Qiagen's SYBR Green probes. Both the QC PCR array and the custom array have the same protocol for preparing the cDNA and PCR mixes and briefly are as follows, the genomic DNA elimination mix is prepared and centrifuged, incubated for 5 minutes at 42° C and then placed on ice for 1 minute. Next, the reverse-transcription mix is made and is added to each tube containing the genomic DNA elimination mix followed by an incubation at 42° C and then 95° C to stop the reaction. RNase-free water is added and the reactions are placed on ice and then the real-time PCR protocol was followed using an aliquot of the diluted cDNA template. Next, the RT² SYBR Green Mastermix, water and cDNA synthesis reaction is centrifuged and then the PCR component mixes are added into the RT² RNA QC PCR Array, the array is sealed and centrifuged at 1000xg for 1 minute to remove any bubbles and then placed in the Applied Biosystems real time cycler. Lastly, the C_T values for all wells were exported to a blank Excel® spreadsheet for analysis with the RT² RNA QC PCR Array Data Analysis Excel template and the RT² Profiler qPCR Array Data Analysis template.

SAMPLE		↓ 96-well →																					
		1	2	3	4	5	6	7	8	9	10	11	12	13	14	15	16	17	18	19	20	21	22
cDNA template	A	HK1				HK1				HK1				HK1				HK1					
	B	HK2				HK2				HK2				HK2				HK2					
	C	RTC				RTC				RTC				RTC				RTC					
	D	PPC				PPC				PPC				PPC				PPC					
	E	GDC				GDC				GDC				GDC				GDC					
	F	NRT				NRT				NRT				NRT				NRT					
	G	PPC				PPC				PPC				PPC				PPC					
	H	NTC				NTC				NTC				NTC				NTC					
RNA	F	NRT				NRT				NRT				NRT				NRT					
H ₂ O	G	PPC				PPC				PPC				PPC				PPC					
	H	NTC				NTC				NTC				NTC				NTC					

Figure 5.1. RT² RNA QC PCR Array layout. Row A contains replicate assays for a highly expressed housekeeping gene, HK1 (the ACTB gene). Row B contains replicate assays for a lowly expressed housekeeping gene, HK2 (The HPRT1 gene). Expression levels of these housekeeping genes enable prediction of C_T values in future analyses and assessment of RNA integrity. Row C contains replicate assays for the reverse transcription control (RTC), which test the efficiency of the RT² First Strand Kit. These assays detect external RNA control template built in to the RT² First Strand Kit. Rows D and G contain replicate positive PCR controls (PPC), which comprise an artificial DNA sequence and the assay that detects it. Template cDNA is added to row D and water is added to row G. This tests for PCR inhibitors. Row E contains replicate assays for the genomic DNA control (GDC). These assays specifically detect nontranscribed genomic DNA contamination with a high level of sensitivity. Row F contains replicate assays for the no reverse transcription control (NRT). These assays test for genomic DNA contamination in the RNA sample by trying to amplify a housekeeping gene directly from the RNA sample. Row H contains replicate assays for the no template control (NTC). These assays test for general DNA contamination in the PCR system introduced during plate setup. During experimental setup, template cDNA and master mix are added to rows A-E; RNA and master mix are added to row F; and master mix only is added to rows G and H. The 384-well format of the RT² RNA QC PCR Array includes 4 replicates of each well of the 96-well format.

Results.

All 24 RNA samples pass rigorous quality control measures.

The results of the quality control steps are shown in Table 5.1. The majority of the samples passed with A_{260}/A_{280} ratios above 1.8 and acceptable RNA integrity numbers above 7 which were generated on a bioanalyzer, that also generated an electropherogram with sharp peaks for the 18S and 28S ribosomal RNA with no shoulders or smearing of the associated bands indicating degradation of the sample. The two samples with low A_{260}/A_{280} ratios, OF6 CAF and OF50, had acceptable RIN numbers and very reasonable bioanalyzer tracings and bands, so it was decided to proceed with these samples. It is notable that our original protocol did not include a DNase digestion step and that there were samples that had significant genomic DNA contamination resulting in failure of the quality control measures, specifically the bioanalyzer electropherogram and RIN number. We altered the protocol to include an RNA purification step using the RNeasy Mini Kit with an on-column DNase digestion step, which resulted in a high pass rate for the RNA samples.

Unsupervised hierarchical clustering of the top 10% most differentially expressed genes in the entire data set indicates possible clustering in the tongue versus gingival groups.

Using the statistical analysis described in the methods, the top 10% most differentially expressed genes in the entire data set were subjected to unsupervised

hierarchical clustering in an attempt to define group specific clusters based on those genes. Although there was nothing statistically significant there was an indication of

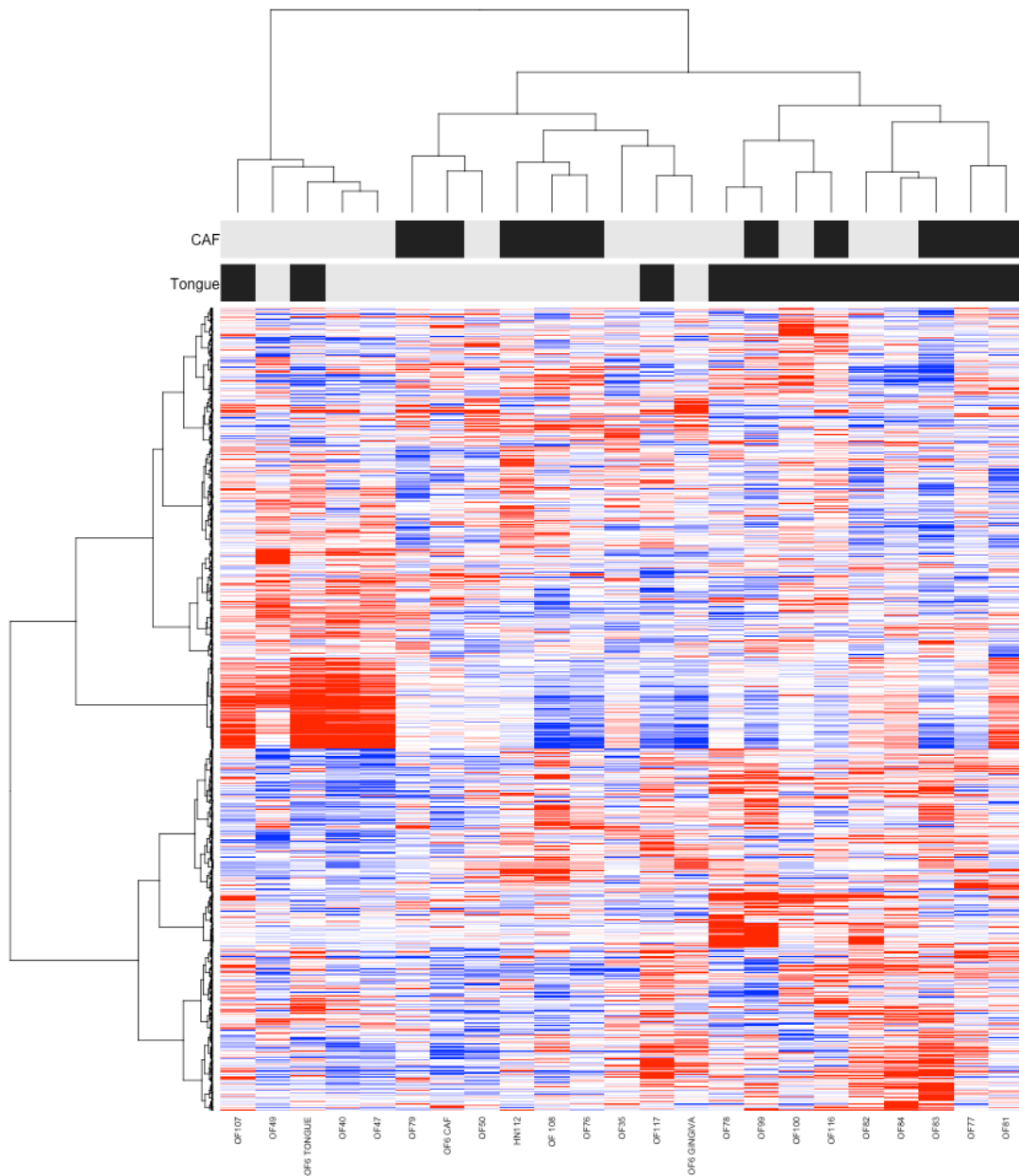


Figure 5.2. Unsupervised hierarchical clustering of top 10% most differentially expressed genes in the entire 24-sample data set. Top row CAFs are black, NFs are white and bottom row tongues are black and gingiva is white. This reveals the heterogeneous nature of the fibroblast populations; there is an indication of clustering in the tongues versus the gingival groups. Red represents areas of over-expression and blue under-expression.

clustering between the tongue and gingiva groups (Figure 5.2). As described in detail in Chapter 4, the reasons for this most probably reflect the relatively small n and also the very heterogeneous nature of the fibroblast strains themselves. Such fibroblast gene expression heterogeneity has been described for other tumors such as for breast cancer ^{95,101}.

There is an indication of group clustering between the gingiva CAFs and NFs.

When examining the results of the unsupervised hierarchical clustering of the top 10% most differentially expressed genes within the gingival data set, there does seem to be clustering in the gingiva CAFs compared to the gingiva NFs. As for the entire data set there is no statistically significant clustering, however this is consistent with the results seen for the total data set (Figure 5.3). This is contrary to the results of the unsupervised hierarchical clustering within the tongue groups, where there was not even a clear indication of separation between the CAFs and NFs (Figure 5.4).

Ten genes have been identified as being differentially expressed between the gingival CAF and NF groups.

Based on the level of fold change in expression and the significance level, ten genes have emerged as being differentially expressed between the gingival CAF and NF groups. All ten of the genes display a higher level of expression in the gingival CAFs

compared to the gingival NFs and their differential expression is demonstrated in Figure 5.5. Of the genes (*ACTA2*, *OLFML1*, *USP53*, *RHOJ*, *PHLDB2*, *TNSF18*, *FLJ21075*, *CYYR1*, *TIAM1*, *TUFT1*), it is most reassuring that *ACTA2* appears as more highly expressed in the gingival CAFs compared to the gingival NFs, this verifies the

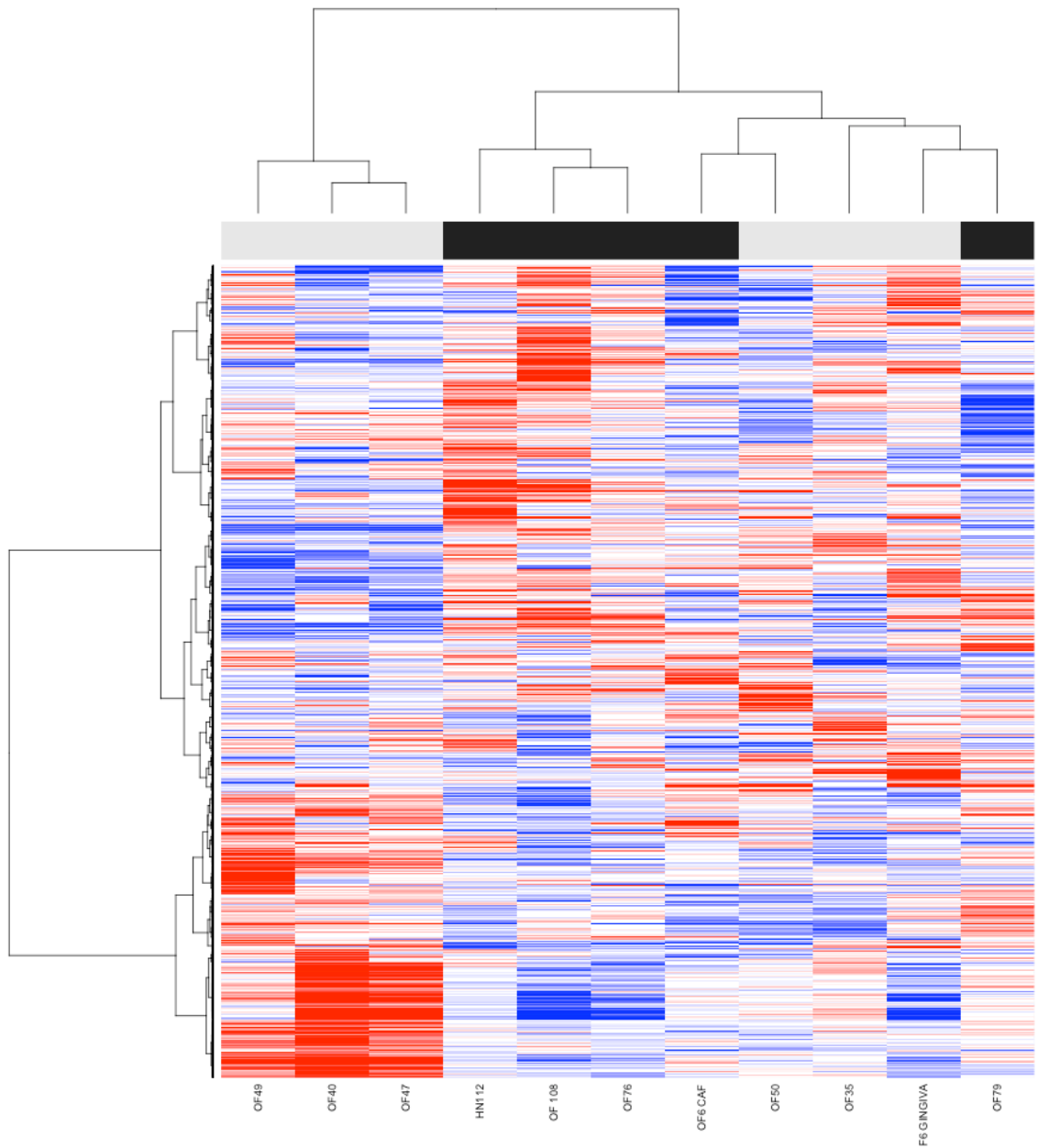


Figure 5.3. Unsupervised hierarchical clustering of top 10% most differentially expressed genes among the gingival data set. CAFs are black and NFs are white. There does seem to be clustering indicating differential expression between the CAFs and NFs in the gingival group.

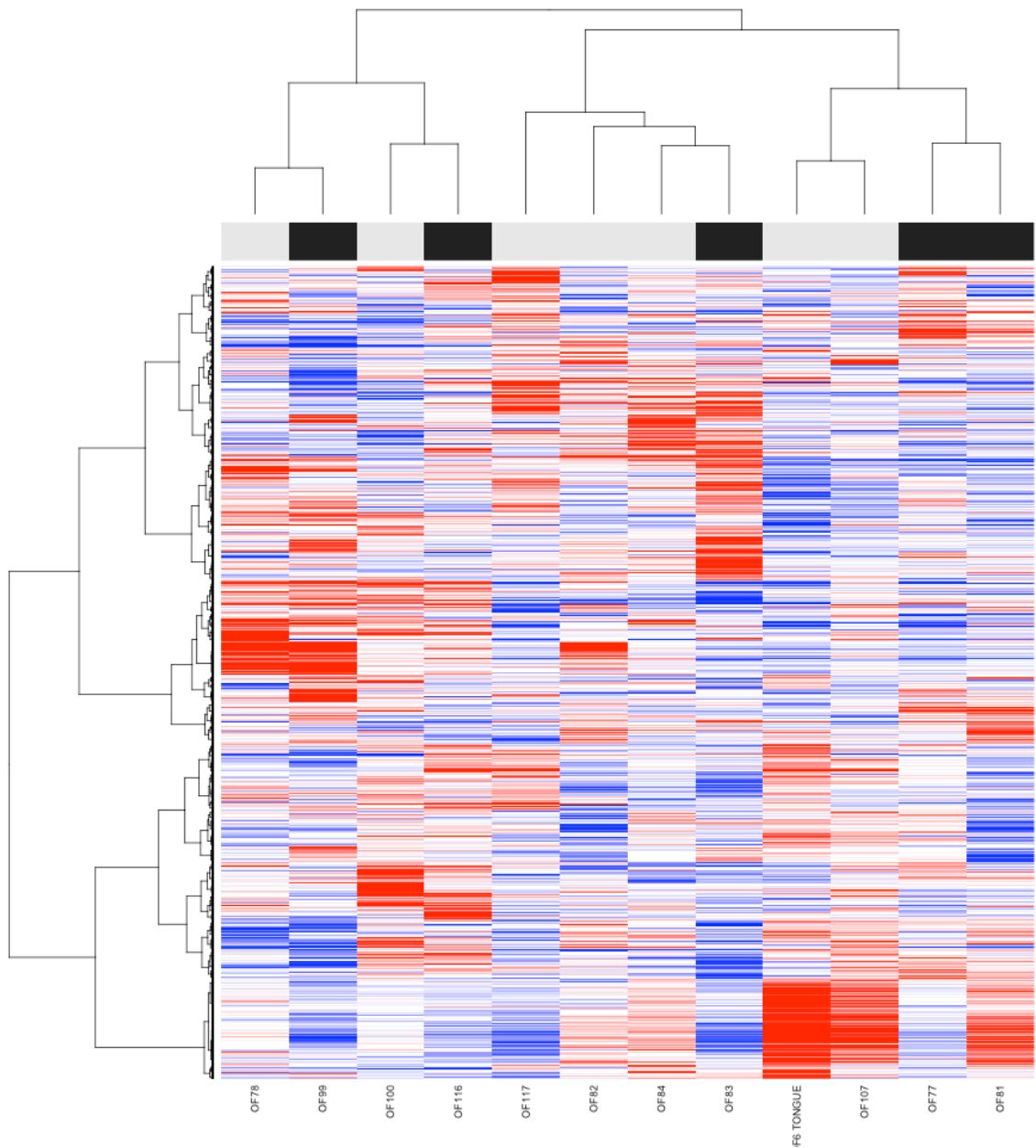


Figure 5.4. Unsupervised hierarchical clustering of top 10% most differentially expressed genes among the tongue fibroblast data set. CAFs are black and NFs are white. The expression in this group is very heterogeneous with no apparent clustering appreciated.

findings in Chapter 4 as well as being consistent with the established literature^{94,102}, which describes the over-expression of α SMA (ACTA2) in CAFs compared to NFs in the stroma surrounding tumors.

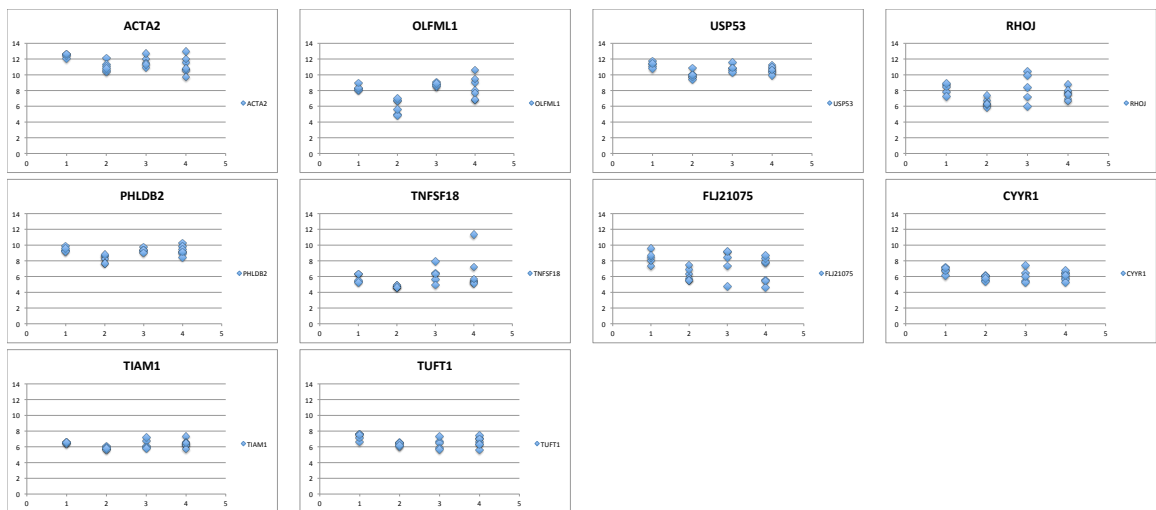


Figure 5.5. Ten genes were identified as being differentially expressed based on the level of fold change in expression and the significance level for gingival CAFs compared to gingival NFs. There were no such genes identified for the tongue anatomic subgroup. For each panel; column 1 represents gingival CAFs, column 2 represents gingival NFs, column 3 represents tongue CAFs and column 4 tongue NFs.

Eight genes have been identified as being differentially expressed between the tongue and gingival groups.

In comparing the total tongue group with the total gingiva groups (CAFs and NFs, together) one finds seven genes that have a lower expression in the gingival group (*MEIS2, PDPN, ZNF608, FHL1, ALDH1A1, TXNDC16, LAMB1*) and only one gene had a lower expression in the tongue group (*MAB21L2*, Figure 5.6). The gene specific function and possible implications for cancer for both groups of differentially expressed genes are given in Table 5.2.

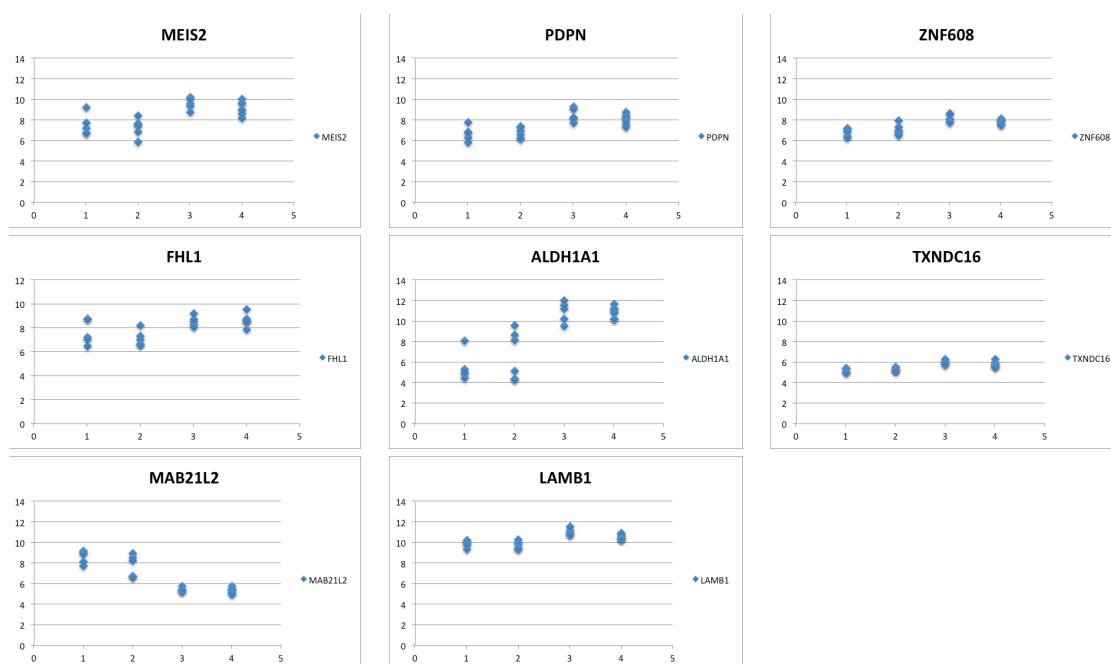


Figure 5.6. Eight genes were identified as being differentially expressed based on the level of fold change in expression and the significance level for tongue fibroblasts compared to gingival fibroblasts. For each panel; column 1 represents gingival CAFs, column 2 represents gingival NFs, column 3 represents tongue CAFs and column 4 tongue NFs.

The qPCR validation study affirms the differential expression of the genes in the gingival CAF/NF and the tongue/gingival groupings.

The total RNA from all 24 samples was run on the RT² RNA QC PCR Array to test for RNA integrity and to ensure there was an acceptable level of contamination (Figure 5.1). The results of this quality control measure indicated that OF6 CAF, OF50 and OF108 RNA were not acceptable and they were excluded from further analysis (Supplementary Data A). This did not reflect the RNA quality of the samples used for the Affymetrix expression array because those samples each passed their own independent quality control measures both prior to array loading (Nanodrop and

Bioanalyzer) and internal controls built into the array. Table 5.3 lists the genes that were included in the validation study, of note there are only 15 genes that were validated, this was due to the limitations of the qPCR array, which could only accommodate a total of 16 genes, including a housekeeping gene. Three genes were excluded from the validation study either due to a marginal differential expression or a paucity of literature to identify functional significance.

Of the seven genes from the gingival CAF/NF grouping, six were validated as being differentially expressed. In addition, *ACTA2* and *C7orf69* were differentially expressed in the CAF/NF grouping and *OLFML1* was differentially expressed in the tongue/gingiva grouping. Of the eight genes from the tongue/gingiva grouping, six were validated as being differentially expressed with no additional significance differences in any of the other groupings.

Exon-level microarray analyses of the 18 identified differentially expressed genes did not reveal alternative splicing.

Often, genes will display alternative splicing events, which produce alternative transcripts that may be undetected with conventional mRNA expression quantification methods such as a typical Taqman® assay, which has a defined set of probes and primers that identify a transcript over a specific region. In such a situation, if an alternative splicing event occurs outside of this defined region, the message may not be accurately quantified. Past authors have identified alternative

Table 5.2. The gene symbol, function and relevance to cancer are listed in the table. The gene symbols and associated references are as follows; ACTA¹⁰⁵, OLFML1¹⁰⁶, RHOJ¹⁰⁷, PHLDB2¹⁰⁸, C7orf69¹⁰⁹, Tiam1^{110,111}, MEIS2¹¹², FHL1¹¹³, PDPN¹¹⁴, MAB21L2¹¹⁵, ALDH1A1^{116,117}, LAMB1^{118,119}, ZNF608 and TXNDC16¹²⁰

Gene Symbol	Gene Function	Gene Relevance to Cancer
ACTA2	highly conserved protein being a major constituent of the contractile apparatus	hallmark of a carcinoma-associated fibroblast
OLFML1	highly N-glycosylated secreted protein may play a role in cell proliferation	has been shown to increase proliferation of cancer cells
RHOJ	regulation of the assembly of cytoskeletal components during cell proliferation and motility and the establishment of cell polarity	involvement in cell transformation and metastasis
PHLDB2	C-terminal Pleckstrin homology domain that binds phosphatidylinositol (3,4,5)-triphosphates	PI3 kinase pathway has been implicated in many stages of cancer
C7orf69	hypothetical protein FJ121075	unknown
CYR1	unknown function	has alternative splicing and expressin in human neuroendocrine tumors
TIAM1	guanine nucleotide exchange factor	regulates cell adhesion, migration and apoptosis in colon tumor cells
MEIS2	myeloid ecotropic insertion site 2 a homeodomain protein with a conserved homothorax domain	may co-operate with proto-oncogenes in T-cell leukemia
FHL1	four and a half LIM domain protein 1, LIM domain is a protein-interaction motif involved in linkining proteins with both the actin cytoskeleton and transcriptional machinery	expression is suppressed in a variety of cancers
PDPN	transmembrane glycoprotein	expression linked to increased cell migration and invasiveness, possibly through interaction with CD44
MAB21L2	male abnormal 21 family, may interact with SMAD1	possible influence on the TGFβ superfamily
ALDH1A1	metabolize a wide spectrum of endogenous and exogenous alphatic and aromatic aldehydes	cancer stem cell marker, predicts poor survival in multiple tumor types including head and neck cancer
LAMB1	laminin β1 chain genes, extracellular matrix glycoprotein, functions in cell adhesion, cell migration, proliferation, differentiation and tumor metastasis	identified as a contributing gene in metastasis in an oral cancer cell line
ZNF608	unknown function	unknown
TXNDC16	thioredoxin-related transmembrane protein	part of the thioredoxin-thioredoxin reductase system known to be involved in oncogenesis and tumorigenesis

splicing events that differed between tumors and normal tissue¹⁰³ with such discoveries possibly leading to development of protein isoform specific markers or even targeted cancer treatment¹⁰⁴. The Affymetrix Human 1.0 ST Exon Array is designed to have multiple probes across the entire transcript (in the range of 30-50 probes), which allows for alternative transcript detection. However, analysis of the 18 genes that were determined to be differentially expressed failed to reveal any alternative splicing events and no alternative transcripts (Supplementary Data B).

Table 5.3. Validation of 15 of the differentially expressed genes from figures 5.4 and 5.5. The SABiosciences catalog numbers are listed along with the gene symbol, alias, Refseq # and official full name. RPL13A is the control gene for the 384 RT² Custom Profiler PCR array.

Gene Symbol	Alias	Refseq #	Official Full Name	RT2 Catalog Number
ACTA2	AAT6/ACTSA	NM_001613	Actin, alpha 2, smooth muscle, aorta	PPH01300
OLFML1	UNQ564	NM_198474	Olfactomedin-like 1	PPH22736
RHOJ	ARHJ/FLJ14445/MGC34777/RASL7B/TC10B/TCL	NM_020663	Ras homolog gene family, member J	PPH05845
PHLDB2	DKFZp313O2433/DKFZp434G227/DKFP686J05113/FLJ21791/LL5b/LL5beta	NM_145753	Pleckstrin homology-like domain, family B, member 2	PPH07509
C7orf69	FLJ21075	NM_025031	Chromosome 7 open reading frame 69	PPH16084
CYYR1	C21orf95	NM_052954	Cysteine/tyrosine-rich 1	PPH12163
TIAM1	FLJ36302	NM_003253	T-cell lymphoma invasion and metastasis 1	PPH05973
MEIS2	HsT18361/MGC2820/MRG1	NM_172316	Meis homeobox 2	PPH17891
FHL1	FHL1B/FLH1A/KYOT/MGC111107/SLIM1/SLIMMER/XMPMA	NM_001449	Four and a half LIM domains 1	PPH05549
PDPN	AGGRUS/GP36/GP40/Gp38/HT1A-1/OTS8/PA2.26/T1A/T1A-2	NM_006474	Podoplanin	PPH22397
MAB21L2	FLJ31103	NM_006439	Mab-21-like 2 (C. elegans)	PPH15106
ALDH1A1	ALDC/ALDH-E1/ALDH1/ALDH11/MGC2318/PUMB1/RALDH1	NM_000689	Aldehyde dehydrogenase 1 family, member A1	PPH01723
LAMB1	CLM/MGC142015	NM_002291	Laminin, beta 1	PPH00183
ZNF608	DKFZp781C0723/MGC166851/NY-REN-36	NM_020747	Zinc finger protein 608	PPH58101
TXNDC16	KIAA1344	NM_020784	Thioredoxin domain containing 16	PPH16246
RPL13A	-	NM_012423	Ribosomal protein L13a	PPH01020

Discussion.

Expression array analysis reveals differential expression between the gingiva CAF/NF and tongue/gingival groupings.

In this chapter we have demonstrated and validated differential expression of genes in the gingiva CAF versus the gingiva NF groups and the entire set of tongue fibroblast strains versus the gingiva fibroblast strains. These data further define the potential molecular differences that exist between CAFs and NFs, hopefully leading to a better understanding of how the CAF functions to produce a more tumor permissive microenvironment. Additionally, the results will hopefully lead to an increased understanding of how anatomic context may alter fibroblast biology contributing to site-specific differences in tumor biology and clinical characteristics. The results of the expression array provide further evidence of the inter-individual heterogeneity of gene expression in CAF and NF cell populations. Similar heterogeneity has been demonstrated for CAFs and NFs derived from breast cancer stroma and normal mammary tissue where it was found, to the authors surprise, that the inter-individual NF gene expression variability actually was more than the matched CAF variability, suggesting a relative synchronization of gene expression⁹⁵. Others have shown that the fibroblast gene expression profile is able to distinguish between genomically stable and unstable oral squamous cell carcinomas⁹⁶, indicating another possible application of our data set.

Table 5.4. The qPCR results validate the majority of the differences found from the Affymetrix expression array. There was additional significant differential expression detected between groups that was not apparent from the original comparisons; *ACTA2* and *C7orf69* are differentially expressed between the CAF and NF groups and *OLFML1* is differentially expressed between the tongue and gingiva groups. *LAMB1*, *TXNDC16* and *PLCXD2* show no significant differences between any of the groups.

Gene	Differential Expression (Affymetrix Array)	Validation qPCR Significantly different Groups	P value
ACTA2	Gingival CAF/Gingiva NF	Gingiva CAF/Gingiva NF CAF/NF	0.002 0.02
OLFML1	Gingiva CAF/Gingiva NF	Gingiva CAF/Gingiva NF Tongue/Gingiva	0.02 0.04
RHOJ	Gingiva CAF/Gingiva NF	Gingiva CAF/Gingiva NF	0.002
PLCXD2	Gingiva CAF/Gingiva NF	**	n.s.
C7orf69	Gingiva CAF/Gingiva NF	Gingiva CAF/Gingiva NF CAF/NF	0.001 0.01
CYYR1	Gingiva CAF/Gingiva NF	Gingiva CAF/Gingiva NF	0.004
TIAM1 (sybr)	Gingiva CAF/Gingiva NF	Gingiva CAF/Gingiva NF	0.006
MEIS2	Tongue/Gingiva	Tongue/Gingiva	0.01
FHL1	Tongue/Gingiva	Tongue/Gingiva	0.002
PDPN	Tongue/Gingiva	Tongue/Gingiva	0.0001
MAB21L2	Tongue/Gingiva	Tongue/Gingiva	2.51X10 ⁻⁸
ALDH1A1	Tongue/Gingiva	Tongue/Gingiva	2.39X10 ⁻⁵
LAMB1	Tongue/Gingiva	**	n.s.
ZNF608	Tongue/Gingiva	Tongue/Gingiva	0.05
TXNDC16	Tongue/Gingiva	**	n.s.

TIAM1 and OLFML1 are proteins that may be secreted by CAFs and have the potential to directly affecting tumor cell activity.

Of the differentially expressed genes that have been identified, *TIAM1* and *OLFML1* are two genes that produce a secreted protein, which may then directly influence tumor cells in the microenvironment. Increased *TIAM1* expression in colon tumor cells is associated with increased migratory activity and metastatic potential¹¹⁰.

TIAM1 is a guanine nucleotide exchange factor, which may be recruited to integrin complexes on a cell's leading edge by 14-3-3 ζ , where it mediates integrin-dependent RAC1 activation, thereby initiating downstream motility-inducing pathways¹¹¹. In order to test whether this is a possible tumor promoting mechanism is present in our population of CAFs, one would first have to verify that *TIAM1* was secreted into the culture media with a *TIAM1* specific ELISA or another detection method. Then a functional assay could be established, such as demonstrated in Chapter 6, where a Boyden-type chamber could be used to assess for the differential affects of varying levels of *TIAM1* on cancer cell migration and invasion. This could be done by either varying the levels of the *TIAM1* protein in the cell media, or through siRNA technology to reduce *TIAM1* expression in a high *TIAM1* expressing cell strain.

OLFML1 is a novel secreted extracellular glycoprotein with an olfactamine domain in its C-terminus that has been demonstrated to increase the percentage of HeLa cells in S phase and to promote proliferation, while knock down of *OLFML1* protein expression by siRNA lead to decreased cellular proliferation and a delayed entry into S phase¹⁰⁶. Considering the robust differential expression of *OLFML1* in gingiva

CAFs compared to gingiva NFs it may be worthwhile to follow a similar discovery strategy as described for TIAM1 to determine whether this novel secreted protein plays a role in oral cancer microenvironment.

PDPN and TXNDC16 are membrane-associated proteins that may be expressed by CAFs and affect the progression of tumorogenesis.

Among the possible classes of mediators, which are expressed by CAFs, that are most likely to directly affect the progression of the carcinoma-associated microenvironment is secreted proteins and cell surface or membrane-associated proteins, for the obvious reason that they are available to interact extracellularly with either other cells or matrix components. Podoplanin (PDPN) is a sialomucin-like transmembrane glycoprotein that is currently being used as a marker for lymphatic vessels¹²¹. PDPN has been shown to mediate signaling that facilitates collective cell migration and invasion both in vivo and in vitro^{122,123}. Additionally, PDPN has been observed in squamous cell carcinomas from different anatomic regions, including oral squamous cell carcinomas¹²⁴ as well as the intratumoral stroma in cervical cancers where the strongest signal for PDPN expression was observed at the proliferating edge of tumor nests¹²⁵. It is interesting that PDPN is overexpressed in the tongue fibroblasts compared to the gingival fibroblasts. Increased PDPN in the tongue microenvironment may provide a mechanism to explain why tongue oral squamous cell carcinoma has a higher rate of lymph node metastasis than gingival oral squamous cell carcinoma; the PDPN could create a

stroma, which is more permissive to invasion by acting on the leading edge of the advancing tumor cells.

TXNDC16 is a thioredoxin-related transmembrane protein, which has been shown to be involved in oncogenesis and tumorigenesis. This member of the thioredoxin-thioredoxin reductase system provides a unique mechanism of microenvironment alteration in that it is primarily involved in metabolism and may function to buffer the waste products of the highly metabolic carcinoma cells¹⁰⁸.

The approach to investigating the functions of membrane-associated proteins is different than for secreted proteins. One does first have to verify that the individual fibroblast strain expresses the protein and that it is localized to the membrane, again this is best done with either immunohistochemistry or immunofluorescence. Then, as in Chapter 3, a 3 dimensional organotypic co-culture system would be best suited to investigate the effects of the fibroblast strains which either differentially express PDPN or TXNDC16 on an epidermal cell type either normal, benign or neoplastic. One would be able to observe any leading edge effects or indications of metabolic distress through specific immunohistochemical stains.

Future directions.

There are several additional strategies we can employ to investigate the possible role of the genes found to be differentially expressed in the fibroblast strains. One method would be to carry out immunohistochemistry or immunofluorescence on a sample of oral squamous cell carcinoma tumors, dysplasia and normal tissue. This would provide verification that the protein was present in the tumor

microenvironment and the specific cellular localization may provide clues to its functional significance. Another method is to over-express a gene of interest in a fibroblast cell line and then use that over-expressing cell line in a functional assay such as the one described above and used in the final chapter. In the final chapter we assess the ability of the various fibroblast cell strains to influence the proliferative capacity of a tongue oral squamous cell carcinoma cell line and an immortalized keratinocyte cell line in a 2 dimensional co-culture assay and then we assess if the same fibroblast cell strains can affect the migratory or invasive capacity in a 3 dimensional Boyden-type co-culture system. We will then use the expression data generated in this chapter to identify genes that may be preferentially expressed.

**Chapter 6: Proliferation and Invasion/Migration Assays Reveal Subsets of
Fibroblasts with Differential Gene Expression.**

Introduction.

Fibroblasts have been proposed to modify growth, migration and invasion of keratinocytes and carcinoma cells. Recent work has demonstrated several methodologies used to discover the molecular mechanisms underlying these effects. Some authors have used high-throughput fibroblast/cancer cell co-culture systems and have found largely inhibitory effects¹, while others have observed both inhibitory and stimulatory effects, combining the results with gene expression profiling².

The overall aim of this chapter is to assess whether NF and CAFs differentially affect proliferation of a tumor and “normal” cell line. We will use a straightforward 2-dimensional co-culture assay to assess for effects on proliferation and a Boyden chamber type of assay to assess for effects on invasion/migration. Then using the expression data derived in Chapter 5, it is hoped that we will be able to produce a list of differentially expressed genes, which are amenable for molecular and functional validation in the future.

Methods.

Proliferation

Fibroblast cell strains were grown to approximately 80% confluence in 10 ml of DMEM H16 with 10% FBS and were released from T75 culture flasks (Corning, NY) using 4ml of 0.25% trypsin, pelleted by centrifugation at 1 g for 3 minutes and resuspended in 3ml of DMEM with 10% FBS. A haemocytometer (Reichert, Buffalo,

NY) was used to determine the numbers of fibroblasts per ml so that 2×10^4 cells were plated onto a black flat bottom 96-well plate (Corning, Corning, NY) in a 150 μ l volume of DMEM H16 with 10% FBS. These were allowed to attach over a 24-hour period.

Next, HaCaT (human epidermal keratinocyte) and OSC20 (human tongue oral squamous cell carcinoma cell line, ATCC, Manassas, VA) cells were transfected with an FG12 vector construct³ highly overexpressing the eGFP gene through lentiviral transduction. Briefly, the FG12 lentivirus construct was transiently transfected into 293FT cells using 36 μ l of Lipofectamine 2000 (Invitrogen, Carlsbad, CA) in a total of 3 ml of Opti-MEM I (Invitrogen). Thereafter, cells were maintained in DMEM H21 and 10% FBS. Culture supernatants containing lentiviral particles were harvested 24 hours after a fresh media change and then again 24 hours after that, with centrifugation at 1 g for 3 minutes to remove cell debris and filter sterilized (45 μ m PES filter, Whatman, Piscataway, NJ). The processed supernatant was added to a T75 tissue culture flask containing either OSC20 or HaCaT cells and incubated for a 24-hour period with this process being repeated once. Then, the HaCaT and OSC20 FG12 eGFP over-expressing cells were sorted using a flow cytometer (BD FACS Aria, BD Biosciences, San Jose, CA) and grown in DMEM H16 with 10% FBS and with gentamycin (50 μ g/ml) or penicillin (100 units/ml and streptomycin (100 μ g/ml) and fungizone (2.5 μ g/ml). (All antimicrobials were obtained from the University of California San Francisco Cell Culture Facility). HaCaT and OSC20 cells that were not transfected to over-express eGFP were also grown in T75 culture flasks with DMEM

H16 with 10% FBS containing antimicrobials. All cell lines were harvested at confluence (logarithmic growth) by addition of 4mls of 0.25% trypsin to detach the cells and then subsequently 5 ml of DMEM H16 with 10% FBS was used to neutralize the trypsin. The cell suspension was centrifuged at 1 g for 3 minutes. The resulting cell pellet was re-suspended in 3 ml of DMEM H16 with 10% FBS and the cellular concentration was determined using a hemocytometer (Reichert, Buffalo, NY). Either 2×10^3 or 5×10^3 cells (HaCaT or OSC20, both eGFP overexpressing and non-transfected cells) in a volume of 50 μ l were added to the appropriate wells in the 96-well plates containing the fibroblast strains. The plates were then maintained for a period of 14 days with media changes on days 3, 6, 9 and 12. Twenty-four hours after the addition of the epithelial cells and then every 24 hours thereafter, fluorescence readings were taken using a plate reader (Biotek Synergy II, Winooski, VT) at 485 nm (excitation) and 528 nm (emission). Filter settings and measurements were reported as relative fluorescence units (RFUs). Six replicates were tested in the following co-cultures: fibroblast strain + OSC20 FG12 eGFP, fibroblast strain + OSC20, fibroblast strain + HaCaT FG12 eGFP, fibroblast strain + HaCaT. The wells with the non-transfected epithelial cell lines allowed for the subtraction of the autofluorescence generated by the fibroblast/epithelial cell co-culture. Monocultures of HaCaT eGFP, OSC20 eGFP, HaCaT and OSC20 were also grown in 6 replicate wells and were used as a control to compare against the growth rates of the co-cultures.

To assess for cell detachment, on days 6 and 15 the media in each well of the 96-well plate containing the co-cultures was collected and placed in an empty 96-well plate. The collection plate was then centrifuged at 1 g for 2 minutes to concentrate any detached cells towards the bottom of the plate to facilitate fluorescence detection. As above, a plate reader (485 nm/529 nm, excitation/emission) was used to measure the fluorescent signal emanating from the eGFP cells that had detached from the co-cultures.

Invasion/migration experiment

For the following experiment, the invasion and migration chambers refer to a Boyden-type chamber consisting of a basal well and an apical insert (refer to diagram). The fibroblast cell strains are grown on the bottom surface of the basal wells. This allows for the production of chemotactic factors by the fibroblasts that can influence the activity of the epithelial cells that are placed in the apical insert or wells. For the invasion assays, the apical insert has as the bottom limit a plastic membrane with 8 μm holes allowing for cellular movement from the top to the bottom surfaces of the membrane. In the invasion system, the membrane has a thin coating of matrigel, which consists of basement membrane proteins that serve as the “barrier” to cellular invasion, forcing the cells to possess the ability to alter those membrane components and meet at least a minimal requirement for a cell to be considered invasive. For the migration system, the chambers have exactly the same design except for the absence of the matrigel layer, thus there is no basement membrane alteration required for movement of the cells from the top of the

membrane to the bottom where they adhere and are ultimately measured.

Fibroblast cell strains were grown to approximately 80% confluence in 10 ml of DMEM H16 with 10% FBS and were released from T75 culture flasks (Corning, NY) using 4ml of 0.25% trypsin, pelleted by centrifugation at 1 g for 3 minutes and resuspended in 3ml of DMEM with 10% FBS. A haemocytometer (Reichert, Buffalo, NY) was used to determine the number of fibroblasts per ml so that 8×10^4 cells were plated into the basal chambers of a 24-well plate tumor invasion system (matrigel, 8.0 μm membrane, BD Biosciences, Bedford, MA) and a 24-well plate migration assay (non-matrigel, 8.0 μm membrane, BD Biosciences, Bedford, MA) in a volume of 500 μl . The cells were allowed to attach overnight and the next day the medium was changed from DMEM H16 with 10% FBS to 750 μl of DMEM H16 with 0.5% FBS. The plates were returned to the incubator for an additional 24-hour period. Next, HaCaT cells grown in DMEM H16 with 10% FBS and antimicrobials were released by 0.25% trypsin, pelleted by centrifugation at 1 g for 3 minutes and then resuspended in 3ml of DMEM H16 with antimicrobials but without serum. A haemocytometer was used to determine the numbers of HaCaT cells so that 5×10^4 cells were plated in the apical chambers of the invasion and migration systems in a volume of 500 μl . The plates were then incubated for 22 hours at 37°C and 5% CO₂. Next, the invasion and migration systems were removed from the incubator and the membranes on the inserts were stained with crystal violet (4% in 12 % aqueous methanol, Sigma, St. Louis, MO), rinsed in water and a moist cotton applicator used to clear the upper-side of the membrane in the insert of non-invading or migrating cells. Then, using a

Zeiss inverted microscope (Germany), invading or migrating cells were counted in three random fields of the under-side of the membrane at 40X.

Results.

All of the fibroblast/keratinocyte co-cultures were less proliferative than either HaCaT or OSC20 alone.

A 2-dimensional co-culture system was used to assess whether CAFs derived from the tumor microenvironment and NFs derived from the dermis of normal tissue have an affect on the proliferation rate of the human tongue oral squamous cell carcinoma cell line, OSC20, or the well-characterized, immortalized keratinocyte cell line, HaCaT. The daily fluorescent readings for each co-culture over the course of the 14-day experiment were tabulated and the trapezoid rule was applied to calculate the area under the curve, which was then normalized to the area under the curve for the cell lines grown in monoculture. This analysis reveals that all of the co-cultures were less proliferative than either of the HaCaT or OSC20 monocultures (Figure 6.1). When the proliferation rates are compared between CAFs versus NFs and across anatomically defined groups, tongue versus gingiva, there was no significant difference observed in either the HaCaT or OSC20 co-cultures (Figure 6.2).

Additionally, the effects on proliferation rates did not differ with respect to keratinocyte line as seen in the scatter plot of HaCaT proliferation versus OSC20 proliferation in Figure 6.3. However, there were significant differences found between three paired samples derived from the tumor stroma and normal tissue

stroma of the same individual (OF6 gingiva/OF6 CAF, OF82/OF81 and OF84/OF83) where two of the NFs produced a greater inhibition of the proliferation rate compared to CAFs (Table 6.1). This was true for the OF82/OF81 pair when co-cultured with both HaCaT and OSC20, and for OF84/OF83 only when co-cultured

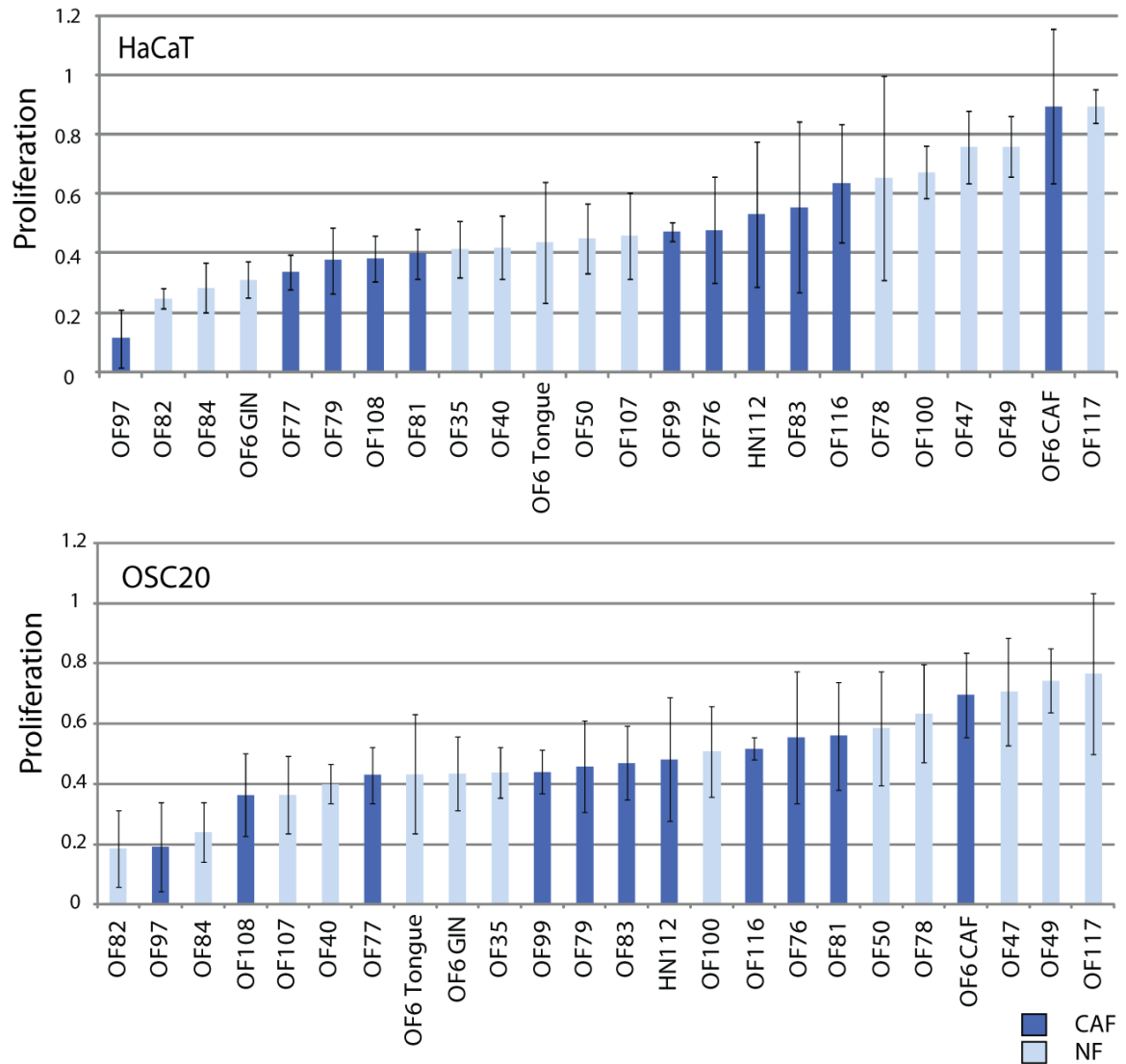


Figure 6.1. The results of the co-culture experiments demonstrate that all fibroblast cell strain/HaCaT pairings (top panel) and all fibroblast cell strain/OSC20 pairings were less proliferative compared to the monoculture of the respective cell line.

with OSC20. On the other hand, for the OF6 gingiva/OF6 CAF pair, a significant reduction in proliferation was observed when the OF6 CAF fibroblasts were co-cultured with HaCaT cells compared to the OF6 gingiva fibroblasts (NF).

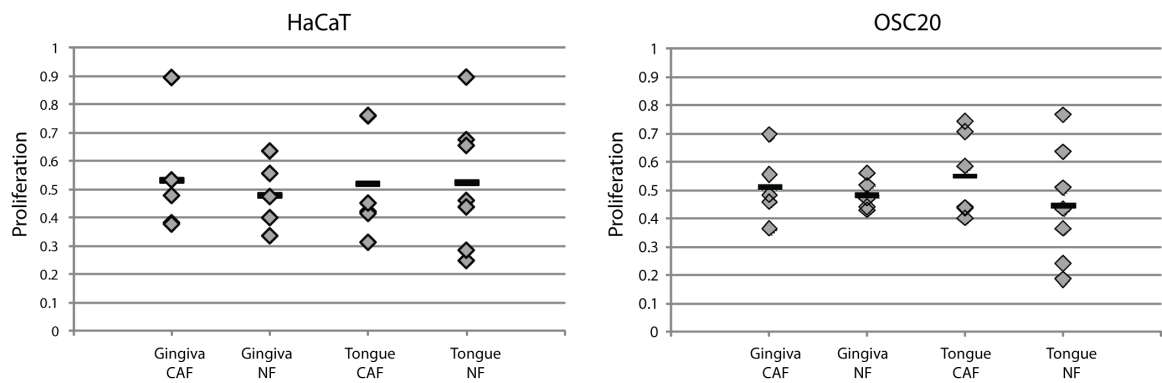


Figure 6.2. The effect of the fibroblast strains on proliferation of the HaCaT (left panel) or OSC20 (right panel) cell lines did not differ significantly for NF versus CAF or tongue versus gingiva groups. The solid black line represents the mean for that group.

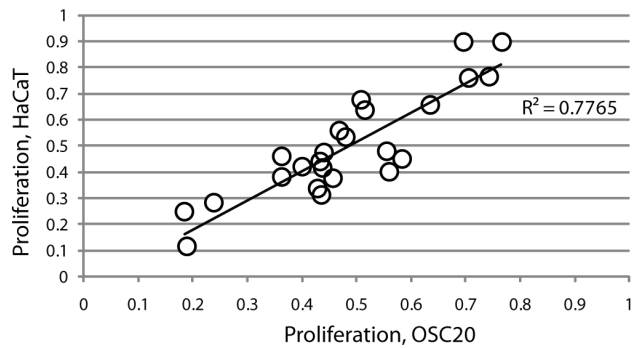


Figure 6.3. Scatter plot of HaCaT versus OSC20 proliferation shows that the effect on proliferation did not differ with respect to keratinocyte line ($R^2=0.78$).

Table 6.1. Same individual paired samples with significantly greater inhibition of proliferation for the NF compared to the CAF.

Fibroblast strain	Type	Sex	Age	Site	OSC20			HaCaT		
					Area	SD	TTEST	Area	SD	TTEST
OF82	NF	F	66	Tongue	0.19	0.13	0.025	0.25	0.03	0.049
OF81	CAF				0.56	0.18		0.40	0.08	
OF84	NF	F	71	Tongue	0.24	0.10	0.048	0.28	0.09	0.12
OF83	CAF				0.47	0.12		0.56	0.29	
OF117	NF	M	61	Tongue	0.77	0.27	0.14	0.63	0.20	0.1
OF116	CAF				0.52	0.04		0.90	0.06	
OF100	NF	F	65	Tongue	0.51	0.15	0.56	0.67	0.09	0.08
OF99	CAF				0.44	0.07		0.47	0.03	
OF78	NF	F	60	Tongue	0.63	0.16	0.07	0.65	0.35	0.19
OF77	CAF				0.43	0.09		0.33	0.06	
OF6 GIN	NF	M	63	Gingiva	0.44	0.12	0.13	0.90	0.26	0.017
OF6 CAF	CAF				0.70	0.14		0.31	0.06	

Discovery of differential gene expression amongst the fibroblast strains which were most or least inhibitory for proliferation of HaCaTs in 2-dimensional co-culture.

The most and least inhibitory fibroblast strains for proliferation of HaCaT and OSC20 were identified from Figure 6.1. The proliferation rate between the least and most inhibitory fibroblast groups was significantly different (least inhibitory group; mean=0.26 s.d.=0.05 and most inhibitory group; mean=0.79 s.d.=0.10, $p=7.02 \times 10^{-5}$, t-test). To generate a list of differentially expressed genes, the mean expression levels of genes within the two groups was determined and the list was filtered on fold change greater than 1.5 and $p < 0.05$ (two-sided t-test). Genes mapping to the Y chromosome were excluded. Then we mean centred and clustered the genes and samples by Euclidean distance and complete linkage using Cluster software and Java TreeView to show the expression values of the 51 differentially expressed genes as

color maps (Figure 6.4). The majority of the identified differentially expressed genes were expressed more highly in the more inhibitory fibroblasts, while only 11 genes were more highly expressed in the least inhibitory fibroblast strains.

Table 6.2. Fibroblast strains were divided into least and most inhibiting for the proliferation of HaCaTs in co-culture.

Strain	Site	Type	Sex	Inhibition	Proliferation	SD
OF82	Tongue	NF	F	Most	0.25	0.03
OF84	Tongue	NF	F	Most	0.28	0.09
OF77	Tongue	CAF	F	Most	0.33	0.06
OF108	Gingiva	CAF	M	Most	0.38	0.08
OF78	Tongue	NF	F	Least	0.65	0.35
OF47	Gingiva	NF	M	Least	0.76	0.12
OF49	Gingiva	NF	M	Least	0.76	0.10
OF6 CAF	Gingiva	CAF	F	Least	0.90	0.26
OF117	Tongue	NF	M	Least	0.90	0.06

The invasion/migration experiments reveal highly reproducible fibroblast strains that confer increased or decreased invasive capacity to HaCaTs.

A modified Boyden chamber was used to determine the migration and invasion rates of the HaCaT keratinocyte line. The chamber consists of an upper well with a porous membrane, into which keratinocytes (benign or carcinoma cells) are seeded. Cells can migrate through the 8 µm wide pores of the membrane in response to an

attractant or the membrane can be coated with a thin layer of modified basement membrane to model invasion. The top chamber sits in a bottom chamber, which has

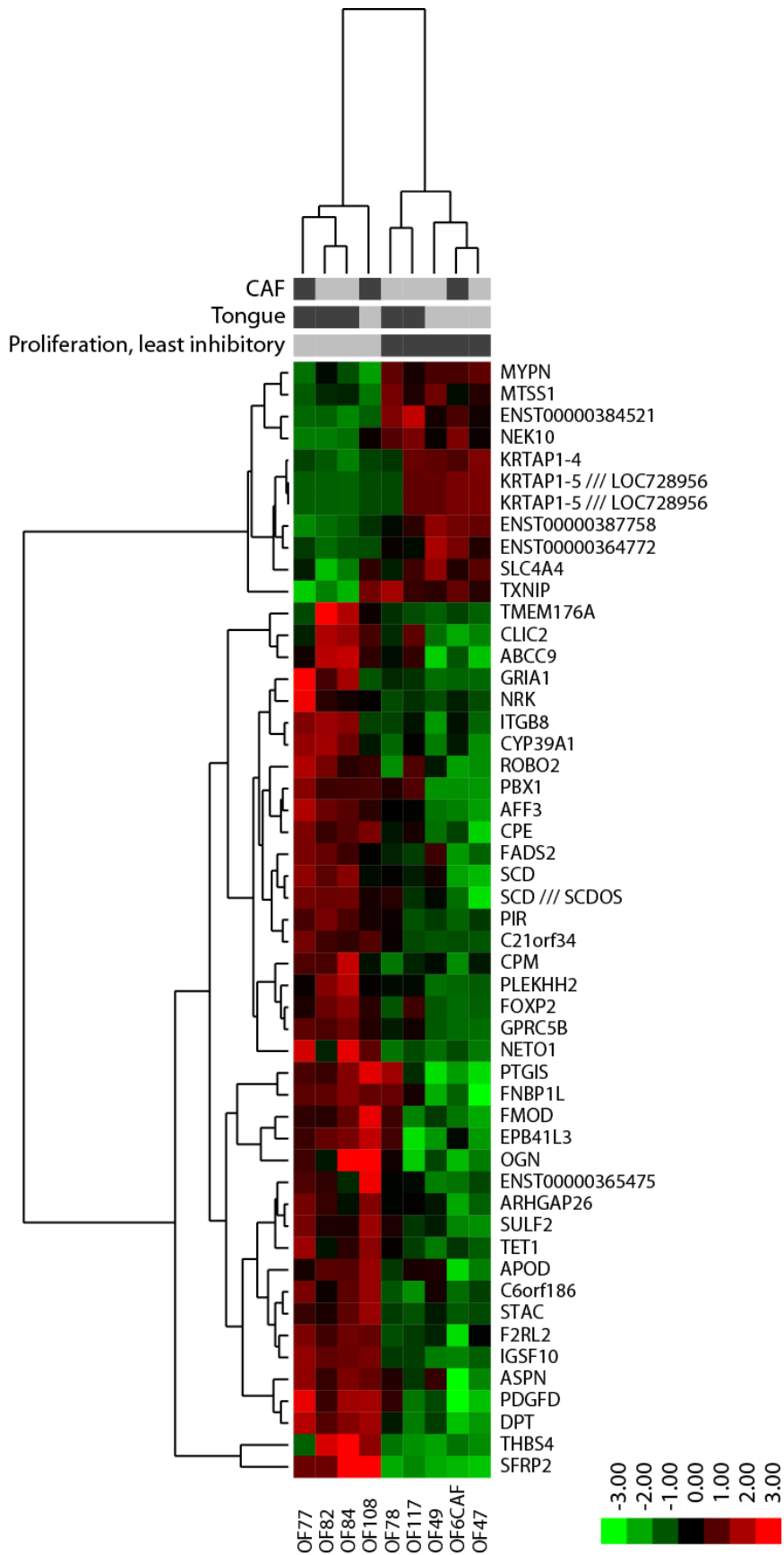


Figure 6.4. The color map shows the 51 differentially expressed genes in the least and most inhibitory fibroblast strains. The top rows indicate CAF/NF, tongue/gingiva and least/most inhibitory status of the cell strains listed on the bottom of the color map. Red indicates high expression and green indicates low expression, as demonstrated by the scale bar on the right.

serum depleted media alone or including fibroblasts seeded on the bottom of the well. Thus, the assays without the matrigel component are the migration assays and determine the rate at which the keratinocytes move from the top of the membrane to the bottom of the membrane through the pores in a specified time period.

Similarly, the assays with the matrigel component are the invasion assays and determine the rate at which the keratinocytes are able to invade through the basement membrane-like matrigel, move through the pores and end up on the underside. In our experimental system we measured the invasion rates and the migration rates of the various keratinocyte/fibroblast pairs as well as for the keratinocyte/serum depleted pairs and then calculated an invasion ratio by dividing the invasion rate by the migration rate. All keratinocyte cell lines are going to have a certain invasion and migration capacity, so to account for this, we finally divide the test assay invasion ratios (keratinocyte/fibroblast co-culture) by the control assay ratios and arrive at an invasion index for each individual fibroblast strain, which is a true measure of stimulatory or inhibitory signals affects.

For the majority of the fibroblast strains, we repeated the experiment twice in triplicate wells each time, the results of which are displayed in Figure 6.5. We then

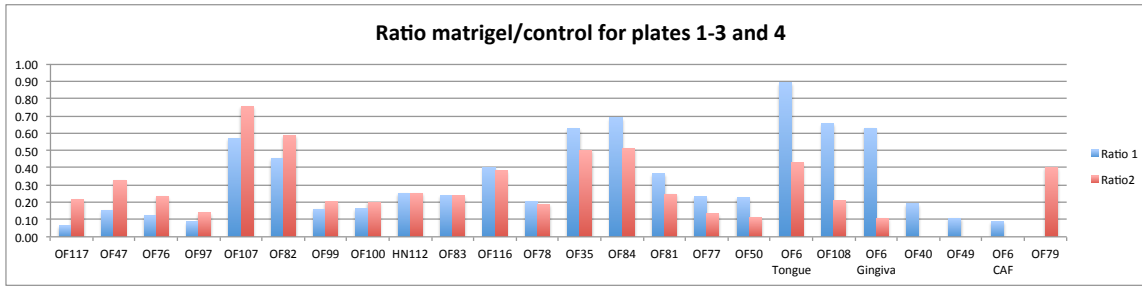


Figure 6.5. Represented are the ratios of invasion/migration for each of the fibroblast strains. Series 1 and series 2 are separate experiments done in triplicate. The higher ratios represent increased invasion relative to migration of the HaCaT cell line.

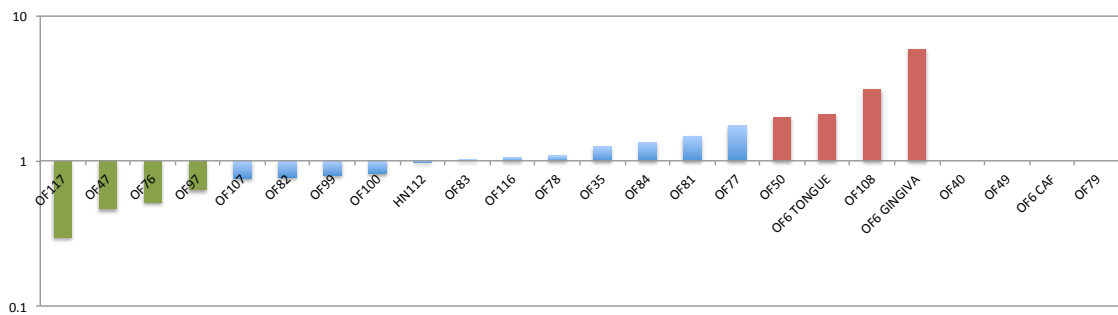


Figure 6.6. The ratios of the ratios from Figure 6.5 were calculated and displayed. The blue bars represent the fibroblast strains that had highly reproducible effects on HaCaT invasion and migration and the fibroblast strains represented by the green and red bars were less reproducible and not included in further analysis.

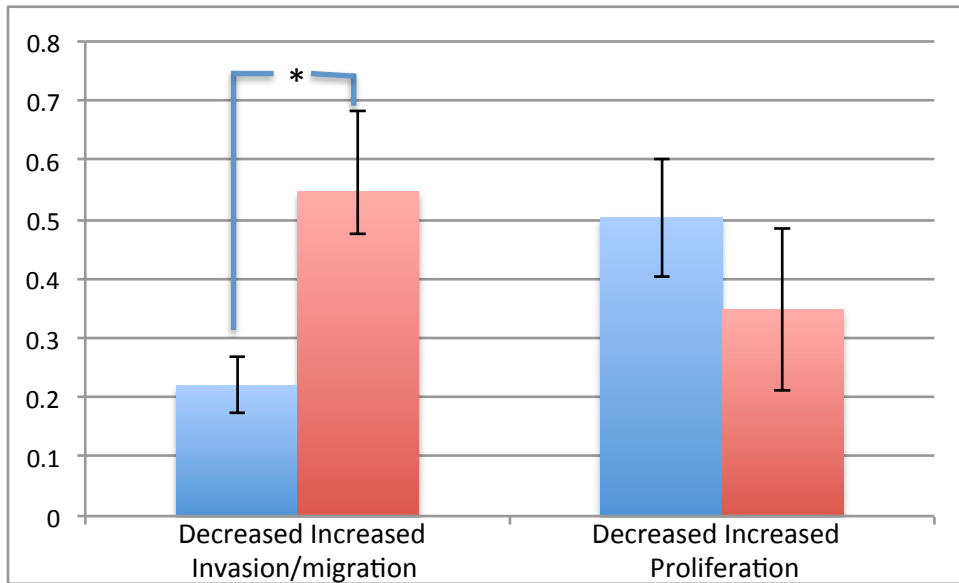


Figure 6.7. There is a significant difference between the fibroblast strains that increased versus decreased the invasion/migration index. Upon examination of the same groupings affects on proliferation rate, there is a trend for the group that increased invasion/migration towards a lower proliferation rate and for the group that decreased invasion/migration towards a higher proliferation rate. The figure represents the mean \pm s.d. values (Invasion/migration; decreased=0.22 \pm 0.04, increased=0.55 \pm 0.1, * p=1.87x10⁻⁵, Proliferation; decreased=0.34 \pm 0.13, increased=0.5 \pm 0.07, not significant)

took the ratios of the two experiments, which resulted in fibroblast/keratinocyte pairings that were considered highly reproducible and those that were not. The highly reproducible strains consisted of those that had either increased (OF116, OF84, OF107, OF82, OF35) or decreased (OF78, OF99, OF77, OF81, HN112, OF83, OF100) invasion indexes and were the only ones considered for further analysis (Figure 6.6).

The fibroblast strains that increased the invasion index trended towards a lower proliferation rate compared to the strains that decreased the invasion index, which trended towards a higher proliferation rate.

Upon examination of the affect on proliferation rate of HaCaTs in the fibroblast groups that increased versus decreased the invasion index, one finds that the group that increased the invasion index trended towards a lower proliferation rate and the groups that decreased the invasion index trended towards a higher proliferation rate (Figure 6.7).

DKK1 is one of the differentially expressed genes that emerged from the analysis of the fibroblast strains, which displayed increased or decreased affects on the invasion index of HaCaT keratinocytes.

The fibroblast strains were divided into two groups based on whether they affected an increase or a decrease in the invasion index of HaCaTs as described above. Then a procedure similar to that followed to generate the differentially expressed genes in the proliferation assay resulted in a list of 14 genes that were either over-expressed or under-expressed in the invasion index subgroups (Figure 6.8). Among the more interesting genes is Dickkopf-1 or *DKK1*, which has significantly lower expression levels in the group of fibroblasts that had an increased invasion index, the ramifications of which will be explored in the discussion section.

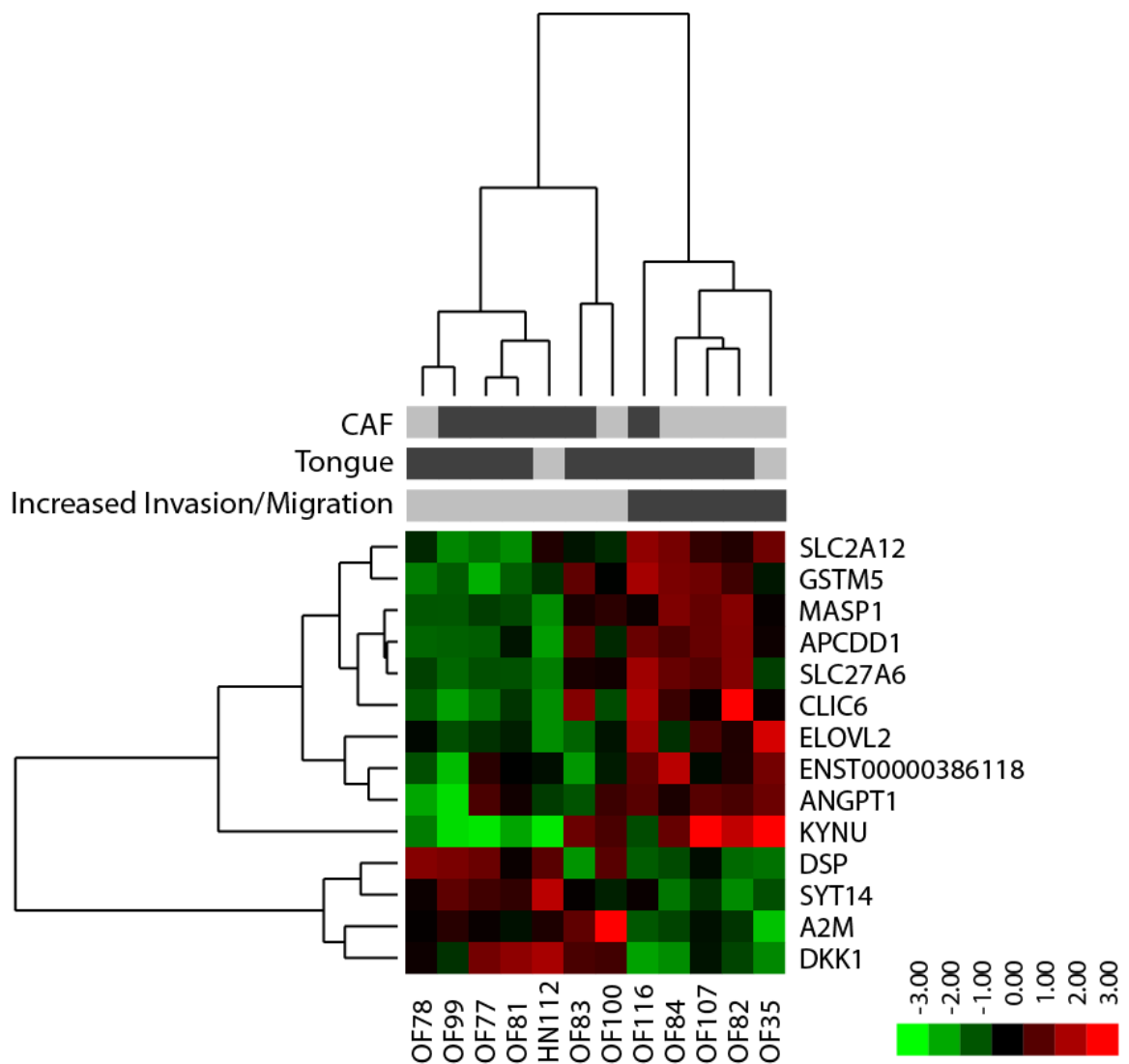


Figure 6.8. Differential expression of 14 genes is displayed following a similar algorithm as for Figure 6.4 a color map was generated separating fibroblast strains that had increased versus decreased invasion/migration ratio. The top rows indicate CAF/NF, tongue/gingiva and increase/decreased invasion/migration ratio status of the cell strains listed on the bottom of the color map. Red indicates high expression and green indicates low expression, as demonstrated by the scale bar on the right.

Discussion.

All fibroblast/keratinocyte interactions were inhibitory with NFs producing a significantly greater inhibition than CAFs in individually paired fibroblast strains.

In the 2-dimensional co-culture system, proliferation of HaCaTs or OSC20 was monitored in real-time over a 14-day period. The results demonstrate that all of the fibroblast/keratinocyte interactions resulted in a decreased proliferation rate of the epithelial cells as compared their proliferation rate in monocultures. Further, there were three same individual CAF/NF pairs, which showed differentially effects on proliferation. For two pairs, the NF was more inhibitory than the CAF, while for the third pair the CAF was more inhibitory. These results are generally in agreement with what is reported in the literature. Wadlow et al. found fibroblast/carcinoma co-cultures that were both growth promoting and inhibiting, although the percentage of growth promoting cells were a clear minority^{1,2}. In a study by Flaberg et al., it was demonstrated that all fibroblast cells types were growth inhibiting and indicated that normal fibroblasts were more inhibiting than fibroblasts derived from areas close to tumors, specifically fibroblasts that could potentially be CAFs derived from a prostate biopsy of a prostate cancer patient. They go on to suggest that expression profiling of most and least inhibitory fibroblasts could lead to the discovery of novel molecular mechanisms. This is the general approached that we followed in deriving the list of differentially expressed genes in Figure 6.4.

SFRP2 and THBS4 are secreted proteins that are more highly expressed in fibroblast cell strains that inhibit proliferation the most

Fifty-one genes have been identified as being differentially expressed between the least and most inhibitory fibroblast strains. Of those genes, two secreted proteins over-expressed in the most inhibitory fibroblast strains are of particular interest, the soluble frizzled receptor protein (*SFRP2*) and thrombospondin 4 (*THBS4*).

Interestingly, *SFRP2* is methylated in oral cancer and cell lines [4,5](#) and the up-regulated expression of this soluble mediator inhibits colony formation.

Additionally, the WNT-pathway is often activated in the absence of beta-catenin and/or APC/Axin mutations during oral carcinogenesis. Thus, if *SFRP2*, an inhibitory mediator of the proliferative WNT-pathway, is epigenetically silenced in cancer cells, then over-production and secretion by CAFs may be able to overcome the inhibitory affect leading to decreased proliferation. *THBS4* is similarly, a secreted protein, belonging to the extracellular calcium-binding protein family. Proposed functions include calcium binding, cell attachment, cell migration and proliferation, cytoskeletal organization, neurite growth, binding other extracellular matrix components and cell-cell interactions. It has been promoted as being a putative tumour-suppressor gene that is hypermethylated in colorectal cancer [6](#), with the additional observation that over-expression in colon carcinoma cells suppressed growth as demonstrated by a failure to recover colonies. *THBS4* has also been found to be over-expressed by stromal CAFs in diffuse type gastric adenocarcinomas [7](#) and secretion by CAFs is stimulated by the presence of tumor cells in a co-culture model but its role has yet to be fully elucidated.

DKK1, a WNT antagonist, is a differentially expressed gene, which has lower expression levels in fibroblast strains associated with an increased invasion index.

Similar to the proliferation experiments, the invasion/migration experiments yielded a list of differentially expressed genes derived from the comparison of fibroblasts that increased or decreased the invasion/migration ratios. Of all of the genes, *DKK1* had the largest differential expression. *DKK1* is a secreted glycoprotein that has been shown to act as a potent inhibitor of the canonical Wnt/ β -catenin signalling pathway^{8,9}. Through competitive binding of the low-density lipoprotein receptor-related proteins, *DKK1* results in degradation of cytosolic β -catenin¹⁰. Epigenetic silencing of *DKK1* has been described in colorectal cancer¹¹ and overexpression of *DKK1* inhibits epithelial cell proliferation in a mouse model¹². Proinflammatory cytokines have been shown to induce expression of *DKK1*, where its presence or absence may have direct consequences on a cancer-associated microenvironment. In an LOH study looking at head and neck squamous cell carcinoma, cases that retained *DKK1* had less distant metastasis and a tendency for longer disease free survival¹³ and in oral squamous cell carcinoma, *DKK1* positive cases were correlated significantly with a low risk of regional lymph node metastasis¹⁴.

Emergence of the WNT signalling system and future plans on investigating its role in shaping the tumor/stromal relationship.

Our analysis of the differentially expressed genes derived from the 2-dimensional and 3-dimensional co-culture experiments has yielded a very strong signal from two

genes that are involved in regulating WNT signalling, *SFRP2* and *DKK1*. In fact, another group has found that tumor fibroblasts secretes *WNT2* to promote tumor progression in oesophageal cancers¹⁵. So, perhaps there exists a balancing act between the promoters and inhibitors of the WNT system, which helps determine the fate of a carcinoma and its microenvironment. Future experiments to further elucidate this question involve verification that *SFRP2* and *DKK1* are secreted at different levels by the least/most inhibiting fibroblasts and increasing/decreasing fibroblasts in relation to proliferation and invasion/migration, respectively. Then *SFRP2* and *DKK1* can be applied exogenously to HaCaT or OSC20 cultures to determine the affect on proliferation and invasion.

.

References.

- 1 Hiscox, S., Barrett-Lee, P. & Nicholson, R. I. Therapeutic targeting of tumor-stroma interactions. *Expert Opin Ther Targets* **15**, 609-621, doi:10.1517/14728222.2011.561201 (2011).
- 2 Margaritescu, C. *et al.* VEGF expression and angiogenesis in oral squamous cell carcinoma: an immunohistochemical and morphometric study. *Clin Exp Med* **10**, 209-214, doi:10.1007/s10238-010-0095-4 (2010).
- 3 Connelly, S. T. & Schmidt, B. L. Evaluation of pain in patients with oral squamous cell carcinoma. *J Pain* **5**, 505-510, doi:10.1016/j.jpain.2004.09.002 (2004).
- 4 Kolokythas, A., Connelly, S. T. & Schmidt, B. L. Validation of the University of California San Francisco Oral Cancer Pain Questionnaire. *J Pain* **8**, 950-953, doi:10.1016/j.jpain.2007.06.012 (2007).
- 5 Wang, S. J. & Bourguignon, L. Y. Role of hyaluronan-mediated CD44 signaling in head and neck squamous cell carcinoma progression and chemoresistance. *Am J Pathol* **178**, 956-963, doi:10.1016/j.ajpath.2010.11.077 (2011).
- 6 DeNardo, D. G., Andreu, P. & Coussens, L. M. Interactions between lymphocytes and myeloid cells regulate pro- versus anti-tumor immunity. *Cancer Metastasis Rev* **29**, 309-316, doi:10.1007/s10555-010-9223-6 (2010).
- 7 Al-Qahtani, D., Anil, S. & Rajendran, R. Tumour infiltrating CD25+ FoxP3+ regulatory T cells (Tregs) relate to tumour grade and stromal inflammation in oral squamous cell carcinoma. *J Oral Pathol Med*, doi:10.1111/j.1600-0714.2011.01020.x (2011).
- 8 Silverman, S., Jr. & Gorsky, M. Proliferative verrucous leukoplakia: a follow-up study of 54 cases. *Oral Surg Oral Med Oral Pathol Oral Radiol Endod* **84**, 154-157 (1997).
- 9 Liu, Y., Messadi, D. V., Wu, H. & Hu, S. Oral lichen planus is a unique disease model for studying chronic inflammation and oral cancer. *Med Hypotheses* **75**, 492-494, doi:10.1016/j.mehy.2010.07.002 (2010).
- 10 Hansen, L. S., Olson, J. A. & Silverman, S., Jr. Proliferative verrucous leukoplakia. A long-term study of thirty patients. *Oral Surg Oral Med Oral Pathol* **60**, 285-298 (1985).
- 11 Paget, S. The distribution of secondary growths in cancer of the breast. 1889. *Cancer Metastasis Rev* **8**, 98-101 (1889).
- 12 Hart, I. R. & Fidler, I. J. Role of organ selectivity in the determination of metastatic patterns of B16 melanoma. *Cancer Res* **40**, 2281-2287 (1980).
- 13 Cesson, V. *et al.* MAGE-A3 and MAGE-A4 specific CD4(+) T cells in head and neck cancer patients: detection of naturally acquired responses and identification of new epitopes. *Cancer Immunol Immunother* **60**, 23-35, doi:10.1007/s00262-010-0916-z (2011).

- 14 Ruffell, B., DeNardo, D. G., Affara, N. I. & Coussens, L. M. Lymphocytes in cancer development: polarization towards pro-tumor immunity. *Cytokine Growth Factor Rev* **21**, 3-10, doi:10.1016/j.cytogfr.2009.11.002 (2010).
- 15 Gannot, G., Gannot, I., Vered, H., Buchner, A. & Keisari, Y. Increase in immune cell infiltration with progression of oral epithelium from hyperkeratosis to dysplasia and carcinoma. *Br J Cancer* **86**, 1444-1448, doi:10.1038/sj.bjc.6600282 (2002).
- 16 Shih, B., Garside, E., McGrouther, D. A. & Bayat, A. Molecular dissection of abnormal wound healing processes resulting in keloid disease. *Wound Repair Regen* **18**, 139-153, doi:10.1111/j.1524-475X.2009.00553.x (2010).
- 17 Prime, S. S., Eveson, J. W., Guest, P. G., Parkinson, E. K. & Paterson, I. C. Early genetic and functional events in the pathogenesis of oral cancer. *Radiat Oncol Investig* **5**, 93-96 (1997).
- 18 Mueller, M. M. & Fusenig, N. E. Tumor-stroma interactions directing phenotype and progression of epithelial skin tumor cells. *Differentiation* **70**, 486-497, doi:10.1046/j.1432-0436.2002.700903.x (2002).
- 19 Willhauck, M. J. *et al.* Reversion of tumor phenotype in surface transplants of skin SCC cells by scaffold-induced stroma modulation. *Carcinogenesis* **28**, 595-610, doi:10.1093/carcin/bgl188 (2007).
- 20 Siveen, K. S. & Kuttan, G. Role of macrophages in tumour progression. *Immunol Lett* **123**, 97-102, doi:10.1016/j.imlet.2009.02.011 (2009).
- 21 Sica, A. *et al.* Macrophage polarization in tumour progression. *Semin Cancer Biol* **18**, 349-355, doi:10.1016/j.semcancer.2008.03.004 (2008).
- 22 Marsh, D. *et al.* Stromal features are predictive of disease mortality in oral cancer patients. *J Pathol* **223**, 470-481, doi:10.1002/path.2830 (2011).
- 23 Bello, I. O. *et al.* Cancer-associated fibroblasts, a parameter of the tumor microenvironment, overcomes carcinoma-associated parameters in the prognosis of patients with mobile tongue cancer. *Oral Oncol* **47**, 33-38, doi:10.1016/j.oraloncology.2010.10.013 (2011).
- 24 Alberts, B. *Molecular biology of the cell*. 3rd edn, (Garland Pub., 1994).
- 25 Daniels, J. T., Kearney, J. N. & Ingham, E. Human keratinocyte isolation and cell culture: a survey of current practices in the UK. *Burns* **22**, 35-39 (1996).
- 26 Rakhorst, H. A. *et al.* Mucosal keratinocyte isolation: a short comparative study on thermolysin and dispase. *Int J Oral Maxillofac Surg* **35**, 935-940, doi:10.1016/j.ijom.2006.06.011 (2006).
- 27 Supaprutsakul, S., Chotigeat, W., Wanichpakorn, S. & Kedjarune-Leggat, U. Transfection efficiency of depolymerized chitosan and epidermal growth factor conjugated to chitosan-DNA polyplexes. *J Mater Sci Mater Med* **21**, 1553-1561, doi:10.1007/s10856-010-3993-9 (2010).
- 28 Moharamzadeh, K., Brook, I. M., Van Noort, R., Scutt, A. M. & Thornhill, M. H. Tissue-engineered oral mucosa: a review of the scientific literature. *J Dent Res* **86**, 115-124 (2007).
- 29 Cristofalo, V. J. & Pignolo, R. J. Replicative senescence of human fibroblast-like cells in culture. *Physiol Rev* **73**, 617-638 (1993).

- 30 Montes, D. M. & Schmidt, B. L. Oral maxillary squamous cell carcinoma: management of the clinically negative neck. *J Oral Maxillofac Surg* **66**, 762-766, doi:S0278-2391(07)02139-8 [pii]10.1016/j.joms.2007.12.017 (2008).
- 31 Snijders, A. M. *et al.* Rare amplicons implicate frequent deregulation of cell fate specification pathways in oral squamous cell carcinoma. *Oncogene* **24**, 4232-4242, doi:1208601 [pii]10.1038/sj.onc.1208601 (2005).
- 32 Mantovani, A., Allavena, P., Sica, A. & Balkwill, F. Cancer-related inflammation. *Nature* **454**, 436-444, doi:nature07205 [pii]10.1038/nature07205 (2008).
- 33 Snijders, A. M. *et al.* Stromal control of oncogenic traits expressed in response to the overexpression of GLI2, a pleiotropic oncogene. *Oncogene*, doi:onc2008421 [pii]10.1038/onc.2008.421 (2008).
- 34 Brigstock, D. R. *et al.* Proposal for a unified CCN nomenclature. *Mol Pathol* **56**, 127-128 (2003).
- 35 De Wever, O., Demetter, P., Mareel, M. & Bracke, M. Stromal myofibroblasts are drivers of invasive cancer growth. *Int J Cancer* **123**, 2229-2238, doi:10.1002/ijc.23925 (2008).
- 36 De Wever, O. *et al.* Tenascin-C and SF/HGF produced by myofibroblasts in vitro provide convergent pro-invasive signals to human colon cancer cells through RhoA and Rac. *FASEB J* **18**, 1016-1018, doi:10.1096/fj.03-1110fje03-1110fje [pii] (2004).
- 37 Gaggioli, C. *et al.* Fibroblast-led collective invasion of carcinoma cells with differing roles for RhoGTPases in leading and following cells. *Nat Cell Biol* **9**, 1392-1400, doi:ncb1658 [pii]10.1038/ncb1658 (2007).
- 38 Kellermann, M. G. *et al.* Myofibroblasts in the stroma of oral squamous cell carcinoma are associated with poor prognosis. *Histopathology* **51**, 849-853, doi:HIS2873 [pii]10.1111/j.1365-2559.2007.02873.x (2007).
- 39 Kellermann, M. G. *et al.* Mutual paracrine effects of oral squamous cell carcinoma cells and normal oral fibroblasts: induction of fibroblast to myofibroblast transdifferentiation and modulation of tumor cell proliferation. *Oral Oncol* **44**, 509-517, doi:S1368-8375(07)00183-2 [pii]10.1016/j.oraloncology.2007.07.001 (2008).
- 40 Surowiak, P. *et al.* Stromal myofibroblasts in breast cancer: relations between their occurrence, tumor grade and expression of some tumour markers. *Folia Histochem Cytobiol* **44**, 111-116 (2006).
- 41 Galie, M. *et al.* Mammary carcinoma provides highly tumourigenic and invasive reactive stromal cells. *Carcinogenesis* **26**, 1868-1878, doi:bgi158 [pii]10.1093/carcin/bgi158 (2005).
- 42 Dvorak, H. F. Tumors: wounds that do not heal. Similarities between tumor stroma generation and wound healing. *N Engl J Med* **315**, 1650-1659 (1986).
- 43 Kane, C. J., Hebda, P. A., Mansbridge, J. N. & Hanawalt, P. C. Direct evidence for spatial and temporal regulation of transforming growth factor beta 1 expression during cutaneous wound healing. *J Cell Physiol* **148**, 157-173, doi:10.1002/jcp.1041480119 (1991).

- 44 Leask, A. & Abraham, D. J. TGF-beta signaling and the fibrotic response. *FASEB J* **18**, 816-827, doi:10.1096/fj.03-1273rev18/7/816 [pii] (2004).
- 45 Leask, A. Targeting the TGFbeta, endothelin-1 and CCN2 axis to combat fibrosis in scleroderma. *Cell Signal* **20**, 1409-1414, doi:S0898-6568(08)00026-0 [pii]10.1016/j.cellsig.2008.01.006 (2008).
- 46 McWhirter, A., Colosetti, P., Rubin, K., Miyazono, K. & Black, C. Collagen type I is not under autocrine control by transforming growth factor-beta 1 in normal and scleroderma fibroblasts. *Lab Invest* **71**, 885-894 (1994).
- 47 Mori, T. *et al.* Role and interaction of connective tissue growth factor with transforming growth factor-beta in persistent fibrosis: A mouse fibrosis model. *J Cell Physiol* **181**, 153-159, doi:10.1002/(SICI)1097-4652(199910)181:1<153::AID-JCP16>3.0.CO;2-K [pii]10.1002/(SICI)1097-4652(199910)181:1<153::AID-JCP16>3.0.CO;2-K (1999).
- 48 Shah, M., Foreman, D. M. & Ferguson, M. W. Neutralising antibody to TGF-beta 1,2 reduces cutaneous scarring in adult rodents. *J Cell Sci* **107 (Pt 5)**, 1137-1157 (1994).
- 49 Teder, P. & Noble, P. W. A cytokine reborn? Endothelin-1 in pulmonary inflammation and fibrosis. *Am J Respir Cell Mol Biol* **23**, 7-10 (2000).
- 50 Shi-Wen, X. *et al.* Constitutive ALK5-independent c-Jun N-terminal kinase activation contributes to endothelin-1 overexpression in pulmonary fibrosis: evidence of an autocrine endothelin loop operating through the endothelin A and B receptors. *Mol Cell Biol* **26**, 5518-5527, doi:26/14/5518 [pii]10.1128/MCB.00625-06 (2006).
- 51 Levin, E. R. Endothelins. *N Engl J Med* **333**, 356-363 (1995).
- 52 Ortega Mateo, A. & de Artinano, A. A. Highlights on endothelins: a review. *Pharmacol Res* **36**, 339-351, doi:S1043661897902462 [pii] (1997).
- 53 Galie, N., Manes, A. & Branzi, A. Emerging medical therapies for pulmonary arterial hypertension. *Prog Cardiovasc Dis* **45**, 213-224, doi:10.1053/pcad.2002.130160S0033062002500499 [pii] (2002).
- 54 Abraham, D., Ponticos, M. & Nagase, H. Connective tissue remodeling: cross-talk between endothelins and matrix metalloproteinases. *Curr Vasc Pharmacol* **3**, 369-379 (2005).
- 55 Lalich, M., McNeel, D. G., Wilding, G. & Liu, G. Endothelin receptor antagonists in cancer therapy. *Cancer Invest* **25**, 785-794, doi:783553274 [pii]10.1080/07357900701522588 (2007).
- 56 Xu, S. W. *et al.* Endothelin-1 induces expression of matrix-associated genes in lung fibroblasts through MEK/ERK. *J Biol Chem* **279**, 23098-23103, doi:10.1074/jbc.M311430200M311430200 [pii] (2004).
- 57 Shi-Wen, X. *et al.* Endothelin-1 promotes myofibroblast induction through the ETA receptor via a rac/phosphoinositide 3-kinase/Akt-dependent pathway and is essential for the enhanced contractile phenotype of fibrotic fibroblasts. *Mol Biol Cell* **15**, 2707-2719, doi:10.1091/mbc.E03-12-0902E03-12-0902 [pii] (2004).

- 58 Shi-Wen, X. *et al.* Endogenous endothelin-1 signaling contributes to type I collagen and CCN2 overexpression in fibrotic fibroblasts. *Matrix Biol* **26**, 625-632, doi:S0945-053X(07)00085-6 [pii]10.1016/j.matbio.2007.06.003 (2007).
- 59 Shi-wen, X. *et al.* Endothelin is a downstream mediator of profibrotic responses to transforming growth factor beta in human lung fibroblasts. *Arthritis Rheum* **56**, 4189-4194, doi:10.1002/art.23134 (2007).
- 60 Salani, D. *et al.* Role of endothelin-1 in neovascularization of ovarian carcinoma. *Am J Pathol* **157**, 1537-1547 (2000).
- 61 Spinella, F., Rosano, L., Di Castro, V., Natali, P. G. & Bagnato, A. Endothelin-1 induces vascular endothelial growth factor by increasing hypoxia-inducible factor-1alpha in ovarian carcinoma cells. *J Biol Chem* **277**, 27850-27855, doi:10.1074/jbc.M202421200M202421200 [pii] (2002).
- 62 Rosano, L. *et al.* Therapeutic targeting of the endothelin a receptor in human ovarian carcinoma. *Cancer Res* **63**, 2447-2453 (2003).
- 63 Salani, D. *et al.* Endothelin-1 induces an angiogenic phenotype in cultured endothelial cells and stimulates neovascularization in vivo. *Am J Pathol* **157**, 1703-1711 (2000).
- 64 Perbal, B. CCN proteins: multifunctional signalling regulators. *Lancet* **363**, 62-64, doi:S0140-6736(03)15172-0 [pii]10.1016/S0140-6736(03)15172-0 (2004).
- 65 Bork, P. The modular architecture of a new family of growth regulators related to connective tissue growth factor. *FEBS Lett* **327**, 125-130, doi:0014-5793(93)80155-N [pii] (1993).
- 66 Holmes, A. *et al.* CTGF and SMADs, maintenance of scleroderma phenotype is independent of SMAD signaling. *J Biol Chem* **276**, 10594-10601, doi:10.1074/jbc.M010149200M010149200 [pii] (2001).
- 67 Van Beek, J. P., Kennedy, L., Rockel, J. S., Bernier, S. M. & Leask, A. The induction of CCN2 by TGFbeta1 involves Ets-1. *Arthritis Res Ther* **8**, R36, doi:ar1890 [pii]10.1186/ar1890 (2006).
- 68 Shi-wen, X. *et al.* CCN2 is necessary for adhesive responses to transforming growth factor-beta1 in embryonic fibroblasts. *J Biol Chem* **281**, 10715-10726, doi:M511343200 [pii]10.1074/jbc.M511343200 (2006).
- 69 Uchio, K., Graham, M., Dean, N. M., Rosenbaum, J. & Desmouliere, A. Down-regulation of connective tissue growth factor and type I collagen mRNA expression by connective tissue growth factor antisense oligonucleotide during experimental liver fibrosis. *Wound Repair Regen* **12**, 60-66, doi:10.1111/j.1067-1927.2004.012112.xWRR12112 [pii] (2004).
- 70 Lang, C. *et al.* Connective tissue growth factor: a crucial cytokine-mediating cardiac fibrosis in ongoing enterovirus myocarditis. *J Mol Med* **86**, 49-60, doi:10.1007/s00109-007-0249-3 (2008).
- 71 Rinn, J. L., Bondre, C., Gladstone, H. B., Brown, P. O. & Chang, H. Y. Anatomic demarcation by positional variation in fibroblast gene expression programs.

- PLoS Genet* **2**, e119, doi:06-PLGE-RA-0156R1 [pii]10.1371/journal.pgen.0020119 (2006).
- 72 Chang, H. Y. *et al.* Diversity, topographic differentiation, and positional memory in human fibroblasts. *Proc Natl Acad Sci U S A* **99**, 12877-12882, doi:10.1073/pnas.162488599162488599 [pii] (2002).
- 73 Shannon, D. B., McKeown, S. T., Lundy, F. T. & Irwin, C. R. Phenotypic differences between oral and skin fibroblasts in wound contraction and growth factor expression. *Wound Repair Regen* **14**, 172-178, doi:WRR107 [pii]10.1111/j.1743-6109.2006.00107.x (2006).
- 74 Stephens, P., Davies, K. J., al-Khateeb, T., Shepherd, J. P. & Thomas, D. W. A comparison of the ability of intra-oral and extra-oral fibroblasts to stimulate extracellular matrix reorganization in a model of wound contraction. *J Dent Res* **75**, 1358-1364 (1996).
- 75 Irwin, C. R. *et al.* Inter- and intra-site heterogeneity in the expression of fetal-like phenotypic characteristics by gingival fibroblasts: potential significance for wound healing. *J Cell Sci* **107 (Pt 5)**, 1333-1346 (1994).
- 76 Gron, B., Stoltze, K., Andersson, A. & Dabelsteen, E. Oral fibroblasts produce more HGF and KGF than skin fibroblasts in response to co-culture with keratinocytes. *APMIS* **110**, 892-898, doi:apm1101208 [pii] (2002).
- 77 Hughes, M. W. & Chuong, C. M. A mouthful of epithelial-mesenchymal interactions. *J Invest Dermatol* **121**, vii-viii, doi:12651 [pii]10.1111/j.1523-1747.2003.12651.x (2003).
- 78 Winning, T. A. & Townsend, G. C. Oral mucosal embryology and histology. *Clin Dermatol* **18**, 499-511, doi:S0738-081X(00)00140-1 [pii] (2000).
- 79 Sukotjo, C. *et al.* Oral fibroblast expression of wound-inducible transcript 3.0 (wit3.0) accelerates the collagen gel contraction in vitro. *J Biol Chem* **278**, 51527-51534, doi:10.1074/jbc.M309616200M309616200 [pii] (2003).
- 80 Okazaki, M., Yoshimura, K., Suzuki, Y. & Harii, K. Effects of subepithelial fibroblasts on epithelial differentiation in human skin and oral mucosa: heterotypically recombined organotypic culture model. *Plast Reconstr Surg* **112**, 784-792, doi:10.1097/01.PRS.0000069710.48139.4E (2003).
- 81 Chinnathambi, S. *et al.* Recapitulation of oral mucosal tissues in long-term organotypic culture. *Anat Rec A Discov Mol Cell Evol Biol* **270**, 162-174, doi:10.1002/ar.a.10021 (2003).
- 82 Lu, S. L. *et al.* Overexpression of transforming growth factor beta1 in head and neck epithelia results in inflammation, angiogenesis, and epithelial hyperproliferation. *Cancer Res* **64**, 4405-4410, doi:10.1158/0008-5472.CAN-04-1032 (2004).
- 83 Rasanen, K. & Vaheri, A. Activation of fibroblasts in cancer stroma. *Exp Cell Res* **316**, 2713-2722, doi:10.1016/j.yexcr.2010.04.032 (2010).
- 84 Ostman, A. & Augsten, M. Cancer-associated fibroblasts and tumor growth--bystanders turning into key players. *Curr Opin Genet Dev* **19**, 67-73, doi:10.1016/j.gde.2009.01.003 (2009).

- 85 Sugimoto, H., Mundel, T. M., Kieran, M. W. & Kalluri, R. Identification of fibroblast heterogeneity in the tumor microenvironment. *Cancer Biol Ther* **5**, 1640-1646 (2006).
- 86 Rasanen, K., Virtanen, I., Salmenpera, P., Grenman, R. & Vaheri, A. Differences in the chemotaxis response of normal and cancer-associated fibroblasts from patients with oral squamous cell carcinoma. *PLoS One* **4**, e6879, doi:10.1371/journal.pone.0006879 (2009).
- 87 Kalluri, R. & Zeisberg, M. Fibroblasts in cancer. *Nat Rev Cancer* **6**, 392-401, doi:10.1038/nrc1877 (2006).
- 88 Radisky, D. C., Kenny, P. A. & Bissell, M. J. Fibrosis and cancer: do myofibroblasts come also from epithelial cells via EMT? *J Cell Biochem* **101**, 830-839, doi:10.1002/jcb.21186 (2007).
- 89 Zeisberg, E. M., Potenta, S., Xie, L., Zeisberg, M. & Kalluri, R. Discovery of endothelial to mesenchymal transition as a source for carcinoma-associated fibroblasts. *Cancer Res* **67**, 10123-10128, doi:10.1158/0008-5472.CAN-07-3127 (2007).
- 90 Direkze, N. C. *et al.* Bone marrow-derived stromal cells express lineage-related messenger RNA species. *Cancer Res* **66**, 1265-1269, doi:10.1158/0008-5472.CAN-05-3202 (2006).
- 91 Wu, B. H., Xiong, X. P., Jia, J. & Zhang, W. F. MicroRNAs: new actors in the oral cancer scene. *Oral Oncol* **47**, 314-319, doi:10.1016/j.oraloncology.2011.03.019 (2011).
- 92 Keller, S., Ridinger, J., Rupp, A. K., Janssen, J. W. & Altevogt, P. Body fluid derived exosomes as a novel template for clinical diagnostics. *J Transl Med* **9**, 86, doi:10.1186/1479-5876-9-86 (2011).
- 93 Hood, J. L., San, R. S. & Wickline, S. A. Exosomes released by melanoma cells prepare sentinel lymph nodes for tumor metastasis. *Cancer Res* **71**, 3792-3801, doi:10.1158/0008-5472.CAN-10-4455 (2011).
- 94 Saadi, A. *et al.* Stromal genes discriminate preinvasive from invasive disease, predict outcome, and highlight inflammatory pathways in digestive cancers. *Proc Natl Acad Sci U S A* **107**, 2177-2182, doi:10.1073/pnas.0909797107 (2010).
- 95 Bauer, M. *et al.* Heterogeneity of gene expression in stromal fibroblasts of human breast carcinomas and normal breast. *Oncogene* **29**, 1732-1740, doi:10.1038/onc.2009.463 (2010).
- 96 Lim, K. P. *et al.* Fibroblast gene expression profile reflects the stage of tumour progression in oral squamous cell carcinoma. *J Pathol* **223**, 459-469, doi:10.1002/path.2841 (2011).
- 97 Wadlow, R. C. *et al.* Systems-level modeling of cancer-fibroblast interaction. *PLoS One* **4**, e6888, doi:10.1371/journal.pone.0006888 (2009).
- 98 Irizarry, R. A. *et al.* Exploration, normalization, and summaries of high density oligonucleotide array probe level data. *Biostatistics* **4**, 249-264, doi:10.1093/biostatistics/4.2.249 (2003).

- 99 Lempicki, R. A. *et al.* Gene expression profiles in hepatitis C virus (HCV) and HIV coinfection: class prediction analyses before treatment predict the outcome of anti-HCV therapy among HIV-coinfected persons. *J Infect Dis* **193**, 1172-1177, doi:10.1086/501365 (2006).
- 100 Smyth, G. K. Linear models and empirical bayes methods for assessing differential expression in microarray experiments. *Stat Appl Genet Mol Biol* **3**, Article3, doi:10.2202/1544-6115.1027 (2004).
- 101 Perou, C. M. *et al.* Molecular portraits of human breast tumours. *Nature* **406**, 747-752, doi:10.1038/35021093 (2000).
- 102 Thode, C., Jorgensen, T. G., Dabelsteen, E., Mackenzie, I. & Dabelsteen, S. Significance of myofibroblasts in oral squamous cell carcinoma. *J Oral Pathol Med* **40**, 201-207, doi:10.1111/j.1600-0714.2010.00999.x (2011).
- 103 Venables, J. P. *et al.* Identification of alternative splicing markers for breast cancer. *Cancer Res* **68**, 9525-9531, doi:10.1158/0008-5472.CAN-08-1769 (2008).
- 104 Lapuk, A. *et al.* Exon-level microarray analyses identify alternative splicing programs in breast cancer. *Mol Cancer Res* **8**, 961-974, doi:10.1158/1541-7786.MCR-09-0528 (2010).
- 105 Orimo, A. & Weinberg, R. A. Stromal fibroblasts in cancer: a novel tumor-promoting cell type. *Cell Cycle* **5**, 1597-1601 (2006).
- 106 Wan, B. *et al.* hOLFML1, a novel secreted glycoprotein, enhances the proliferation of human cancer cell lines in vitro. *FEBS Lett* **582**, 3185-3192, doi:10.1016/j.febslet.2008.08.009 (2008).
- 107 Kaur, S. *et al.* RhoJ/TCL regulates endothelial motility and tube formation and modulates actomyosin contractility and focal adhesion numbers. *Arterioscler Thromb Vasc Biol* **31**, 657-664, doi:10.1161/ATVBAHA.110.216341 (2011).
- 108 Carles, A. *et al.* Head and neck squamous cell carcinoma transcriptome analysis by comprehensive validated differential display. *Oncogene* **25**, 1821-1831, doi:10.1038/sj.onc.1209203 (2006).
- 109 Venter, J. C. *et al.* The sequence of the human genome. *Science* **291**, 1304-1351, doi:10.1126/science.1058040 (2001).
- 110 Minard, M. E., Ellis, L. M. & Gallick, G. E. Tiam1 regulates cell adhesion, migration and apoptosis in colon tumor cells. *Clin Exp Metastasis* **23**, 301-313, doi:10.1007/s10585-006-9040-z (2006).
- 111 O'Toole, T. E., Bialkowska, K., Li, X. & Fox, J. E. Tiam1 is recruited to beta1-integrin complexes by 14-3-3zeta where it mediates integrin-induced rac1 activation and motility. *J Cell Physiol*, doi:10.1002/jcp.22644 (2011).
- 112 Milech, N. *et al.* MEIS proteins as partners of the TLX1/HOX11 oncoprotein. *Leuk Res* **34**, 358-363, doi:10.1016/j.leukres.2009.06.003 (2010).
- 113 Shathasivam, T., Kislinger, T. & Gramolini, A. O. Genes, proteins and complexes: the multifaceted nature of FHL family proteins in diverse tissues. *J Cell Mol Med* **14**, 2702-2720, doi:10.1111/j.1582-4934.2010.01176.x (2010).

- 114 Martin-Villar, E. *et al.* Podoplanin associates with CD44 to promote directional cell migration. *Mol Biol Cell* **21**, 4387-4399, doi:10.1091/mbc.E10-06-0489 (2010).
- 115 Baldessari, D., Badaloni, A., Longhi, R., Zappavigna, V. & Consalez, G. G. MAB21L2, a vertebrate member of the Male-abnormal 21 family, modulates BMP signaling and interacts with SMAD1. *BMC Cell Biol* **5**, 48, doi:10.1186/1471-2121-5-48 (2004).
- 116 Kahlert, C. *et al.* Low expression of aldehyde dehydrogenase 1A1 (ALDH1A1) is a prognostic marker for poor survival in pancreatic cancer. *BMC Cancer* **11**, 275, doi:10.1186/1471-2407-11-275 (2011).
- 117 Chen, Y. C. *et al.* Aldehyde dehydrogenase 1 is a putative marker for cancer stem cells in head and neck squamous cancer. *Biochem Biophys Res Commun* **385**, 307-313, doi:10.1016/j.bbrc.2009.05.048 (2009).
- 118 Shen, J., Li, C. & Gudas, L. J. Regulation of the laminin beta 1 (LAMB1), retinoic acid receptor beta, and bone morphogenetic protein 2 genes in mutant F9 teratocarcinoma cell lines partially deficient in cyclic AMP-dependent protein kinase activity. *Cell Growth Differ* **8**, 1297-1304 (1997).
- 119 Zhuang, Z., Jian, P., Longjiang, L., Bo, H. & Wenlin, X. Oral cancer cells with different potential of lymphatic metastasis displayed distinct biologic behaviors and gene expression profiles. *J Oral Pathol Med* **39**, 168-175, doi:10.1111/j.1600-0714.2009.00817.x (2010).
- 120 Lincoln, D. T., Ali Emadi, E. M., Tonissen, K. F. & Clarke, F. M. The thioredoxin-thioredoxin reductase system: over-expression in human cancer. *Anticancer Res* **23**, 2425-2433 (2003).
- 121 Gonzalez-Alva, P. *et al.* Podoplanin expression in odontomas: clinicopathological study and immunohistochemical analysis of 86 cases. *J Oral Sci* **53**, 67-75 (2011).
- 122 Wicki, A. *et al.* Tumor invasion in the absence of epithelial-mesenchymal transition: podoplanin-mediated remodeling of the actin cytoskeleton. *Cancer Cell* **9**, 261-272, doi:10.1016/j.ccr.2006.03.010 (2006).
- 123 Dumoff, K. L. *et al.* Low D2-40 immunoreactivity correlates with lymphatic invasion and nodal metastasis in early-stage squamous cell carcinoma of the uterine cervix. *Mod Pathol* **18**, 97-104, doi:10.1038/modpathol.3800269 (2005).
- 124 Yuan, P. *et al.* Overexpression of podoplanin in oral cancer and its association with poor clinical outcome. *Cancer* **107**, 563-569, doi:10.1002/cncr.22061 (2006).
- 125 Carvalho, F. M. *et al.* Prognostic value of podoplanin expression in intratumoral stroma and neoplastic cells of uterine cervical carcinomas. *Clinics (Sao Paulo)* **65**, 1279-1283 (2010).
- 126 Flaberg, E. *et al.* High-throughput live-cell imaging reveals differential inhibition of tumor cell proliferation by human fibroblasts. *Int J Cancer* **128**, 2793-2802, doi:10.1002/ijc.25612 (2011).

- 127 Qin, X. F., An, D. S., Chen, I. S. & Baltimore, D. Inhibiting HIV-1 infection in human T cells by lentiviral-mediated delivery of small interfering RNA against CCR5. *Proc Natl Acad Sci U S A* **100**, 183-188, doi:10.1073/pnas.232688199 (2003).
- 128 Sogabe, Y. *et al.* Epigenetic inactivation of SFRP genes in oral squamous cell carcinoma. *Int J Oncol* **32**, 1253-1261 (2008).
- 129 Pannone, G. *et al.* WNT pathway in oral cancer: epigenetic inactivation of WNT-inhibitors. *Oncol Rep* **24**, 1035-1041 (2010).
- 130 Greco, S. A. *et al.* Thrombospondin-4 is a putative tumour-suppressor gene in colorectal cancer that exhibits age-related methylation. *BMC Cancer* **10**, 494, doi:10.1186/1471-2407-10-494 (2010).
- 131 Forster, S., Gretschel, S., Jons, T., Yashiro, M. & Kemmner, W. THBS4, a novel stromal molecule of diffuse-type gastric adenocarcinomas, identified by transcriptome-wide expression profiling. *Mod Pathol*, doi:10.1038/modpathol.2011.99 (2011).
- 132 Glinka, A. *et al.* Dickkopf-1 is a member of a new family of secreted proteins and functions in head induction. *Nature* **391**, 357-362, doi:10.1038/34848 (1998).
- 133 Fedi, P. *et al.* Isolation and biochemical characterization of the human Dkk-1 homologue, a novel inhibitor of mammalian Wnt signaling. *J Biol Chem* **274**, 19465-19472 (1999).
- 134 Bafico, A., Liu, G., Yaniv, A., Gazit, A. & Aaronson, S. A. Novel mechanism of Wnt signalling inhibition mediated by Dickkopf-1 interaction with LRP6/Arrow. *Nat Cell Biol* **3**, 683-686, doi:10.1038/35083081 (2001).
- 135 Gonzalez-Sancho, J. M. *et al.* The Wnt antagonist DICKKOPF-1 gene is a downstream target of beta-catenin/TCF and is downregulated in human colon cancer. *Oncogene* **24**, 1098-1103, doi:10.1038/sj.onc.1208303 (2005).
- 136 Kuhnert, F. *et al.* Essential requirement for Wnt signaling in proliferation of adult small intestine and colon revealed by adenoviral expression of Dickkopf-1. *Proc Natl Acad Sci U S A* **101**, 266-271, doi:10.1073/pnas.2536800100 (2004).
- 137 Katase, N. *et al.* Frequent allelic loss of Dkk-1 locus (10q11.2) is related with low distant metastasis and better prognosis in head and neck squamous cell carcinomas. *Cancer Invest* **28**, 103-110, doi:10.3109/07357900903095680 (2010).
- 138 Ogoshi, K. *et al.* Dickkopf-1 in human oral cancer. *Int J Oncol* **39**, 329-336, doi:10.3892/ijo.2011.1046 (2011).
- 139 Fu, L. *et al.* Wnt2 secreted by tumour fibroblasts promotes tumour progression in oesophageal cancer by activation of the Wnt/{beta}-catenin signalling pathway. *Gut*, doi:10.1136/gut.2011.241638 (2011).

Appendices

Supplementary Material

Supplementary Figure A. RT2 QC Profiler Results. OF108, OF6 CAF and OF50 did not pass and were not included in the validation study.

	OF51	OF51	OF52	OF52	OF78	OF78	OF77	OF77
ACTB	17.82	17.70	19.30	19.27	20.57	20.64	16.78	16.76
HPRT1	24.85	24.99	28.28	28.21	26.72	26.86	24.86	25.14
RTC	22.50	22.42	21.66	21.53	23.13	22.91	22.17	22.18
PPC	18.30	18.30	18.38	18.45	18.27	18.63	18.21	18.30
GDC	39.87	Undeterm	Undeterm	Undeterm	33.17	Undeterm	Undeterm	Undetermined
NRT	Undeterm	Undeterm	35.29	Undeterm	Undeterm	39.37	Undeterm	Undetermined
PPC - H2C	15.91	18.66	18.29	18.53	18.40	18.74	18.52	18.70
NTC	37.74	Undeterm	36.35	Undeterm	Undeterm	38.99	Undeterm	Undetermined

	OF82	OF82	OF81	OF81	OF84	OF84	OF83	OF83
ACTB	18.88	18.63	18.33	18.37	17.46	17.41	18.74	18.75
HPRT1	26.13	26.29	25.61	25.72	24.38	24.75	25.49	25.37
RTC	21.81	21.76	21.98	21.79	21.74	21.83	22.25	22.19
PPC	18.46	18.64	18.27	18.40	18.70	17.95	17.99	17.92
GDC	Undeterm	Undeterm	Undeterm	Undeterm	34.98	Undeterm	34.99	31.33
NRT	Undeterm	Undeterm	Undeterm	36.33	Undeterm	Undeterm	33.76	34.27
PPC - H2C	18.46	18.33	18.61	18.48	18.25	18.39	18.50	18.60
NTC	Undeterm	Undeterm	38.06	Undeterm	Undeterm	Undeterm	Undeterm	Undetermined

	OF99	OF99	OF100	OF100	OF6 TONG	OF6 TONG	OF107	OF107
ACTB	21.22	21.25	16.89	16.98	17.45	17.53	16.31	16.41
HPRT1	27.87	28.16	25.61	25.94	24.31	24.47	24.10	24.30
RTC	22.75	22.68	22.61	22.44	22.54	22.41	22.16	22.22
PPC	18.00	17.94	18.21	18.28	17.90	18.20	17.89	18.20
GDC	Undeterm	Undeterm	39.99	Undeterm	33.23	Undeterm	Undeterm	39.30
NRT	33.93	36.16	Undeterm	Undeterm	35.90	33.22	31.84	Undetermined
PPC - H2C	18.12	18.44	18.35	18.45	18.27	18.49	18.29	18.53
NTC	Undeterm	Undeterm	Undeterm	Undeterm	Undeterm	Undeterm	31.76	Undetermined

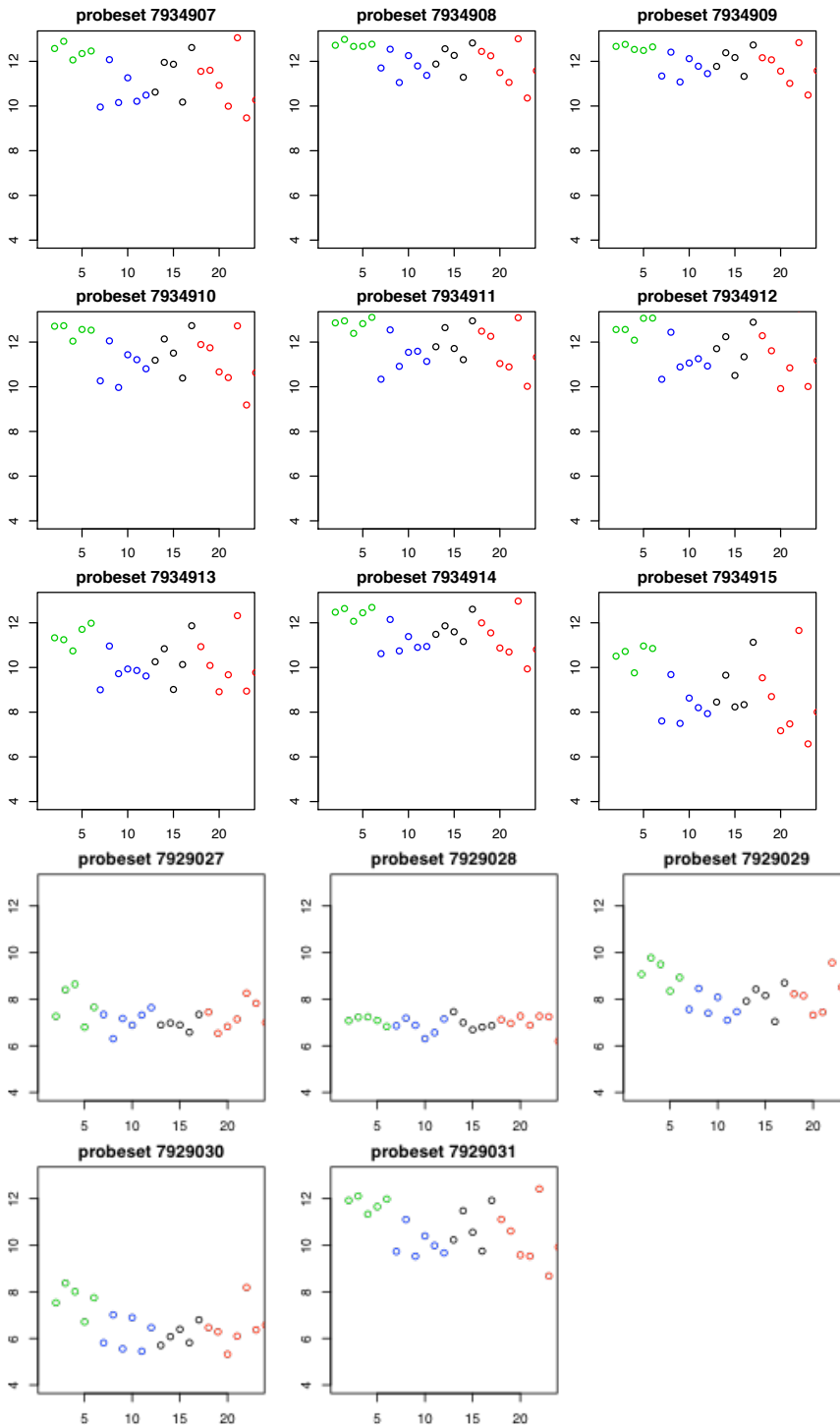
	OF 108	OF 108	OF6 GING	OF6 GING	OF6 CAF	OF6 CAF	OF40	OF40
ACTB	24.16	24.10	18.39	18.45	32.91	Undeterm	18.40	18.36
HPRT1	27.60	27.64	27.22	27.45	32.93	32.82	25.14	25.22
RTC	23.96	23.88	22.91	22.81	28.81	28.26	23.01	22.72
PPC	19.12	18.32	18.39	18.32	18.44	18.34	18.44	18.37
GDC	Undeterm	Undeterm	39.12	Undeterm	Undeterm	Undeterm	Undeterm	Undetermined
NRT	Undeterm	Undeterm	Undeterm	Undeterm	Undeterm	Undeterm	Undeterm	Undetermined
PPC - H2C	18.64	18.61	18.58	18.76	18.75	18.85	18.40	18.65
NTC	Undeterm	Undeterm	Undeterm	Undeterm	Undeterm	Undeterm	Undeterm	39.99

	HN112	HN112	OF50	OF50	OF79	OF79	OF49	OF49
ACTB	17.67	17.68	25.51	25.37	16.97	16.77	17.76	17.70
HPRT1	25.93	25.92	28.90	28.80	24.82	25.13	25.30	25.26
RTC	22.60	22.59	24.34	24.12	22.45	22.43	21.88	21.77
PPC	18.21	18.28	18.27	18.23	18.34	18.12	18.25	18.02
GDC	Undeterm	Undeterm	Undeterm	Undeterm	Undeterm	Undeterm	Undeterm	Undetermined
NRT	Undeterm	Undeterm	Undeterm	Undeterm	Undeterm	Undeterm	Undeterm	Undetermined
PPC - H2C	18.59	18.56	18.43	18.86	18.57	18.60	18.52	18.54
NTC	Undeterm	Undeterm	38.97	Undeterm	Undeterm	Undeterm	Undeterm	Undetermined

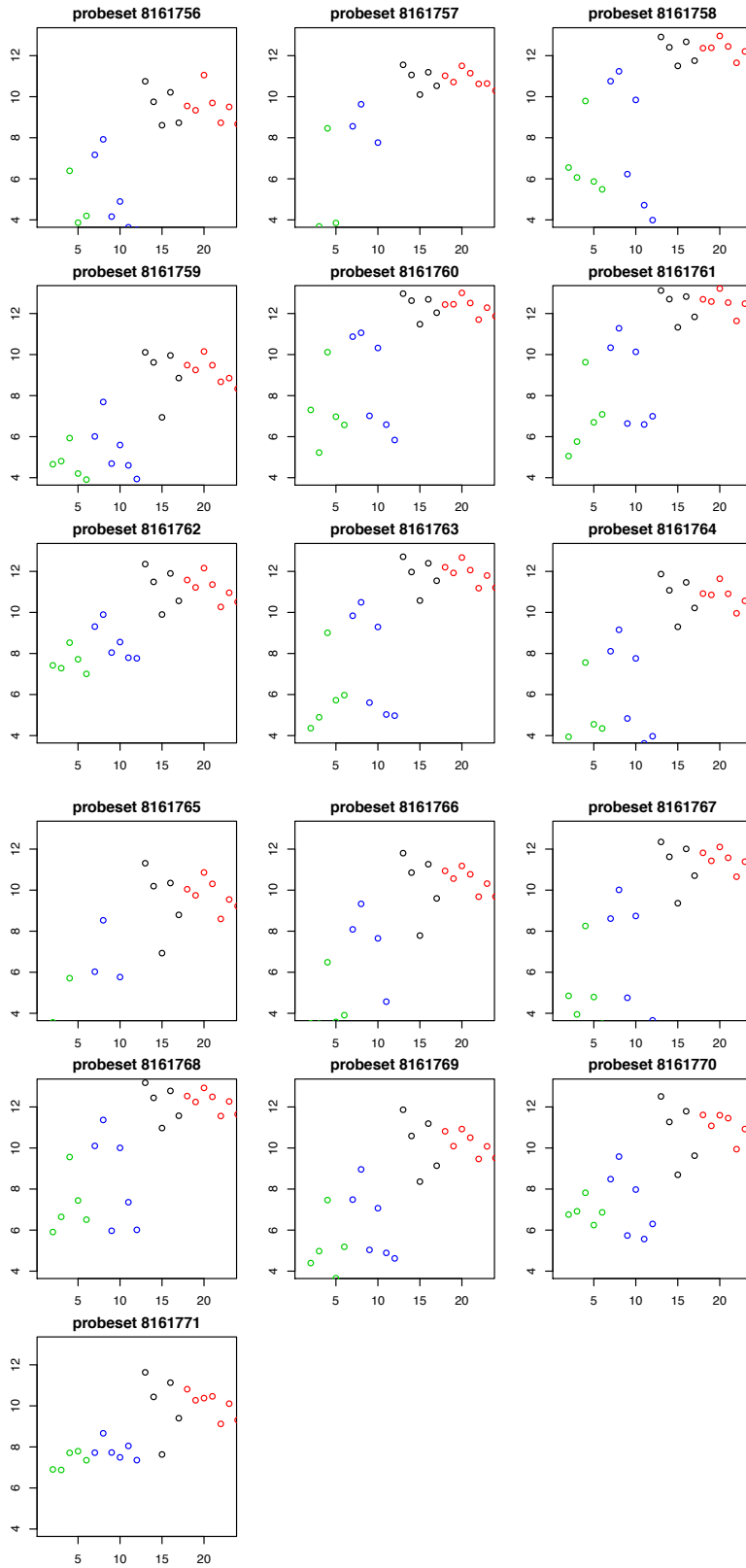
	OF97	OF97	OF76	OF76	OF47	OF47
ACTB	16.71	16.72	17.34	17.22	17.99	17.99
HPRT1	22.97	23.04	25.94	25.84	28.81	25.68
RTC	22.38	22.28	22.44	22.24	22.55	22.53
PPC	18.51	18.19	18.24	18.01	19.17	18.55
GDC	38.69	33.00	Undeterm	Undeterm	32.56	31.53
NRT	Undeterm	Undeterm	Undeterm	34.17	32.51	26.96
PPC - H2C	18.56	18.64	18.63	18.57	18.66	18.59
NTC	Undeterm	Undeterm	Undeterm	Undeterm	Undeterm	Undetermined

Supplementary Figure B. Probe set graphs for representative genes. For the validated genes, no alternative splicing events were detected. Green circles = gingival CAF, Blue circles = gingival NF, Black circles = tongue CAF, Red circles = tongue NF.

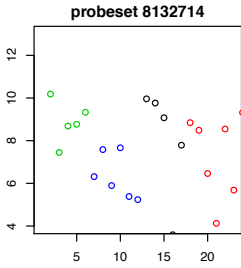
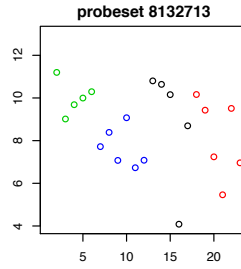
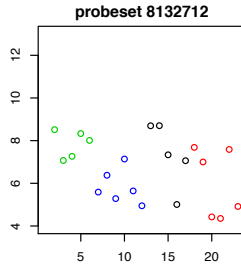
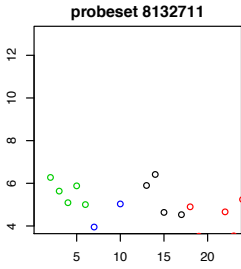
ACTA2



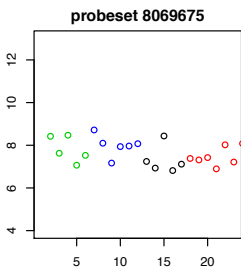
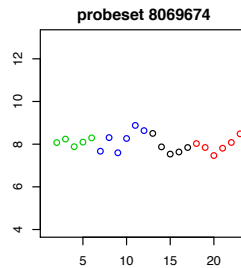
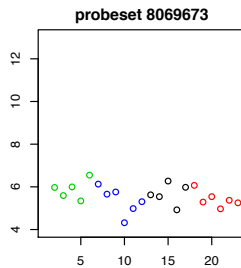
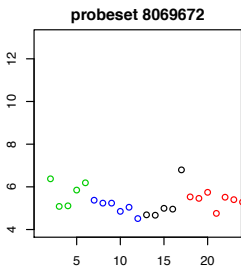
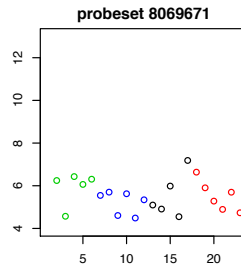
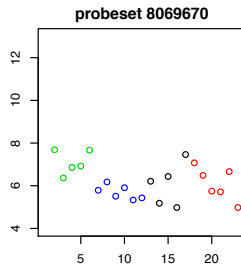
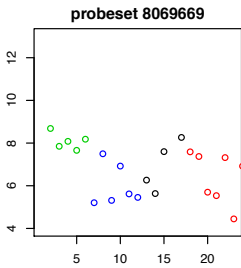
ALDH1A1



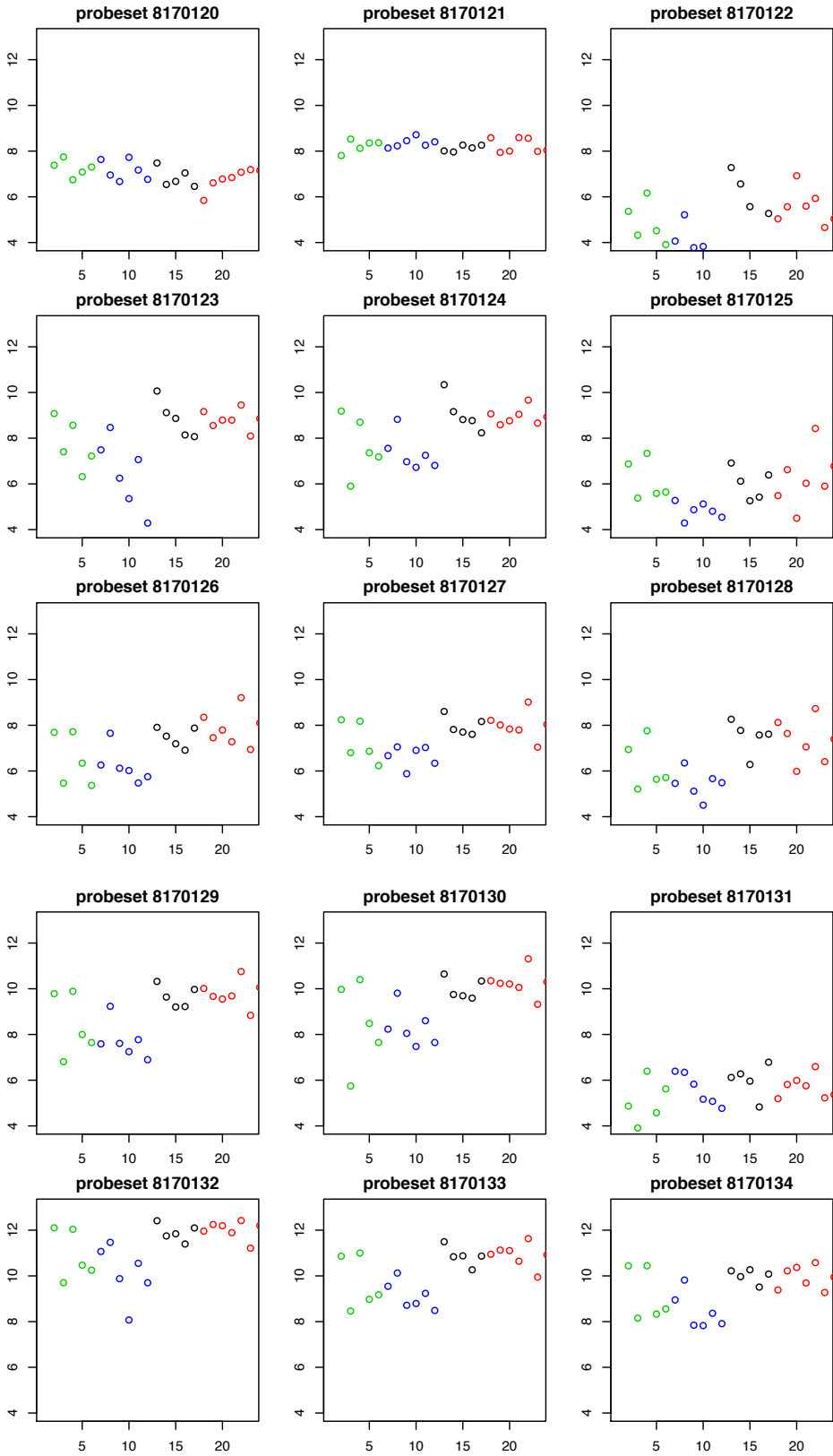
C7orf69



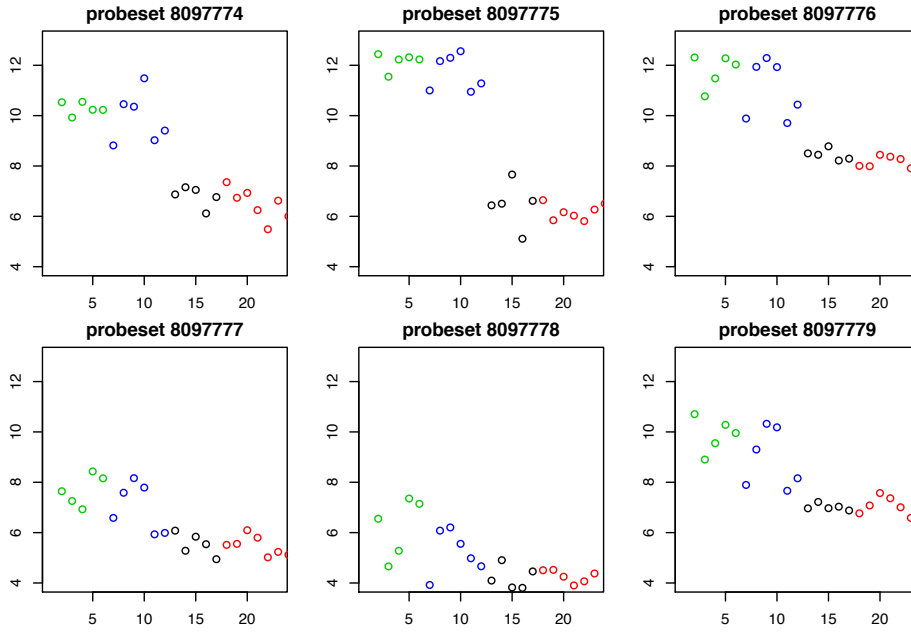
CYR-1



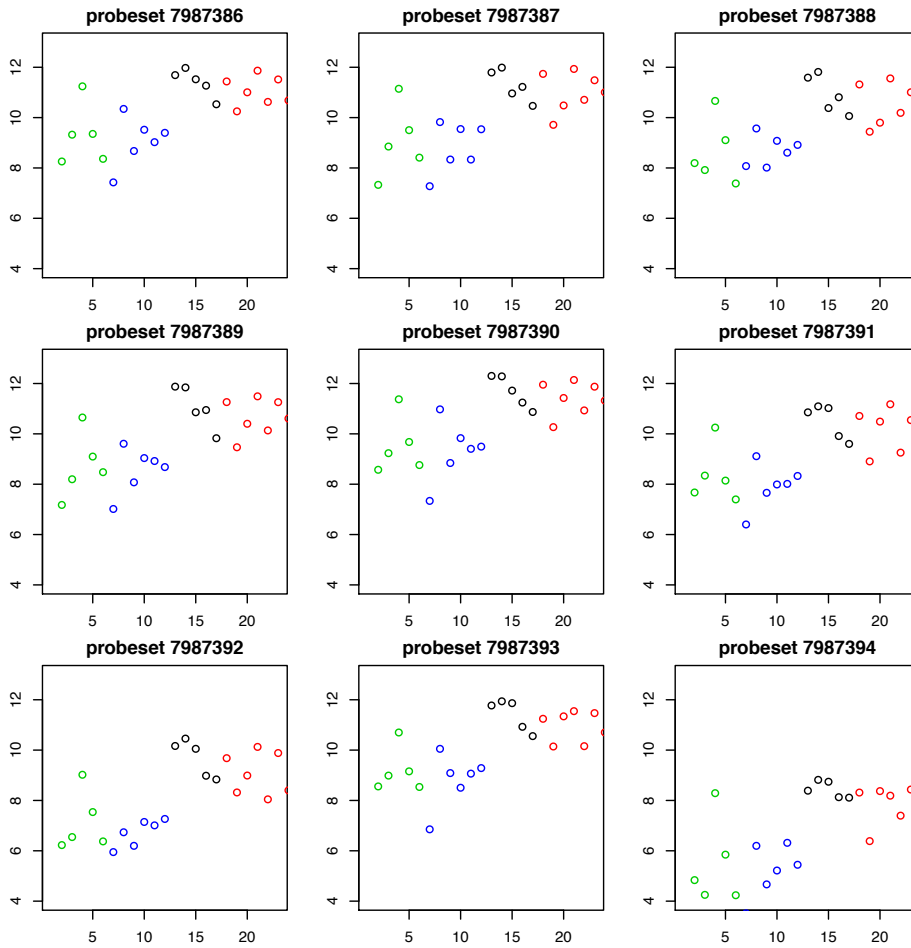
FHL-1



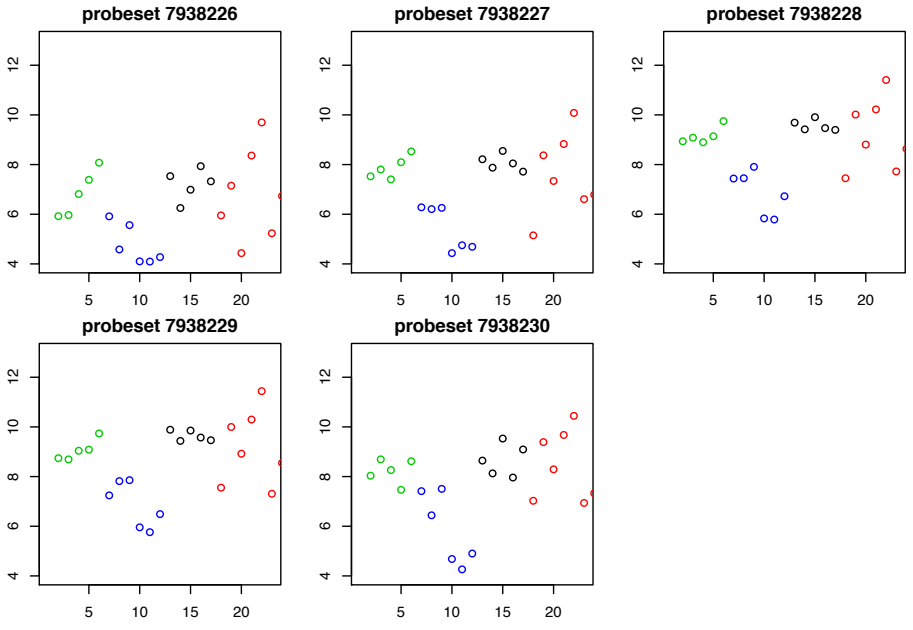
MAB21L2



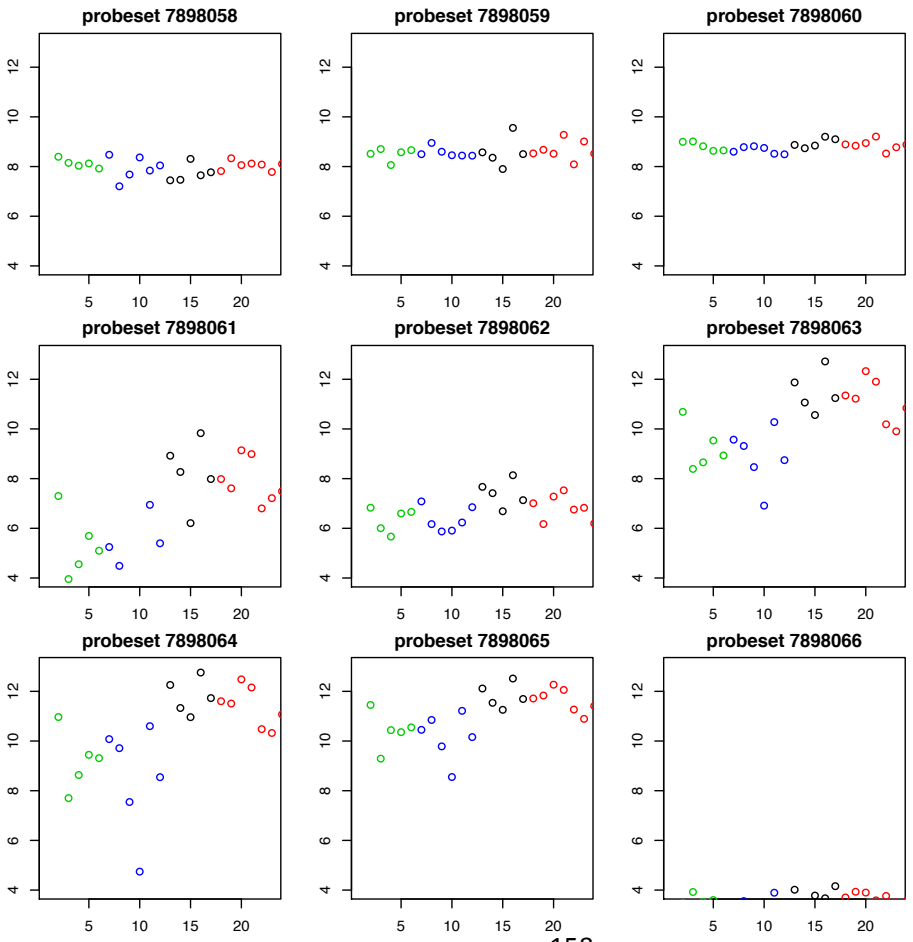
MEIS2



OLFML-1



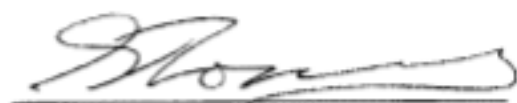
PDPN



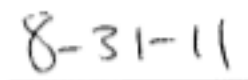
Publishing Agreement

It is the policy of the University to encourage the distribution of all theses, dissertations and manuscripts. Copies of all UCSF theses, dissertations and manuscripts will be routed to the library via the Graduate Division. The library will make all theses, dissertations and manuscripts accessible to the public and will preserve these to the best of their abilities, in perpetuity.

I hereby grant permission to the Graduate Division of the University of California, San Francisco to release copies of my thesis, dissertation or manuscript to the Campus Library to provide access and preservation, in whole or in part, in perpetuity.

A handwritten signature in black ink, appearing to be "Thomas", written over a horizontal line.

Author Signature

A handwritten date "8-31-11" in black ink, written over a horizontal line.

Date